THE QUARTERLY JOURNAL OF

MECHANICS AND APPLIED MATHEMATICS

VOLUME XI PART 3

AUGUST 1958

OXFORD

AT THE CLARENDON PRESS

1958

Price 18*s. net*

PRINTED IN GREAT BRITAIN BY CHARLES BATEY AT THE UNIVERSITY PRESS, OXFORD

THE QUARTERLY JOURNAL OF MECHANICS AND APPLIED MATHEMATICS

THE QUARTERLY JOURNAL OF MECHANICS AND APPLIED MATHEMATICS is published at 18*s.* net for a single number with an annual subscription (for four numbers) of 60*s.* post free.

NOTICE TO CONTRIBUTORS

1. *Communication.* Papers should be communicated to Dr. D. M. A. Leggett, Department of Mathematics, King's College, Strand, London, W.C. 2.

If possible, to expedite publication, papers should be submitted in duplicate.

2. *Presentation.* Papers should be typewritten (double spacing) and should be preceded by a summary not exceding 300 words in length. References to literature should be given in standard order, *author, title of journal, volume number, date, page.* These should be placed at the end of the paper and arranged according to the order of reference in the paper.

3. *Diagrams.* The number of diagrams should be kept to the minimum consistent with clarity. The lines of the figures should be drawn in ink either on draughtsman's paper or on good quality white paper. Each individual line in the figure should bear reducing to one-half of the size of the original, and great care should be exercised to see that the lines are regular in thickness, especially where they meet. Lettering of the figure should be in pencil and should be sufficient to define clearly the lines and curves in it. The writing of formulae or of explanations on the diagram itself should be avoided. All explanations of symbols, etc., should be given in underline. Contributors should indicate on their manuscripts where figures should be inserted.

4. *Tables.* Tables should preferably be arranged so that they can be printed with the columns parallel to the longer edge of the page.

5. *Notation.* All single letters used to denote vectors in the manuscript should be marked by underlining with a wavy line. Scalar and vector products should be denoted by $\underset{\sim}{a} . \underset{\sim}{b}$ and $\underset{\sim}{a} \wedge \underset{\sim}{b}$ respectively. Real and imaginary parts of complex quantities should be denoted by re and im respectively.

6. *Offprints.* Authors of papers will be entitled to 25 free offprints. This number is available for sharing between authors of joint papers.

7. All correspondence other than that dealing with contributions should be addressed to the publishers:

OXFORD UNIVERSITY PRESS
AMEN HOUSE, LONDON, E.C. 4

HEAT TRANSFER BY LAMINAR FREE CONVECTION IN ENCLOSED PLANE GAS LAYERS

By G. POOTS (*Department of Theoretical Mechanics, University of Bristol*)

[Received 31 May 1957]

SUMMARY

A numerical method based on the use of orthogonal polynomials is given for the solution of two simultaneous partial differential equations which govern the heat transfer by laminar free convection in enclosed horizontal, oblique, and vertical gas layers. The heat transfer through the enclosed gas layer depends only on the Rayleigh number $A = g\beta(T_1 - T_0)d^3/T_0k\nu$, the Prandtl number $\sigma = \nu/k$, the aspect ratio of the rectangular cell $x = l/d$, the angle of inclination ϕ of the hot and cold walls to the vertical, and finally the temperature distribution in the remaining two walls or border strips.

Preliminary thermal results are given for air taking $\sigma = 0{\cdot}73$, $x = 1$, $\phi = 0$ and $A = 5 \cdot 10^2$, 10^3, $2{\cdot}5 \cdot 10^3$, $5 \cdot 10^3$, and 10^4, and the temperature distribution along the border strips to be $T = T_0 + (T_1 - T_0)y/d$. A comparison of the theoretical prediction of the heat transfer across the cell with the experimental data of Mull and Reiher (**1**), as correlated by Jakob (**2**), can only be made in the region $A = 10^4$. Calculated results and empirical formulae obtained by Jakob agree favourably in this region considering that all the measurements of Mull and Reiher were made for large values of the aspect ratio and virtually non-conducting border-strips.

Streamlines and isothermals have been plotted for $A = 10^4$ which clearly indicate the existence of an isothermal core in the cavity having constant vorticity, as postulated by Batchelor (**3**).

1. Introduction and basic theory

The heat transmission through horizontal, oblique, and vertical enclosed gas layers was investigated experimentally by Mull and Reiher (**1**) and the thermal results correlated by Jakob (**2**). Batchelor (**3**) derived the equations governing heat transmission across an air space between two vertical plane boundaries, distant d apart, and held at different temperatures, the air space being closed by two horizontal plane boundaries, or border strips, distant l apart. Quantitative information was given on the rate of heat transfer across the cold boundary for large aspect ratios $x = l/d$. It is the purpose of the present paper to give a numerical method for solving the two simultaneous partial differential equations which govern the heat transmission in a closed rectangular cell having hot and cold walls inclined at an angle ϕ to the vertical. The boundary condition on the border strips is assumed to be either linear and of the form $T = T_0 + (T_1 - T_0)y/d$, or that there is no heat loss into the surrounding medium, namely $\partial T/\partial x = 0$.

Consider an air space enclosed between two plane parallel boundaries

THE QUARTERLY JOURNAL OF MECHANICS AND APPLIED MATHEMATICS

THE QUARTERLY JOURNAL OF MECHANICS AND APPLIED MATHEMATICS is published at 18*s*. net for a single number with an annual subscription (for four numbers) of 60*s*. post free.

NOTICE TO CONTRIBUTORS

1. *Communication.* Papers should be communicated to Dr. D. M. A. Leggett, Department of Mathematics, King's College, Strand, London, W.C. 2.

If possible, to expedite publication, papers should be submitted in duplicate.

2. *Presentation.* Papers should be typewritten (double spacing) and should be preceded by a summary not exceeding 300 words in length. References to literature should be given in standard order, *author, title of journal, volume number, date, page*. These should be placed at the end of the paper and arranged according to the order of reference in the paper.

3. *Diagrams.* The number of diagrams should be kept to the minimum consistent with clarity. The lines of the figures should be drawn in ink either on draughtsman's paper or on good quality white paper. Each individual line in the figure should bear reducing to one-half of the size of the original, and great care should be exercised to see that the lines are regular in thickness, especially where they meet. Lettering of the figure should be in pencil and should be sufficient to define clearly the lines and curves in it. The writing of formulae or of explanations on the diagram itself should be avoided. All explanations of symbols, etc., should be given in underline. Contributors should indicate on their manuscripts where figures should be inserted.

4. *Tables.* Tables should preferably be arranged so that they can be printed with the columns parallel to the longer edge of the page.

5. *Notation.* All single letters used to denote vectors in the manuscript should be marked by underlining with a wavy line. Scalar and vector products should be denoted by $\underset{\sim}{a} . \underset{\sim}{b}$ and $\underset{\sim}{a} \wedge \underset{\sim}{b}$ respectively. Real and imaginary parts of complex quantities should be denoted by re and im respectively.

6. *Offprints.* Authors of papers will be entitled to 25 free offprints. This number is available for sharing between authors of joint papers.

7. All correspondence other than that dealing with contributions should be addressed to the publishers:

OXFORD UNIVERSITY PRESS
AMEN HOUSE, LONDON, E.C. 4

HEAT TRANSFER BY LAMINAR FREE CONVECTION IN ENCLOSED PLANE GAS LAYERS

By G. POOTS (*Department of Theoretical Mechanics, University of Bristol*)

[Received 31 May 1957]

SUMMARY

A numerical method based on the use of orthogonal polynomials is given for the solution of two simultaneous partial differential equations which govern the heat transfer by laminar free convection in enclosed horizontal, oblique, and vertical gas layers. The heat transfer through the enclosed gas layer depends only on the Rayleigh number $A = g(T_1-T_0)d^3/(T_0k\nu)$, the Prandtl number $\sigma = \nu/k$, the aspect ratio of the rectangular cell $\alpha = l/d$, the angle of inclination ϕ of the hot and cold walls to the vertical, and finally the temperature distribution in the remaining two walls or border strips.

Preliminary thermal results are given for air taking $\sigma = 0{\cdot}73$, $\alpha = 1$, $\phi = 0$ and $A = 5\times10^2$, 10^3, $2{\cdot}5\times10^3$, 5×10^3, and 10^4, and the temperature distribution along the border strips to be $T = T_0+(T_1-T_0)y/d$. A comparison of the theoretical prediction of the heat transfer across the cell with the experimental data of Mull and Reiher (**1**), as correlated by Jakob (**2**), can only be made in the region $A = 10^4$. Calculated results and empirical formulae obtained by Jakob agree favourably in this region considering that all the measurements of Mull and Reiher were made for large values of the aspect ratio and virtually non-conducting border strips.

Streamlines and isothermals have been plotted for $A = 10^4$ which clearly indicate the existence of an isothermal core in the cavity having constant vorticity, as postulated by Batchelor (**3**).

1. Introduction and basic theory

THE heat transmission through horizontal, oblique, and vertical enclosed gas layers was investigated experimentally by Mull and Reiher (**1**) and the thermal results correlated by Jakob (**2**). Batchelor (**3**) derived the equations governing heat transmission across an air space between two vertical plane boundaries, distant d apart, and held at different temperatures, the air space being closed by two horizontal plane boundaries, or border strips, distant l apart. Quantitative information was given on the rate of heat transfer across the cold boundary for large aspect ratios $\alpha = l/d$. It is the purpose of the present paper to give a numerical method for solving the two simultaneous partial differential equations which govern the heat transmission in a closed rectangular cell having hot and cold walls inclined at an angle ϕ to the vertical. The boundary condition on the border strips is assumed to be either linear and of the form $T = T_0+(T_1-T_0)y/d$, or that there is no heat loss into the surrounding medium, namely $\partial T/\partial x = 0$.

Consider an air space enclosed between two plane parallel boundaries

inclined at an angle ϕ to the vertical, and by two border strips of length d and distance l apart as shown in Fig. 1. Let T_1 and T_0 be the absolute temperatures of the hot and cold walls respectively. Assuming that

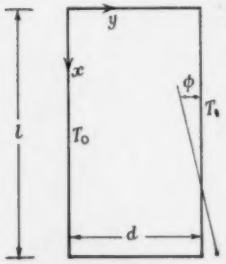

FIG. 1

(i) temperature difference T_1-T_0 is small compared with the absolute temperature T_0 of the cold boundary,

(ii) viscosity, density, and thermal conductivity are constant except for the effect of the density variation in producing buoyancy force,

(iii) fluid is incompressible and viscous heat dissipation may be neglected,

(iv) motion is two-dimensional,

then subject to the above restrictions the equations governing free convection by laminar flow in the cell may be formulated (Goldstein (4)). Thus if the coordinates x, y are chosen as in Fig. 1, and the corresponding velocity components are u, v, then the basic equations of motion are

$$u\frac{\partial u}{\partial x}+v\frac{\partial u}{\partial y}=-\frac{1}{\rho_0}\frac{\partial p}{\partial x}-g\cos\phi\left(\frac{T-T_0}{T_0}\right)+\nu\nabla^2 u, \tag{1.1}$$

$$u\frac{\partial v}{\partial x}+v\frac{\partial v}{\partial y}=-\frac{1}{\rho_0}\frac{\partial p}{\partial y}-g\sin\phi\left(\frac{T-T_0}{T_0}\right)+\nu\nabla^2 v, \tag{1.2}$$

$$\frac{\partial u}{\partial x}+\frac{\partial v}{\partial y}=0, \tag{1.3}$$

and the equation of heat transfer is

$$u\frac{\partial T}{\partial x}+v\frac{\partial T}{\partial y}=k\nabla^2 T, \tag{1.4}$$

where the suffix 0 signifies conditions at the cold wall, ρ is the fluid density, p the pressure, g the gravitational constant, ν the kinematic viscosity, and k the thermometric conductivity. The boundary conditions to be imposed on the variables u, v, and T are

$$u=v=0, \quad T=T_0 \quad \text{at } y=0 \qquad \text{for } 0\leqslant x\leqslant l,$$

$$u=v=0, \quad T=T_1 \quad \text{at } y=d \qquad \text{for } 0\leqslant x\leqslant l,$$

$$u=v=0 \qquad\qquad \text{at } x=0,l \quad \text{for } 0\leqslant y\leqslant d,$$

$$T=T_0+(T_1-T_0)y/d \text{ or } \partial T/\partial x=0 \quad \text{at } x=0,l \text{ for } 0\leqslant y\leqslant d.$$

Following Batchelor (3) by taking d as a representative length for the

coordinates x and y (without changing notation), and defining a dimensionless temperature distribution and stream function by

$$\theta = (T-T_0)/(T_1-T_0), \qquad u = kd^{-1}\frac{\partial\psi}{\partial y}, \qquad v = -kd^{-1}\frac{\partial\psi}{\partial x} \tag{1.5}$$

respectively, then on eliminating the pressure p the governing equations become

$$\nabla^2\theta = \frac{\partial\theta}{\partial x}\frac{\partial\psi}{\partial y} - \frac{\partial\theta}{\partial y}\frac{\partial\psi}{\partial x}, \tag{1.6}$$

$$\nabla^4\psi = A\left(\cos\phi\frac{\partial\theta}{\partial y} - \sin\phi\frac{\partial\theta}{\partial x}\right) + \frac{1}{\sigma}\left\{\frac{\partial}{\partial x}(\nabla^2\psi)\frac{\partial\psi}{\partial y} - \frac{\partial}{\partial y}(\nabla^2\psi)\frac{\partial\psi}{\partial x}\right\}, \tag{1.7}$$

where σ is the Prandtl number, and $A = \sigma G = (T_1-T_0)gd^3/(T_0 k\nu)$ are the Rayleigh and Grashof numbers respectively. The associated boundary conditions are

$$\psi = \frac{\partial\psi}{\partial y} = 0, \qquad \theta = 0 \quad \text{at } y = 0,$$

$$\psi = \frac{\partial\psi}{\partial y} = 0, \qquad \theta = 1 \quad \text{at } y = 1 \quad \text{for } 0 \leqslant x \leqslant \alpha,$$

$$\psi = \frac{\partial\psi}{\partial x} = 0, \qquad \theta = y \text{ (Case I) or } \frac{\partial\theta}{\partial x} = 0 \text{ (Case II)} \quad \text{at } x = 0, \alpha \quad \text{for } 0 \leqslant y \leqslant 1.$$

The form of the governing equations (1.6) and (1.7) and the above boundary conditions shows that the quantities α, ϕ, A, and σ, together with the border strip boundary conditions, are sufficient to determine ψ and θ uniquely.

The thermal quantity measured experimentally is the rate of heat transmission through the cold boundary. If this rate is Q heat units per second per unit depth of boundary in the z-direction, then a dimensionless quantity describing the heat transfer is the Nusselt number

$$N = \frac{Q}{k(T_1-T_0)} = \int_0^\alpha \left(\frac{\partial\theta}{\partial y}\right)_{y=0} dx. \tag{1.8}$$

As has been shown by Batchelor (3) approximations to both θ and ψ may be made enabling quantitative information on N to be obtained for the various types of flow occurring in vertical cavities ($\phi = 0$). For $A < 10^3$ Batchelor develops a power series expansion in terms of A for θ and ψ as follows

$$\psi = \sum_{n=1}^{\infty} A^n\psi_n(x,y), \qquad \theta = y + \sum_{n=1}^{\infty} A^n\theta_n(x,y). \tag{1.9}$$

On substitution of (1.9) into the governing equations (1.6) and (1.7) and

equating coefficients of like powers of A, he reduces the problem to the solution of a series of linear partial differential equations in $\psi_n(x,y)$ and $\theta_n(x,y)$. Due to the symmetry properties of the θ_n,

$$N = \alpha + \sum_{n=1}^{\infty} \gamma_{2n} A^{2n} \qquad \left\{\gamma_{2n} = \int_0^{\alpha} \left(\frac{\partial \theta_{2n}}{\partial y}\right)_{y=0} dx\right\}. \tag{1.10}$$

The value of γ_2 was estimated to be of the order 10^{-8} when $\alpha = l/d$ was not too different from unity. A section is then given on the case of a general value of A as $\alpha \to \infty$. Here Batchelor argues that in the region not near the ends of the cavity θ and ψ take up their asymptotic forms

$$\theta = \psi, \qquad \psi = \frac{A}{24} y^2(1-y^2) \tag{1.11}$$

and since in this region the rising stream loses heat at a rate equal to the net flux of heat across the horizontal plane, he then obtains

$$N \sim \frac{l}{d} + \left(\frac{2\beta - 1}{720}\right) A, \tag{1.12}$$

where β is an undetermined constant taken to be unity. In a final section on the general value of α as $A \to \infty$ Batchelor postulates that inside the cavity there exists an isothermal core having temperature $\theta = \frac{1}{2}$, and having constant vorticity. Boundary layer equations are set up for the surrounding continuous boundary layer in which temperature and velocity make rapid transitions to their assigned values at the boundary. Batchelor found that since θ and the velocity components oscillate in the boundary layer these quantities could not be satisfactorily represented by polynomials of small degree, nor did the equations yield to linearization of the Oseen type. However, although not solving these equations, Batchelor has obtained estimates of the rate of heat transfer by assuming that the flow near each wall bears resemblance to either forced convection of a stream or free convection past a plate under certain boundary conditions.

In section 2 of this paper a technique, based on the use of orthogonal polynomials, is developed for obtaining numerical approximations to the solution of the two partial differential equations (1.6) and (1.7). Numerical solutions are also tabulated, which have been obtained on application of the technique to the case of a cavity having $\alpha = 1, \phi = 0$, and $A = 5 \times 10^2$, 10^3, $2{\cdot}5 \times 10^3$, 5×10^3, and 10^4. Details of the calculations involved are given in Appendixes A and B. From these solutions thermal results may be extracted which are given and compared with existing experimental data in section 3. Finally, in section 4 a statement of conclusions is made on the numerical technique used, and on the thermal results so far obtained.

2. Development and application of the numerical technique

The purpose of this section is to show how, by the use of orthogonal polynomials, the solution of the governing equations (1.6) and (1.7) may be reduced to the numerical solution of two sets of coupled algebraic equations. For convenience in notation we convert the region of integration from that of a rectangle $x = 0, \alpha$ and $y = 0, 1$ to a square region of unit dimension by the substitutions

$$x = \alpha\xi, \qquad y = \eta; \tag{2.1}$$

also to standardize the boundary conditions on θ we introduce

$$\theta(\xi, \eta) = \eta + \Theta(\xi, \eta). \tag{2.2}$$

The governing equations (1.6) and (1.7) then become

$$\nabla_\alpha^2 \Theta = \frac{1}{\alpha^2}\frac{\partial^2\Theta}{\partial\xi^2} + \frac{\partial^2\Theta}{\partial\eta^2} = \frac{1}{\alpha}\left(\frac{\partial\Theta}{\partial\xi}\frac{\partial\psi}{\partial\eta} - \frac{\partial\Theta}{\partial\eta}\frac{\partial\psi}{\partial\xi} - \frac{\partial\psi}{\partial\xi}\right), \tag{2.3}$$

$$\nabla_\alpha^4 \psi = A\left(\cos\phi\frac{\partial\Theta}{\partial\eta} + \cos\phi - \frac{1}{\alpha}\sin\phi\frac{\partial\Theta}{\partial\xi}\right) + \frac{1}{\alpha\sigma}\left\{\frac{\partial}{\partial\xi}(\nabla_\alpha^2\psi)\frac{\partial\psi}{\partial\eta} - \frac{\partial}{\partial\eta}(\nabla_\alpha^2\psi)\frac{\partial\psi}{\partial\xi}\right\}. \tag{2.4}$$

The implied boundary conditions on ψ are

$$\psi = \frac{\partial\psi}{\partial\eta} = 0, \quad \text{at } \eta = 0, 1 \quad \text{for } 0 \leqslant \xi \leqslant 1,$$

$$\psi = \frac{\partial\psi}{\partial\xi} = 0, \quad \text{at } \xi = 0, 1 \quad \text{for } 0 \leqslant \eta \leqslant 1. \tag{2.5}$$

Furthermore, if we take the temperature distribution on the border strips to be linear, then

$$\Theta = 0 \quad \text{at } \eta = 0, 1 \quad \text{for } 0 \leqslant \xi \leqslant 1,$$

and

$$\text{at } \xi = 0, 1 \quad \text{for } 0 \leqslant \eta \leqslant 1 \text{ (Case I)}; \tag{2.6}$$

or if the border strips are perfect insulators, then

$$\Theta = 0 \quad \text{at } \eta = 0, 1 \quad \text{for } 0 \leqslant \xi \leqslant 1,$$

and

$$\frac{\partial\Theta}{\partial\xi} = 0 \quad \text{at } \xi = 0, 1 \quad \text{for } 0 \leqslant \eta \leqslant 1 \text{ (Case II)}. \tag{2.7}$$

Case I. Linear temperature distribution on the border strips

We assume that Θ and Ψ may be represented by the complete double series of orthogonal functions

$$\Theta = \sum_{p=1}^{\infty}\sum_{q=1}^{\infty} A_{p,q}\sin p\pi\xi \sin q\pi\eta \tag{2.8}$$

and

$$\psi = \sum_{p=1}^{\infty}\sum_{q=1}^{\infty} B_{p,q} X_p(\xi) X_q(\eta), \tag{2.9}$$

where the $A_{p,q}$ and $B_{p,q}$ are constants to be evaluated.

The double Fourier series expansion (2.8) satisfies the boundary conditions (2.6); also the expansion (2.9) satisfies the required boundary conditions (2.5), provided the functions $X_p(\xi)$ are chosen to satisfy the fourth order Sturm–Liouville equation

$$\frac{d^4X_p}{d\xi^4} = \mu_p^4 X_p \tag{2.10}$$

with $$X_p(0) = X_p(1) = X_p'(0) = X_p'(1) = 0,$$

and where a prime denotes differentiation with respect to ξ. The differential equation (2.10) is the well-known equation determining the modes of vibration of a uniform beam clamped at both ends. The appropriate eigenfunctions may be given in the form

$$X_p(\xi) = (\cosh\mu_p\xi - \cos\mu_p\xi) - \beta_p(\sinh\mu_p\xi - \sin\mu_p\xi), \tag{2.11}$$

if the eigenvalues μ_p satisfy the transcendental equation

$$\cosh\mu_p\cos\mu_p - 1 = 0,$$

and $$\beta_p = (\cosh\mu_p - \cos\mu_p)/(\sinh\mu_p - \sin\mu_p).\dagger \tag{2.12}$$

Furthermore the functions X_p are orthogonal in the range of integration $(0, 1)$, thus

$$\int_0^1 X_p(\xi)X_q(\xi)\,d\xi = \delta_{p,q} \tag{2.13}$$

where $\delta_{p,q}$ is the Kronecker delta.

We now seek the solution of (2.3) in the assumed form (2.8) where the Fourier coefficients are

$$A_{m,n} = 4\int_0^1\int_0^1 \Theta(\xi,\eta)\sin m\pi\xi\sin n\pi\eta\,d\xi d\eta \tag{2.14}$$

for $m, n = 1, 2, 3,...$, etc. On integration by parts and using the imposed boundary conditions on Θ, we have

$$\begin{aligned} A_{m,n} &= \frac{4}{m\pi}\int_0^1\int_0^1 \frac{\partial\Theta}{\partial\xi}\cos m\pi\xi\sin n\pi\eta\,d\xi d\eta = \frac{4}{n\pi}\int_0^1\int_0^1 \frac{\partial\Theta}{\partial\eta}\sin m\pi\xi\cos n\pi\eta\,d\xi d\eta \\ &= -\frac{4}{(m\pi)^2}\int_0^1\int_0^1 \frac{\partial^2\Theta}{\partial\xi^2}\sin m\pi\xi\sin n\pi\eta\,d\xi d\eta \\ &= -\frac{4}{(n\pi)^2}\int_0^1\int_0^1 \frac{\partial^2\Theta}{\partial\eta^2}\sin m\pi\xi\sin n\pi\eta\,d\xi d\eta. \end{aligned} \tag{2.15}$$

† The values of μ_p and β_p have been tabulated by Young (5), also the integral

$$\int_0^1 X_p'(\xi)X_q'(\xi)\,d\xi.$$

The functions $X_p(\xi)$ for $p = 1(1)6$ at $\xi = 0{\cdot}0(0{\cdot}05)0{\cdot}5$ have been tabulated by Inglis (6) and Corlett (7).

It then follows from (2.15) that on the left-hand side of the governing equation (2.3)

$$\nabla_\alpha^2 \Theta = -\sum_{p=1}^{\infty}\sum_{q=1}^{\infty} \pi^2\left(\frac{p^2}{\alpha^2}+q^2\right)A_{p,q}\sin p\pi\xi \sin q\pi\eta, \tag{2.16}$$

and on the right-hand side

$$\frac{1}{\alpha}\left(\frac{\partial\Theta}{\partial\xi}\frac{\partial\psi}{\partial\eta}-\frac{\partial\Theta}{\partial\eta}\frac{\partial\psi}{\partial\xi}-\frac{\partial\psi}{\partial\xi}\right)$$

$$=\frac{1}{\alpha}\left[-\frac{\partial\psi}{\partial\xi}+\sum_{p=1}^{\infty}\sum_{q=1}^{\infty}A_{p,q}\left(p\pi\cos p\pi\xi\sin q\pi\eta\frac{\partial\psi}{\partial\eta}-q\pi\sin p\pi\xi\cos q\pi\eta\frac{\partial\psi}{\partial\xi}\right)\right]. \tag{2.17}$$

In the usual manner if the double Fourier sine series (2.16) is equal to (2.17), then the Fourier transforms of the two sides must be equal. Hence by multiplying both sides of the equation by $4\sin m\pi\xi\sin n\pi\eta$ and integrating over the region $\xi = 0, 1$ and $\eta = 0, 1$ we obtain an infinite set of algebraic equations in $A_{m,n}$. Thus for $m, n = 1, 2, 3,...,$

$$\left(\frac{m^2}{\alpha^2}+n^2\right)A_{m,n} = \frac{4}{\alpha\pi^2}\int_0^1\int_0^1 \frac{\partial\psi}{\partial\xi}\sin m\pi\xi\sin n\pi\eta\, d\xi d\eta$$

$$-\frac{4}{\alpha\pi}\sum_{p=1}^{\infty}\sum_{q=1}^{\infty}A_{p,q}\int_0^1\int_0^1\left(p\cos p\pi\xi\sin q\pi\eta\frac{\partial\psi}{\partial\eta}-\right.$$

$$\left.-q\sin p\pi\xi\cos q\pi\eta\frac{\partial\psi}{\partial\xi}\right)\sin m\pi\xi\sin n\pi\eta\, d\xi d\eta. \tag{2.18}$$

It remains now to find suitable expressions for the partial derivatives $\partial\psi/\partial\xi$ and $\partial\psi/\partial\eta$. Suppose we expand $\partial\psi/\partial\xi$ as follows:

$$\frac{\partial\psi}{\partial\xi} = \sum_{m=1}^{\infty}\sum_{n=1}^{\infty} b_{m,n}X_m(\xi)X_n(\eta), \tag{2.19}$$

then

$$b_{m,n} = \int_0^1\int_0^1 \frac{\partial\psi}{\partial\xi}X_m(\xi)X_n(\eta)\, d\xi d\eta.$$

On integration by parts and using the boundary conditions (2.5) we find

$$b_{m,n} = -\int_0^1\int_0^1 \psi X_m'(\xi)X_n(\eta)\, d\xi d\eta$$

$$= -\sum_{p=1}^{\infty}\sum_{q=1}^{\infty}B_{p,q}\int_0^1 X_p(\xi)X_m'(\xi)\, d\xi\int_0^1 X_q(\eta)X_n(\eta)\, d\eta$$

$$= -\sum_{p=1}^{\infty}B_{p,n}\int_0^1 X_p(\xi)X_m'(\xi)\, d\xi = \sum_{p=1}^{\infty}B_{p,n}\int_0^1 X_p'(\xi)X_m(\xi)\, d\xi.$$

Thus on substituting in (2.19) we have

$$\frac{\partial\psi}{\partial\xi}=\sum_{m=1}^{\infty}\sum_{n=1}^{\infty}\Big(\sum_{p=1}^{\infty}B_{p,n}\int_0^1 X_p'(\xi)X_m(\xi)\,d\xi\Big)X_m(\xi)X_n(\eta)$$

which on rearrangement gives

$$\begin{aligned}\frac{\partial\psi}{\partial\xi}&=\sum_{p=1}^{\infty}\sum_{n=1}^{\infty}B_{p,n}X_n(\eta)\Big(\sum_{m=1}^{\infty}X_m(\xi)\int_0^1 X_p'(\xi)X_m(\xi)\,d\xi\Big)\\&=\sum_{p=1}^{\infty}\sum_{n=1}^{\infty}B_{p,n}X_p'(\xi)X_n(\eta).\end{aligned}\tag{2.20}$$

Hence term by term differentiation of (2.9) to obtain $\partial\psi/\partial\xi$ and $\partial\psi/\partial\eta$ is justified. Finally substituting (2.20) in (2.18) we find

$$\Big(\frac{1}{\alpha^2}m^2+n^2\Big)A_{m,n}=\frac{1}{\alpha\pi^2}\sum_{r=1}^{\infty}\sum_{s=1}^{\infty}B_{r,s}(a_n^s b_m^r)+\gamma_{m,n},\tag{2.21}$$

where

$$\gamma_{m,n}=-\frac{1}{4\alpha}\sum_{p=1}^{\infty}\sum_{q=1}^{\infty}A_{p,q}\Big[\sum_{r=1}^{\infty}\sum_{s=1}^{\infty}B_{r,s}\{pR(r,p,m)T(s,q,n)-qR(s,q,n)T(r,p,m)\}\Big].\tag{2.22}$$

Definitions and formulae for evaluation of the integrals a_n^s, b_m^r, $R(r,p,m)$ and $T(s,q,n)$ are given in Appendix A.

By a similar procedure to that outlined in obtaining the result (2.20) from (2.9), it can be verified that the remaining partial derivatives occurring in equation (2.4) may be obtained by term-by-term differentiation of the series (2.9). On making use of the properties of the basic functions X_p the partial differential equation (2.4), defining ψ, may be reduced to the numerical solution of a set of algebraic equations in $B_{m,n}$ by the technique employed in treatment of (2.3). Thus for $m, n = 1, 2, 3,\ldots,$

$$\begin{aligned}&\Big(\frac{1}{\alpha^4}\mu_m^4+\frac{2}{\alpha^2}D_{m,m}D_{n,n}+\mu_n^4\Big)B_{m,n}\\&\quad=AC_mC_n\cos\phi-\frac{A}{4}\sum_{p=1}^{\infty}\sum_{q=1}^{\infty}A_{p,q}\Big(a_p^m b_q^n\cos\phi-\frac{1}{\alpha}a_q^n b_p^m\sin\phi\Big)-\\&\qquad\frac{2}{\alpha^2}\sum_{p=1}^{\infty}\sum_{q=1}^{\infty}{}'B_{p,q}D_{p,m}D_{q,n}+\lambda_{m,n},\end{aligned}\tag{2.23}$$

where

$$\begin{aligned}\lambda_{m,n}=\frac{1}{\alpha\sigma}\sum_{p=1}^{\infty}\sum_{q=1}^{\infty}B_{p,q}\Big[\sum_{r=1}^{\infty}\sum_{s=1}^{\infty}B_{r,s}\Big(&\frac{1}{\alpha^3}K(p,r,m)L(s,q,n)+\\&+\frac{1}{\alpha}H(q,s,n)L(p,r,m)-\frac{1}{\alpha^3}H(p,r,m)L(q,s,n)-\\&-\frac{1}{\alpha}H(q,s,n)L(r,p,m)\Big)\Big]\end{aligned}\tag{2.24}$$

and the prime denotes that the (m, n)th term of the double summation has been taken over to the left-hand side of the equation. Definitions and formulae for evaluation of the integrals $D_{p,m}$, C_m, $K(p, r, m)$, $L(p, r, m)$, and $H(p, r, m)$ are given in Appendix A.

TABLE 1

Values of the $A_{m,n}$ coefficients for linear temperature distribution on the border strips, and $\alpha = 1$, $\sigma = 0{\cdot}73$, $\phi = 0$

A	5×10^2	10^3	$2{\cdot}5\times10^3$	5×10^3	10^4
$A_{1,2}$	0·003,747	0·013 55	0·057,08	0·117,3	0·187,5
$A_{2,1}$	0·035,20	0·065,34	0·126,9	0·167,0	0·187,4
$A_{1,4}$	−0·000,238	−0·001,39	−0·003,73	−0·004,9	−0·001,9
$A_{2,3}$	−0·001,55	−0·006,45	−0·008,23	−0·008,0	−0·006,3
$A_{3,2}$	−0·000,102	0·000,42	0·001,61	0·004,4	0·010,7
$A_{4,1}$	0·002,22	0·005,18	0·011,80	0·021,5	0·031,4
$A_{1,6}$	−0·000,027	−0·000,10	−0·000,44	−0·001,0	−0·001,7
$A_{2,5}$	−0·000,24	−0·000,49	−0·001,49	−0·002,7	−0·002,6
$A_{3,4}$	−0·000,017	−0·000,05	0·000,07	0·000,2	0·000,4
$A_{4,3}$	−0·000,13	−0·000,31	−0·000,81	−0·001,6	−0·001,6
$A_{5,2}$	−0·000,011	−0·000,24	−0·000,35	−0·000,8	−0·001,7
$A_{6,1}$	0·000,34	0·000,67	0·001,83	0·003,9	0·007,1
$A_{1,8}$		−0·000,02	−0·000,11	−0·000,4	−0·000,9
$A_{2,7}$		−0·000,09	−0·000,33	−0·000,8	−0·001,8
$A_{3,6}$		−0·000,03	−0·000,18	−0·000,6	−0·000,8
$A_{4,5}$		−0·000,13	−0·000,26	−0·000,6	−0·000,7
$A_{5,4}$		−0·000,06	0·000,04	0·000,1	0·000,3
$A_{6,3}$		0·000,05	−0·000,22	−0·000,4	−0·000,6
$A_{7,2}$		−0·000,03	−0·000,13	−0·000,5	−0·000,8
$A_{8,1}$		0·000,13	0·000,35	0·000,8	0·001,8
$A_{1,10}$					−0·000,1
$A_{2,9}$					−0·000,4
$A_{3,8}$					−0·000,3
$A_{4,7}$					−0·000,3
$A_{5,6}$					0·000,2
$A_{6,5}$					−0·000,1
$A_{7,4}$					−0·000,1
$A_{8,3}$					−0·000,3
$A_{9,2}$					−0·000,3
$A_{10,1}$					0·000,6

The coupled simultaneous algebraic equations (2.21) and (2.23) may be solved to any desired degree of accuracy by using an iterative procedure. The computational procedure adopted for solving these equations when $\alpha = 1$, $\phi = 0$, $\sigma = 0{\cdot}73$, and $A = 5\times10^2$, 10^3, $2{\cdot}5\times10^3$, 5×10^3, and 10^4 is described in Appendix B. Note that in these solutions it follows from symmetry considerations of the basic equations (2.3) and (2.4), that the $A_{m,n}$ can only occur when $m+n$ is odd and $A_{m,n} = 0$ when $m+n$ is even. Furthermore the $B_{m,n}$ can only occur when $m+n$ is even. In Tables 1 and 2

the calculated $A_{m,n}$ and $B_{m,n}$ coefficients are given. It is believed that the last figure quoted may be in error by not more than a few units.

Case II. Border strips being perfect insulators

This case may be treated in exactly the same way as in Case I. We seek solutions of the form

$$\Theta = \sum_{p=0}^{\infty} \sum_{q=1}^{\infty} A_{p,q} \cos p\pi\xi \sin q\pi\eta$$

and

$$\psi = \sum_{p=1}^{\infty} \sum_{q=1}^{\infty} B_{p,q} X_p(\xi) X_q(\eta),$$

TABLE 2

Values of the $B_{m,n}$ coefficients for linear temperature distribution on the border strips, and $\alpha = 1$, $\sigma = 0{\cdot}73$, $\phi = 0$

A	5×10^2	10^3	$2{\cdot}5\times10^3$	5×10^3	10^4
$B_{1,1}$	0·267,1	0·519,3	1·159,9	1·919,1	2·885,6
$B_{1,3}$	0·012,6	0·028,6	0·074,4	0·187,4	0·406,7
$B_{2,2}$	0·001,9	0·008,0	0·031,8	0·059,1	0·051,5
$B_{3,1}$	0·012,2	0·027,2	0·061,1	0·118,0	0·200,4
$B_{1,5}$	0·001,6	0·003,6	0·012,6	0·035,5	0·091,3
$B_{2,4}$	0·000,5	0·001,8	0·008,6	0·021,6	0·040,4
$B_{3,3}$	0·001,2	0·002,4	0·006,0	0·011,9	0·025,5
$B_{4,2}$	−0·000,1	−0·000,4	−0·002,3	−0·005,4	−0·009,6
$B_{5,1}$	0·001,6	0·003,2	0·008,4	0·018,5	0·035,5
$B_{1,7}$	0·000,4	0·000,7	0·002,0	0·004,7	0·010,6
$B_{2,6}$	0·000,1	0·000,2	0·001,6	0·004,6	0·011,3
$B_{3,5}$	0·000,2	0·001,0	0·000,3	−0·000,8	−0·003,8
$B_{4,4}$	0·000,0	0·000,1	0·000,4	0·001,0	0·003,4
$B_{5,3}$	0·000,2	0·001,0	0·001,4	0·002,8	0·006,6
$B_{6,2}$	0·000,0	−0·000,1	−0·000,3	−0·000,8	−0·002,0
$B_{7,1}$	0·000,4	0·000,9	0·001,7	0·003,2	0·005,8
$B_{1,9}$					0·003,4
$B_{2,8}$					0·001,8
$B_{3,7}$					0·002,2
$B_{7,3}$					0·002,2
$B_{8,2}$					−0·000,2
$B_{9,1}$					0·001,8

which satisfy the boundary conditions (2.5) and (2.7). Using the appropriate transforms a set of simultaneous algebraic equations defining the $A_{p,q}$ and $B_{p,q}$ which are similar to (2.21) and (2.23) may be obtained. Since this case is not investigated numerically in the present paper, the actual equations will not be given. However, the integrals to be evaluated are either those already defined in Appendix A or may be obtained from them on integration by parts.

So far in this section no rigorous mathematical discussion has been given

on the validity and convergence of the expansions (2.8) and (2.9). The method can only be considered as approximate since the infinite double expansions have been taken as finite, although sufficient coefficients have been computed in each case to ensure that there is no change in the leading terms. Such proofs of validity and convergence are beyond the scope of the paper. However, it was thought desirable to check by an independent numerical method at least one of the solutions obtained in the present paper. Obviously the standard relaxation method is the only available means. From Tables 1 and 2 the functions Θ and ψ have been evaluated when $A = 10^4$, at the nodal points ξ, $\eta = 0{\cdot}0(0{\cdot}05)0{\cdot}3$ for $\xi+\eta \leqslant 0{\cdot}3$. Hence by standard relaxation methods if Θ and ψ are the correct numerical approximations to the solutions of (2.3) and (2.4), then the residuals at the above nodes must be identically zero, or of such a magnitude that when relaxed to zero the changes in the wanted functions are negligible.† (See Allen (**8**).) It was found that the calculated residuals (using mesh length equal to 0·05) although being non-zero altered Θ by less than 0·2 per cent and ψ by less than 0·4 per cent, when relaxed to zero. Spot checks were also applied in the region of ξ, $\eta = 0{\cdot}5$ and here the residuals were identically zero.

3. Thermal results

From Table 1 we can now calculate, for a range of Rayleigh numbers, the rate of heat transmission across a cavity having square cross-section, vertical hot and cold walls, and a linear temperature distribution on the horizontal walls or the border strips. As defined in equation (1.8), a dimensionless quantity describing the heat transfer is the Nusselt number

$$N = \int_0^\alpha \left(\frac{\partial\theta}{\partial y}\right)_{y=0} dx$$

and on using (2.1), (2.2), and (2.8) we obtain

$$N = \alpha \int_0^1 \left\{1+\left(\frac{\partial\Theta}{\partial\eta}\right)_{\eta=0}\right\} d\xi = \alpha\left(1+4\sum_{p=0}^{\infty}\sum_{q=1}^{\infty}\frac{q}{2p+1}A_{2p+1,2q}\right). \quad (3.1)$$

In Table 3 the calculated values of N are given. These values of N have been plotted against $G^{\frac{1}{4}}$ in Fig. 2.

Considering first values of A less than 10^3, we find from Table 3 that

$$N = 1+5{\cdot}08\times10^{-8}A^2, \quad (3.2)$$

which is in agreement with Batchelor's prediction (1.10), where the con-

† Note the above statement is correct only if the mesh length is small enough for the relaxation solution to converge to a solution of desired accuracy.

stant of proportionality was given to be very roughly of the order 10^{-8}. For $A > 10^3$ the Nusselt number rises rapidly in numerical magnitude until in the region $A \sim 10^4$, N varies linearly as $G^{\frac{1}{4}}$ as in Fig. 2. When $A = 10^4$ ordinary conduction across the cavity accounts for 59 per cent of the total heat transfer and free convection by laminar flow for the remaining 41 per cent. Using the calculated values of N we obtain

$$N = 0{\cdot}16(A/\sigma)^{\frac{1}{4}} \quad \text{for } A \sim 10^4. \tag{3.3}$$

TABLE 3

Calculated values of the Nusselt number N

A	5×10^2	10^3	$2{\cdot}5\times10^3$	5×10^3	10^4
$G^{\frac{1}{4}}$	5·116	6·084	7·649	9·097	10·818
N	$1{\cdot}012_6$	$1{\cdot}041_8$	$1{\cdot}19_2$	$1{\cdot}41_5$	$1{\cdot}70_6$

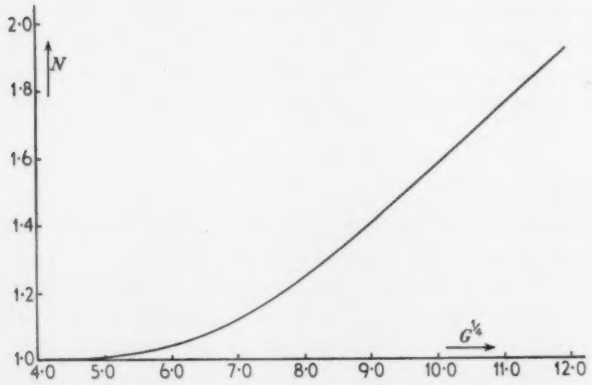

FIG. 2. Variation of heat transfer with Grashof number

From the limited experimental data of Mull and Reiher (1), Jakob suggests that for high aspect ratios N may be represented by the empirical formulae

$$N = 0{\cdot}18(A/\sigma)^{\frac{1}{4}}\alpha^{-8/9} \quad (10^4 < A < 10^5). \tag{3.4}$$

It is questionable how far beyond the range of the experimental data (3.4) is valid, and in particular what is the smallest value of α to be used. Obviously not as far down as $\alpha = 0$ when it would yield an infinite Nusselt number. However, (3.3) and (3.4) are in favourable agreement when $\alpha = 1$ and it seems probable that (3.4) may be valid for $\alpha > 1$.

In Figs. 3 and 4 isothermals and streamlines have been drawn for $A = 10^4$. At this value of A it is apparent that an isothermal core exists in the cavity having uniform temperature $\theta = \frac{1}{2}$, also constant vorticity which was verified numerically. In the region between the core and the cavity walls,

where there exists a continuous boundary layer, θ and ψ oscillate once near the core and then tend smoothly to their appropriate values at the cavity walls. The existence of an isothermal core was postulated by Batchelor (3) in obtaining the equations describing the flow in the continuous boundary layer.

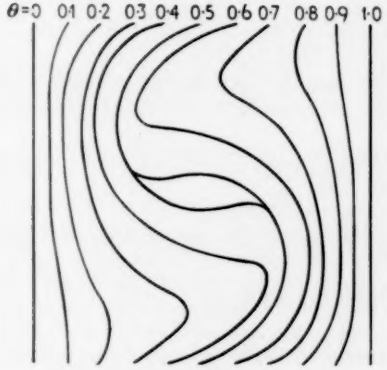

FIG. 3. Isothermals for $A = 10^4$

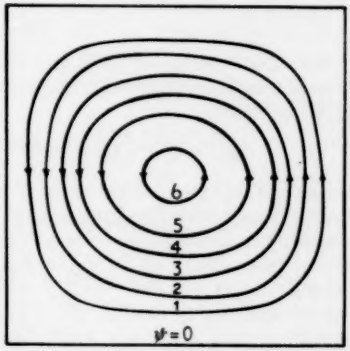

FIG. 4. Streamlines for $A = 10^4$

4. Conclusions

(a) *Numerical technique*

In section 2 of this paper a method is developed for obtaining solutions of the two-dimensional governing equations in the form of approximate double expansions involving orthogonal polynomials. By means of the appropriate transforms the governing equations are reduced to the solution of two sets of coupled simultaneous algebraic equations. It was found that the main computational labour involved was not in solving these simultaneous equations, but in obtaining them. Obviously if only one solution of the governing equations was required the labour involved would be a serious consideration. In this respect the method given is adaptable to the present problem since solutions are required for a range of values of the parameters A, ϕ, and α. It seems likely that the labour involved in obtaining solutions by the present method for $A > 10^4$ and $\alpha > 4$ would be prohibitive.

(b) *Thermal results*

Preliminary thermal results have been obtained for air enclosed in a cavity having square cross-section. The vertical walls are held at different temperatures T_0 and T_1 ($T_1 > T_0$), and the temperature along the horizontal walls is taken to vary linearly from T_0 to T_1. These results indicate that for $A < 10^3$, $N-1$ varies as A^2, with constant of proportionality $5{\cdot}08 \times 10^{-8}$;

for $A \sim 10^4$, N varies as $(A/\sigma)^{\frac{1}{4}}$, with constant of proportionality 0·16 (which is in favourable agreement with the empirical value 0·18 given by Jakob (**2**)). Finally, when $A = 10^4$ an isothermal core exists in the cavity. The vorticity in the core has been verified to be constant. In the region between the core and the cavity walls there is a continuous boundary layer.

APPENDIX A

For completeness we shall give here definitions and formulae for evaluation of certain integrals occurring in section 2. For the integrals occurring in (2.21) and (2.22) we have

$$a_n^s = 2\int_0^1 X_s(\xi)\sin n\pi\xi\, d\xi = \frac{2n\pi}{(n\pi)^4-\mu_s^4}\{X_s''(1)(-1)^n - X_s''(0)\}, \tag{A1}$$

$$b_m^r = 2\int_0^1 X_r'(\eta)\sin m\pi\eta\, d\eta = \frac{2m\pi}{(m\pi)^4-\mu_r^4}\{X_r'''(1)(-1)^m - X_r'''(0)\}, \tag{A2}$$

$$\begin{aligned} R(r,p,m) &= \int_0^1 X_r(\xi)\cos p\pi\xi \sin m\pi\xi\, d\xi \\ &= a_{m+p}^r + a_{m-p}^r, \quad \text{if } m > p \\ &= a_{m+p}^r - a_{p-m}^r, \quad \text{if } m < p, \end{aligned} \tag{A3}$$

and finally

$$\begin{aligned} T(s,q,n) &= \int_0^1 X_s(\eta)\sin q\pi\eta \sin n\pi\eta\, d\eta \\ &= (q-n)a_{q-n}^s - (q+n)a_{q+n}^s, \quad \text{if } q > n \\ &= (n-q)a_{n-q}^s - (q+n)a_{q+n}^s, \quad \text{if } q < n. \end{aligned} \tag{A4}$$

Again with regard to (2.23) and (2.24) we have:

$$\begin{aligned} D_{m,n} &= \int_0^1 X_m'' X_n\, d\xi = -\int_0^1 X_m' X_n'\, d\xi \\ &= -\tfrac{1}{2}\sum_{r=1}^{\infty} b_r^m b_r^n, \quad \text{if } m+n \text{ is even} \\ &= 0, \qquad\qquad \text{if } m+n \text{ is odd.} \end{aligned} \tag{A5}$$

$$C_m = \int_0^1 X_m\, d\xi = \frac{1}{\mu_m^4}\{X_m'''(1) - X_m'''(0)\}, \tag{A6}$$

$$K(p,r,m) = \int_0^1 X_p''' X_r X_m\, d\xi = d_0^{r,m}\{X_p''(1) - X_p''(0)\} - \frac{\mu_p^4}{2}\sum_{n=1}^{\infty}\frac{1}{n\pi} d_n^{r,m} a_n^p, \tag{A7}$$

$$H(q,s,n) = \int_0^1 X_q'' X_s' X_n\, d\xi = \sum_{p=1}^{\infty}\frac{1}{p^2\pi^2} h_p^{s,n}\{X_q'''(-1)^p - X_q'''(0)\} + \frac{\mu_q^4}{2}\sum_{p=1}^{\infty}\frac{1}{p^3\pi^3} h_p^{s,n} l_p^q, \tag{A8}$$

and

$$L(s,q,n) = \int_0^1 X_q' X_s X_n\, d\xi = \sum_{p=1}^{\infty}\frac{1}{p^2\pi^2} d_p^{s,n}\{X_q''(1)(-1)^p - X_q''(0)\} + \frac{\mu_q^4}{2}\sum_{p=1}^{\infty}\frac{1}{p^3\pi^3} d_p^{s,n} a_p^q. \tag{A9}$$

In the above equations (A7)–(A9) the products $X_p(\xi)X_q(\xi)$ and $X_p'(\xi)X_q(\xi)$ have been

expanded as cosine series in the range $(0,1)$, obtaining $X_p X_q = \sum_{n=0}^{\infty} d_n^{p,q} \cos n\pi\xi$, $X_p' X_q = \sum_{n=0}^{\infty} h_n^{p,q} \cos n\pi\xi$, where

$$d_0^{p,q} = \int_0^1 X_p X_q \, d\xi = \delta_{p,q},$$

$$d_n^{p,q} = d_n^{q,p} = 2\int_0^1 X_p X_q \cos n\pi\xi \, d\xi = \tfrac{1}{2}\sum_{r=1}^{\infty} a_r^p (a_{|r-n|}^q - a_{r+n}^q) \quad \text{for } n = 1, 2, 3, \ldots,$$

$$h_0^{p,q} = \int_0^1 X_p' X_q \, d\xi = \tfrac{1}{2}\sum_{n=1}^{\infty} b_n^p a_n^q,$$

$$h_n^{p,q} = 2\int_0^1 X_p' X_q \cos n\pi\xi \, d\xi = \tfrac{1}{2}\sum_{r=1}^{\infty} b_r^p (a_{|r-n|}^q - a_{r+n}^q) \quad \text{for } n = 1, 2, 3, \ldots.$$

The above procedure of evaluation of the required integrals by the aid of Fourier series, and in particular the integrals in equations (A7), (A8), and (A9), whilst looking rather complicated is in fact much more rapid than the evaluation of formulae obtained using the form of $X_p(\xi)$ given by equation (2.11). The Fourier coefficients a_n^r and b_n^r were evaluated for $r = 1(1)9$ and $n = 1(1)60$. (Actually $a_n^r = 0$ except when $r+n$ is even, $b_n^r = 0$ except when $r+n$ is odd). The $d_n^{p,q}$ and $h_n^{p,q}$ are then readily obtained by evaluating the above single summations for $p, q = 1(1)9$, $p+q \leqslant 10$, and $n = 1(1)25$. This task completed, the integrals $K(p,r,m)$, $H(p,r,m)$, and $L(p,r,m)$ can then be obtained. The following relationships, obtained on integration by parts,

$$K(p,r,m) = -\{H(p,r,m)+H(p,m,r)\},$$

$$L(p,r,m) = -\{L(r,p,m)+L(m,p,r)\}$$

were found extremely useful in checking the computations. Tables of $K(p,r,m)$, $H(p,r,m)$, and $L(p,r,m)$ have been completed for $p = 1(1)9$, r, $m = 1(1)9$ for $r+m \leqslant 10$. The calculated double array (A5) agreed exactly with that given by Young (5).

APPENDIX B

The purpose of this appendix is to describe the computational process used in solving the coupled simultaneous algebraic equations (2.21) and (2.23) when $\alpha = 1$, $\phi = 0$ for various Rayleigh numbers. This process could be used, without modification, to treat other values of the parameters α and ϕ.

Some mention should first be made of the way in which an individual equation, say for A_{12}, is recorded. The first double summation on the right-hand side of (2.21) will involve, by virtue of the symmetry properties of the functions $X_r(\xi)$, the $B_{r,s}$ for $r, s = 2(2)8$, $r+s \leqslant 10$. A double array of the product $a_q^s b_1^r$ is then calculated from values already computed using equations (A1) and (A2). The quadruple summation γ_{12} is treated in a similar fashion. First when r and s are both even, taking $r, s = 2(2)8$, $r+s \leqslant 10$, double arrays for

$$pR(r,p,1)\,T(s,q,2) - qR(s,q,2)\,T(r,p,1) \tag{B1}$$

were evaluated using (A3) and (A4) for $p = 1(2)9$, $q = 2(2)8$, and $p+q \leqslant 10$. Secondly, when r and s are both odd (i.e. $r, s = 1(2)9$, $r+s \leqslant 10$) double arrays of (B1) were evaluated for $p = 2(2)8$ and $q = 1(2)9$. Thus given the values of the $A_{m,n}$

for $A \sim 10^4$, N varies as $(A/\sigma)^{\frac{1}{4}}$, with constant of proportionality 0·16 (which is in favourable agreement with the empirical value 0·18 given by Jakob (**2**)). Finally, when $A = 10^4$ an isothermal core exists in the cavity. The vorticity in the core has been verified to be constant. In the region between the core and the cavity walls there is a continuous boundary layer.

APPENDIX A

For completeness we shall give here definitions and formulae for evaluation of certain integrals occurring in section 2. For the integrals occurring in (2.21) and (2.22) we have

$$a_n^s = 2\int_0^1 X_s(\xi)\sin n\pi\xi\, d\xi = \frac{2n\pi}{(n\pi)^4-\mu_s^4}\{X_s''(1)(-1)^n - X_s''(0)\}, \tag{A1}$$

$$b_m^r = 2\int_0^1 X_r'(\eta)\sin m\pi\eta\, d\eta = \frac{2m\pi}{(m\pi)^4-\mu_r^4}\{X_r'''(1)(-1)^m - X_r'''(0)\}, \tag{A2}$$

$$\begin{aligned} R(r,p,m) &= \int_0^1 X_r(\xi)\cos p\pi\xi \sin m\pi\xi\, d\xi \\ &= a_{m+p}^r + a_{m-p}^r, \quad \text{if } m > p \\ &= a_{m+p}^r - a_{p-m}^r, \quad \text{if } m < p, \end{aligned} \tag{A3}$$

and finally

$$\begin{aligned} T(s,q,n) &= \int_0^1 X_s(\eta)\sin q\pi\eta \sin n\pi\eta\, d\eta \\ &= (q-n)a_{q-n}^s - (q+n)a_{q+n}^s, \quad \text{if } q > n \\ &= (n-q)a_{n-q}^s - (q+n)a_{q+n}^s, \quad \text{if } q < n. \end{aligned} \tag{A4}$$

Again with regard to (2.23) and (2.24) we have:

$$\begin{aligned} D_{m,n} &= \int_0^1 X_m'' X_n\, d\xi = -\int_0^1 X_m' X_n'\, d\xi \\ &= -\tfrac{1}{2}\sum_{r=1}^{\infty} b_r^m b_r^n, \quad \text{if } m+n \text{ is even} \\ &= 0, \qquad\qquad \text{if } m+n \text{ is odd.} \end{aligned} \tag{A5}$$

$$C_m = \int_0^1 X_m\, d\xi = \frac{1}{\mu_m^4}\{X_m'''(1) - X_m'''(0)\}, \tag{A6}$$

$$K(p,r,m) = \int_0^1 X_p''' X_r X_m\, d\xi = d_0^{r,m}\{X_p''(1) - X_p''(0)\} - \frac{\mu_p^4}{2}\sum_{n=1}^{\infty}\frac{1}{n\pi} d_n^{r,m} a_n^p, \tag{A7}$$

$$H(q,s,n) = \int_0^1 X_q'' X_s' X_n\, d\xi = \sum_{p=1}^{\infty}\frac{1}{p^2\pi^2} h_p^{s,n}\{X_q'''(-1)^p - X_q'''(0)\} + \frac{\mu_q^4}{2}\sum_{p=1}^{\infty}\frac{1}{p^3\pi^3} h_p^{s,n} l_p^q, \tag{A8}$$

and

$$L(s,q,n) = \int_0^1 X_q' X_s X_n\, d\xi = \sum_{p=1}^{\infty}\frac{1}{p^2\pi^2} d_p^{s,n}\{X_q''(1)(-1)^p - X_q''(0)\} + \frac{\mu_q^4}{2}\sum_{p=1}^{\infty}\frac{1}{p^3\pi^3} d_p^{s,n} a_p^q. \tag{A9}$$

In the above equations (A7)–(A9) the products $X_p(\xi)X_q(\xi)$ and $X_p'(\xi)X_q(\xi)$ have been

expanded as cosine series in the range (0, 1), obtaining $X_p X_q = \sum_{n=0}^{\infty} d_n^{p,q} \cos n\pi\xi$, $X_p' X_q = \sum_{n=0}^{\infty} h_n^{p,q} \cos n\pi\xi$, where

$$d_0^{p,q} = \int_0^1 X_p X_q \, d\xi = \delta_{p,q},$$

$$d_n^{p,q} = d_n^{q,p} = 2\int_0^1 X_p X_q \cos n\pi\xi \, d\xi = \tfrac{1}{2}\sum_{r=1}^{\infty} a_r^p (a_{|r-n|}^q - a_{r+n}^q) \quad \text{for } n = 1, 2, 3, \ldots,$$

$$h_0^{p,q} = \int_0^1 X_p' X_q \, d\xi = \tfrac{1}{2}\sum_{n=1}^{\infty} b_n^p a_n^q,$$

$$h_n^{p,q} = 2\int_0^1 X_p' X_q \cos n\pi\xi \, d\xi = \tfrac{1}{2}\sum_{r=1}^{\infty} b_r^p (a_{|r-n|}^q - a_{r+n}^q) \quad \text{for } n = 1, 2, 3, \ldots.$$

The above procedure of evaluation of the required integrals by the aid of Fourier series, and in particular the integrals in equations (A7), (A8), and (A9), whilst looking rather complicated is in fact much more rapid than the evaluation of formulae obtained using the form of $X_p(\xi)$ given by equation (2.11). The Fourier coefficients a_n^r and b_n^r were evaluated for $r = 1(1)9$ and $n = 1(1)60$. (Actually $a_n^r = 0$ except when $r+n$ is even, $b_n^r = 0$ except when $r+n$ is odd). The $d_n^{p,q}$ and $h_n^{p,q}$ are then readily obtained by evaluating the above single summations for $p, q = 1(1)9$, $p+q \leqslant 10$, and $n = 1(1)25$. This task completed, the integrals $K(p,r,m)$, $H(p,r,m)$, and $L(p,r,m)$ can then be obtained. The following relationships, obtained on integration by parts,

$$K(p,r,m) = -\{H(p,r,m)+H(p,m,r)\},$$

$$L(p,r,m) = -\{L(r,p,m)+L(m,p,r)\}$$

were found extremely useful in checking the computations. Tables of $K(p,r,m)$, $H(p,r,m)$, and $L(p,r,m)$ have been completed for $p = 1(1)9$, r, $m = 1(1)9$ for $r+m \leqslant 10$. The calculated double array (A5) agreed exactly with that given by Young (5).

APPENDIX B

The purpose of this appendix is to describe the computational process used in solving the coupled simultaneous algebraic equations (2.21) and (2.23) when $\alpha = 1$, $\phi = 0$ for various Rayleigh numbers. This process could be used, without modification, to treat other values of the parameters α and ϕ.

Some mention should first be made of the way in which an individual equation, say for A_{12}, is recorded. The first double summation on the right-hand side of (2.21) will involve, by virtue of the symmetry properties of the functions $X_r(\xi)$, the $B_{r,s}$ for $r, s = 2(2)8$, $r+s \leqslant 10$. A double array of the product $a_2^s b_1^r$ is then calculated from values already computed using equations (A1) and (A2). The quadruple summation γ_{12} is treated in a similar fashion. First when r and s are both even, taking $r, s = 2(2)8$, $r+s \leqslant 10$, double arrays for

$$pR(r,p,1)\,T(s,q,2) - qR(s,q,2)\,T(r,p,1) \tag{B1}$$

were evaluated using (A3) and (A4) for $p = 1(2)9$, $q = 2(2)8$, and $p+q \leqslant 10$. Secondly, when r and s are both odd (i.e. $r, s = 1(2)9$, $r+s \leqslant 10$) double arrays of (B1) were evaluated for $p = 2(2)8$ and $q = 1(2)9$. Thus given the values of the $A_{m,n}$

and $B_{m,n}$ a new estimate of $A_{1,2}$ may be obtained using equation (2.21). The first double summation involving the $B_{r,s}$ coefficients may be readily obtained. The quadruple summation $\gamma_{1,2}$ is written as

$$\gamma_{1,2} = -\frac{1}{4\alpha}\sum_{p=1}^{\infty}\sum_{q=1}^{\infty} A_{p,q}\gamma(1,2;p,q), \tag{B2}$$

where

$$\gamma(1,2;p,q) = \sum_{r=1}^{\infty}\sum_{s=1}^{\infty} B_{r,s}\{pR(r,p,1)T(s,q,2) - qR(s,q,2)T(r,p,1)\}.$$

From the double arrays (B1) calculated for $p = 1(2)9$, $q = 2(2)8$, and $p+q \leqslant 10$ we can then calculate the required $\gamma(1,2;p,q)$ by performing double summations over the $B_{r,s}$. Finally, by means of a double summation over the $A_{p,q}$ and the $\gamma(1,2;p,q)$ as in (B2), $\gamma_{1,2}$ is obtained.

The iterative procedure adopted for the solution of (2.21) and (2.23) was as follows. Initial estimates of the $B_{m,n}$ for m, $n = 1(2)9$, $m+n \leqslant 10$, were obtained using the equation

$$\left(\frac{1}{\alpha^4}\mu_m^4 + \frac{2}{\alpha^2}D_{m,m}D_{n,n} + \mu_n^4\right)B_{m,n} = AC_mC_n - \frac{2}{\alpha^3}\sum_{p=1}^{\infty}\sum_{q=1}^{\infty}{}' B_{p,q}D_{p,m}D_{q,n},$$

the quadruple summations $\gamma_{m,n}$ being neglected at this stage as they are small compared with the term involving the double summation in $A_{m,n}$, about which at this stage we have no information. Returning to equation (2.21) we can now calculate the $A_{m,n}$ for m even and n odd, using

$$\left(\frac{1}{\alpha^2}m^2 + n^2\right)A_{m,n} = \frac{1}{\alpha\pi^2}\sum_{r=1}^{\infty}\sum_{s=1}^{\infty} B_{r,s}(a_n^s b_m^r)$$

since $\gamma_{m,n} = 0$. Values of

$$\sum_{p=1}^{\infty}\sum_{q=1}^{\infty}\left(A_{p,q}\cos\phi\, a_p^m b_q^n - \frac{1}{\alpha}\sin\phi\, a_q^n b_p^m\right)$$

can now be calculated for m and n even and so we obtain the first estimates of $B_{m,n}$ for m and n even. A fairly accurate set of $B_{m,n}$ now exist and from these the $\gamma_{m,n}$ may be obtained giving a complete set of the $A_{m,n}$; $\lambda_{m,n}$ is then computed and then the current set of $B_{m,n}$. Fortunately after a few complete iterations, the values of the quadruple summations $\gamma_{m,n}$ and $\lambda_{m,n}$ remain steady and the main labour involved in each iterative step lies in controlling the sensitive relationship between the main $B_{m,n}$ and $A_{m,n}$ coefficients. The higher the value of A the more serious is the situation. This difficulty was resolved by setting up new equations for the $A_{m,n}$ (taking $m+n = 3$ and 5) and $B_{m,n}$ (taking $m+n = 2$, 4, and 6) which involved only the coefficients indicated, the remaining coefficients having been added in numerically as these achieve their final values at an early stage in the iteration. It was then much easier to control those few coefficients which oscillated about their true values. However, even in the case $A = 10^4$, no more than five complete iterative steps were required.

Acknowledgements

The author is indebted to Miss C. R. Faithfull and Miss E. J. Watkins for their invaluable assistance in the numerical work which occurred in this paper.

REFERENCES

1. W. Mull and H. Reiher, *Gesundh.-Ing. Beihefte*, Reihe 1, No. 28, 1930.
2. M. Jakob, *Heat Transfer*, vol. 1, chap. 25 (Wiley, 1949).
3. G. K. Batchelor, *Quart. App. Math.* 12 (1954), 209–33.
4. S. Goldstein (editor), *Modern Developments in Fluid Dynamics*, vol. 2, chap. 14 (Oxford, 1938).
5. D. Young, *J. App. Mech.* 17 (1950), 448–53.
6. C. E. Inglis, *N.E.C. Inst.* 61 (1944), 111–36.
7. E. C. B. Corlett, ibid. 66 (1949), 51–80.
8. D. N. de G. Allen, *Relaxation Methods* (McGraw-Hill, 1954).

THREE-DIMENSIONAL STEADY, RADIAL FLOW OF VISCOUS, HEAT-CONDUCTING, COMPRESSIBLE FLUID

By AKIRA SAKURAI (*Department of Applied Mathematics, The Weizmann Institute of Science, Israel*†)

[Received 1 August 1957]

SUMMARY

The case of flow at large Reynolds number is investigated, special attention being paid to the problem of finding deviations from the well-known inviscid flow. The fundamental equations in this case are reduced to a single second-order differential equation of the singular perturbation type, which is quite similar to the corresponding equation obtained in the case of two-dimensional radial flow. Utilizing this similarity and the knowledge obtained from the solution of the two-dimensional case as a guide, the solutions which contain shock waves are studied in detail.

1. Introduction

THE purpose of the present paper is to investigate the solution of the Navier–Stokes equations in the case of steady, three-dimensional, radial flow of both source and sink types, taking into account the effects of compressibility, viscosity, and heat conduction. This problem in the absence of viscosity and heat conduction (inviscid problem) is one of the few examples whose exact solutions are known and expressed in simple closed form. Thus it is of special interest to find the deviation from the inviscid solution due to the effects of viscosity and heat conduction.

The same kind of problem has been discussed in the corresponding case of two-dimensional radial flow. The present author (**1**) reduced the problem to a differential equation of the first order for source flow and solved it for a certain Reynolds number. Levey (**2**) investigated the equation in detail and proved the existence of shock waves in a class of flows at large Reynolds numbers. The case of sink type flow was considered by Wu (**3**). He expressed a solution in an analytical form at large Reynolds numbers using Lighthill's method. Prosnak (**4**) investigated the problem for both cases of source and sink flows from a different point of view in order to find the separate effect of either viscosity or heat conduction alone.

Under the assumption of large Reynolds number, the system of equations for the present problem is reduced and simplified to one equation:

$$aw^2\frac{d^2w}{dx^2}-(1-w^2)\frac{dw}{dx}+\frac{2}{x}w(1-\beta w^2)=0, \qquad \text{(A)}$$

† Now at Tokyo Electrical Engineering College, Kanda, Tokyo.

where $w = u/c_1$, $x = r_1/r$, $\beta = (\gamma-1)/(\gamma+1)$ (see (8), (9), (15), (25) below) and a is a small number proportional to the reciprocal of the Reynolds number. The corresponding equation for the two-dimensional case is found in the papers referred to above, and is

$$aw^2\frac{d^2w}{dt^2}-(1-w^2)\frac{dw}{dt}+w(1-\beta w^2)=0, \qquad t=\log r. \tag{B}$$

Comparing these two equations, we can see that they are similar except for the factor $2/x$ in the equation (A) and solutions of these equations would be expected to be similar. Actually, the factor $2/x$ is almost constant in a narrow range of x, and thus a solution of (B) which includes shock waves may also be expected to be a solution of (A), since in the shock wave the change in w takes place in a narrow region of x.

The equation (A) is non-linear and of singular perturbation type, having a small coefficient a of the highest derivative. It is difficult to express the solution in a single analytical form in the whole range of x. Utilizing the similarity between (A) and (B), and using the knowledge of the solution of (B) as a guide, the domain of x is divided into several sub-regions where approximate solutions can be obtained. By connecting these approximate solutions in different regions using boundary layer technique (Carrier, **5**), the solution can be constructed.

After reducing the fundamental equations to the equation (A) in section 2, the properties of the solution of (B) are displayed in section 3 for the purpose of obtaining qualitative information about the solution of (A). Detailed study is given in section 4 to the typical solution of (A) which, in the limit of large Reynolds number, reduces to a solution consisting of inviscid solutions and shock waves. Other types of solutions are briefly discussed in section 5.

2. The fundamental equations

Let r, u, p, ρ, T denote respectively the radial distance from the origin, velocity, pressure, density, and absolute temperature. The system of Navier–Stokes equations specialized to the case of three-dimensional steady radial flow of a perfect gas with viscosity μ and heat conductivity λ are as follows:

The continuity equation is $\qquad \rho u r^2 = m, \tag{1}$

where m is a constant and

$$\begin{cases} m > 0 & \text{for a source flow,} \\ m < 0 & \text{for a sink flow;} \end{cases}$$

the momentum equation is

$$\rho u\frac{du}{dr}=-\frac{dp}{dr}+\frac{4}{3}\frac{d}{dr}\left(\mu\frac{1}{r^2}\frac{d}{dr}(r^2u)\right)-\frac{4u}{r}\frac{d\mu}{dr}; \tag{2}$$

the energy equation, after one integration and taking the integration constant as mE, is

$$2mc_pT+(m+\tfrac{8}{3}\mu T)u^2=2\lambda r^2\frac{dT}{dr}+\tfrac{4}{3}\mu r^2\frac{du^2}{dr}+2mE; \tag{3}$$

these equations are supplemented by the equation of state

$$p=\rho RT. \tag{4}$$

The equations for the inviscid fluid are obtained by putting $\lambda, \mu = 0$ in the above system of equations. Then (2), (3) become

$$\rho u\frac{du}{dr}=-\frac{dp}{dr}, \tag{5}$$

$$2c_pT+u^2=2E=2c_pT_0, \tag{6}$$

where T_0 is the temperature at the stagnation point. Eliminating p, ρ, T from (1), (4), (5), (6), we get an equation for u,

$$\frac{du}{dr}\left(\frac{\gamma+1}{\gamma-1}u^2-2c_pT_0\right)+\frac{2}{r}u(u^2-2c_pT_0)=0, \tag{7}$$

where γ is the ratio of the specific heats. Introducing a new variable w defined by

$$w=u/c_1, \tag{8}$$

where c_1 is the critical velocity defined by

$$c_1^2=2\beta c_pT, \qquad \beta=(\gamma-1)/(\gamma+1), \tag{9}$$

(7) is reduced to

$$\frac{dw}{dr}(1-w^2)+\frac{2}{r}w(1-\beta w^2)=0. \tag{10}$$

This equation gives, on integration,

$$\frac{r}{r_1}=w^{-1}\left(\frac{1-\beta w^2}{1-\beta}\right)^{-(1-\beta)/4\beta}, \tag{11}$$

where we have put $r=r_1$ at $w=1$. The graph of $w(r)$ given by (11) is plotted in Fig. 1. The graph shows almost the same features as in the two-dimensional case, i.e. it has two branches—one supersonic one subsonic—in $r>r_1$, terminating at $r=r_1$ with an infinite gradient and there is no solution in $r<r_1$.

For $r\gg r_1$ the slope of the curve $w(r)$ of (11) is much smaller than unity, and consequently viscous effects should become comparatively unimportant there, and so the inviscid solution (11) itself can be considered to be an approximate solution of the system of equations (1)–(4) with non-

zero but small λ, μ, provided $E = 2c_p T_0$ and r is large enough. Since our purpose is to find the deviation from the inviscid solution (11) due to the effects of heat conduction and viscosity, it is natural to seek a solution which approximates to the inviscid solution (11) for large value of r. More precisely, we shall find a solution which reduces to the inviscid solution (11) when λ, $\mu \to 0$ at large but finite r. Accordingly E is determined as $E = 2c_p T_0$. We must distinguish this solution from a similar but different one which reduces to the inviscid solution as $r \to \infty$ when λ, μ are small but finite. The second solution cannot always be found, because the supersonic branch of (11) does not satisfy (3) when $r \to \infty$ if λ, μ are finite and fixed.

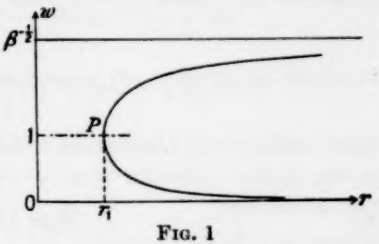

FIG. 1

In the papers quoted above, the effects of varying λ, μ were estimated to be inconsiderable in the case of two-dimensional flow. For the purpose of making the problem as simple as possible, we shall confine our attention to the case when λ, μ are constants.

Now, eliminating p and ρ from equations (1)–(4) and introducing a non-dimensional variable z,

$$z = \frac{r}{r^*}, \qquad r^* = \frac{3m}{4\mu} \quad \begin{cases} z > 0 & \text{for a source flow} \\ z < 0 & \text{for a sink flow,} \end{cases} \tag{12}$$

the equations for u, T, assuming λ, μ, c_p constant, become

$$z^2\frac{d^2u}{dz^2} + (2z-1)\frac{du}{dz} - 2u = \frac{\gamma-1}{\gamma}\left\{\frac{d}{dz}\left(\frac{c_p T}{u}\right) - \frac{2}{z}\frac{c_p T}{u}\right\}, \tag{13}$$

$$c_p T + (1+2z)\frac{u^2}{2} = \frac{3}{4\sigma}z^2\frac{d}{dz}(c_p T) + z^2\frac{d}{dz}\left(\frac{u^2}{2}\right) + c_p T_0, \tag{14}$$

where σ is the Prandtl number and is also assumed to be constant. Unlike the case of two-dimensional flow, r^* in (12) is not a non-dimensional constant interpreted as a Reynolds number but has the dimension of length. Since equations (13) and (14) do not depend explicitly on r^*, the condition for (1)–(4) when λ, $\mu \to 0$ at finite and fixed r becomes the condition at $z \to 0$ for (13), (14). It is convenient to introduce a new variable y and a small number α such that

$$z = \alpha y, \qquad \alpha = \frac{r_1}{r^*} \quad \begin{cases} \alpha > 0 & \text{for a source flow} \\ \alpha < 0 & \text{for a sink flow} \end{cases} \tag{15}$$

and α is interpreted as the reciprocal of the Reynolds number Re ($\alpha^{-1} = Re$) and assumed to be small.

Using (15) together with the non-dimensional variables

$$w = \frac{u}{c_1}, \qquad \theta = \frac{T}{T_1}, \tag{16}$$

where T_1 is the value of T at $r = r_1$ in the inviscid solution, equations (13), (14) are transformed into

$$\alpha y^2 \frac{d^2w}{dy^2} + (2\alpha y - 1)\frac{dw}{dy} - 2\alpha w = \frac{1}{\gamma}\left\{\frac{d}{dy}\left(\frac{\theta}{w}\right) - \frac{2}{y}\frac{\theta}{w}\right\}, \tag{17}$$

$$\theta + \frac{\gamma-1}{2}(1+2\alpha y)w^2 - \frac{\gamma+1}{2} = \alpha y^2\left(\frac{3}{4\sigma}\frac{d\theta}{dy} + \frac{\gamma-1}{2}\frac{dw^2}{dy}\right). \tag{18}$$

The problem is thus reduced to finding a solution of (17), (18) which reduces to the inviscid solution when $\alpha \to 0$ at finite and fixed y. By a further transformation

$$x = 1/y = r_1/r, \tag{19}$$

equations (17), (18) become

$$\alpha\frac{d^2w}{dx^2} + \frac{dw}{dx} - \frac{2\alpha}{x^2}w = -\frac{1}{\gamma}\left\{\frac{d}{dx}\left(\frac{\theta}{w}\right) + \frac{2}{x}\frac{\theta}{w}\right\}, \tag{20}$$

$$\theta + \frac{\gamma-1}{2}\left(1+\frac{2\alpha}{x}\right) - \frac{\gamma+1}{2} = -\alpha\left(\frac{3}{4\sigma}\frac{d\theta}{dx} + \frac{\gamma-1}{2}\frac{dw^2}{dx}\right), \tag{21}$$

which are similar to the corresponding equations in the two-dimensional case.

Now let us write (21) in the different form

$$\theta + \frac{4\sigma}{3}\frac{\gamma-1}{2}w^2 - \frac{\gamma+1}{2}$$

$$= Ae^{-(4\sigma/3\alpha)x} - \frac{\gamma-1}{2}\frac{4\sigma}{3}e^{-(4\sigma/3\alpha)x}\int e^{(4\sigma/3\alpha)x}\left\{\frac{1}{\alpha}\left(1-\frac{4\sigma}{3}\right)+\frac{2}{x}\right\}w^2\,dx, \tag{22}$$

where A is an arbitrary constant. The last term is small if $1-(4\sigma/3)$ $(= \epsilon,$ say) is small enough, i.e. if $\sigma \sim 0{\cdot}75$ (for air $\sigma = 0{\cdot}72$). Now x exceeds a certain fixed value x_1 (say) (we are considering the solution in a range $r < R$ fixed) and it is likely that w will not exceed the maximum value $\beta^{-\frac{1}{2}}$ in the inviscid solution. Then we have

$$\frac{\gamma-1}{2}\frac{4\sigma}{3}e^{-(4\sigma/3\alpha)x}\int e^{(4\sigma/3\alpha)x}\left\{\frac{1}{\alpha}\left(1-\frac{4\sigma}{3}\right)+\frac{2}{x}\right\}w^2\,dx \leqslant \frac{\gamma-1}{2}\left(\epsilon+\frac{2\alpha}{x_1}\right)\beta^{-1}.$$

With regard to the term $Ae^{-(4\sigma/3\alpha)x}$, A must be zero for $\alpha < 0$, otherwise it becomes infinite as $\alpha \to 0$ for finite x; on the other hand, for $\alpha > 0$, $Ae^{-(4\sigma/3\alpha)x}$ becomes smaller than any finite power of α. Then (22) becomes (for both cases $\alpha \gtrless 0$)

$$\theta + \frac{4\sigma}{3}\frac{\gamma-1}{2}w^2 - \frac{\gamma+1}{2} = O\left(\epsilon+\frac{2\alpha}{x_1}\right). \tag{23}$$

Substituting (23) into (20) and neglecting small order terms, we get finally

$$aw^2\frac{d^2w}{dx^2}-(1-w^2)\frac{dw}{dx}+\frac{2}{x}w(1-\beta w^2)=0, \tag{24}$$

where

$$\frac{2\gamma}{\gamma+1}\alpha=a. \tag{25}$$

If we put $a=0$ in (24), the equation reduces to equation (10) having the solution (11).

3. Qualitative properties of the flow from the solution of the two-dimensional case

Let us compare equation (24) with the corresponding equation in the two-dimensional case, namely,

$$aw^2\frac{d^2w}{dt^2}-(1-w^2)\frac{dw}{dt}+(1-\beta w^2)w=0, \qquad t=\log r, \tag{26}$$

neglecting small quantities. Since (24) and (26) are similar, except for the extra factor $2/x$ in the last term of (24), it is to be expected that the solutions

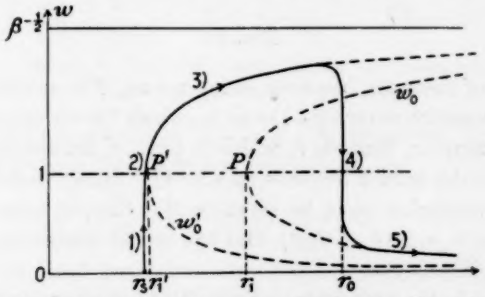

FIG. 2. Sketch of a solution curve for the two-dimensional source type flow ($a>0$)

will be similar, the independent variables being x in (24) and t in (26). In particular, the local properties of the solution of (24) will be the same as for (26), since the factor $2/x$ in (24) varies little if x ranges over a small region. We shall use this fact to find the qualitative properties of the solution of (24). Before doing this, we shall consider the general properties of the solution of (26).

The solution of (26) has not been found in finite form since it is of singular perturbation type. But the important characteristics of the solution are known and may be found in the papers mentioned above. The typical solution curve for $a>0$ is shown in Fig. 2.

The curve starting from the stagnation point at $r=r_s$, (1) rises and

(2) passes the sonic line $w = 1$, then (3) it goes along the supersonic branch of the inviscid solution w_0' until near $r = r_0$, (4) it falls down to the subsonic branch of another inviscid solution w_0 and finally (5) approaches the stagnation point at infinity along w_0. At the limit of $a \to 0$, parts (3) and (5) approach the corresponding parts of inviscid curves while (4) approaches the shock wave. The parts (1), (2) approach the line $P'r_1'$ ('negative shock'). Since the flow is not isentropic but is affected by viscosity and heat conduction, it is natural that the solution as $a \to 0$ corresponds to different inviscid solutions which have different entropies. There is an infinite number of solutions of this type depending on the different choice of

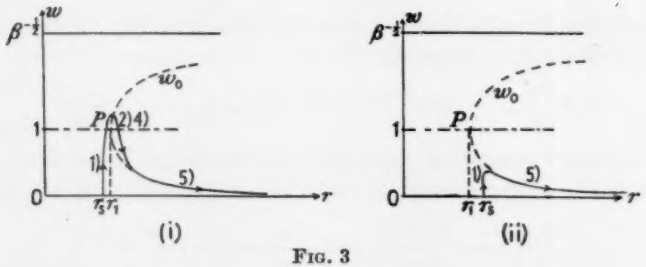

FIG. 3

r_1, r_1', r_0. Two of them are, however, independent. For example, if r_1, r_0 are given, then r_1' must be determined so as to satisfy the shock condition at r_0.

Now, if we move r_0 towards r_1 which is fixed, r_1' moves also towards r_1, and part (3) of the curves becomes smaller and finally disappears.

Special consideration must be given to this case, or more precisely, to the case where $(r_0/r_1) - 1 \leqslant O(a^{\frac{1}{2}})$, and the curve illustrating the solution is as shown in Fig. 3 (i).

The solution in the transition regions (2), (4) is described by a kind of transonic equation. But such a region is small ($O(a^{\frac{1}{2}})$) and becomes zero when $a \to 0$ and then the solution at the limit consists of two parts: (1) negative shock, and (5) the subsonic branch of the inviscid solution w_0. It must be remarked that the limit of this solution corresponds to a single inviscid solution.

Solutions of the same type which consist of the two parts (1), (5) shown in Fig. 3 (ii), are possible, though the transition from (1) to (5) is different from that in the solution shown in Fig. 3 (i).

These main properties of the solution for $a > 0$ appear also in the case of $a < 0$ (sink type flow) except for the fact that the roles of the subsonic and supersonic branches of the inviscid solution are interchanged. A typical solution corresponding to that for $a > 0$ in Fig. 2 is illustrated in Fig. 4.

The curve starts from maximum velocity $\beta^{-\frac{1}{2}}$ as $r \to \infty$ on the supersonic

branch of the inviscid solution w_0', goes down to (3) (the subsonic branch of w_0) through (4) and thereafter passes parts (2), (1) and finally ends at the maximum velocity $w = \beta^{-\frac{1}{2}}$.

In the limit $a \to 0$, the parts (5), (3) approach to the inviscid solutions and the part (4) approaches the shock wave. Since shock transition takes place from low to higher values of the entropy and w_0 has higher entropy than w_0', the transition must be from w_0' to w_0 as was true for the case $a > 0$. Solutions of a special type similar to that shown for the case $a > 0$ in Fig. 3 also exist.

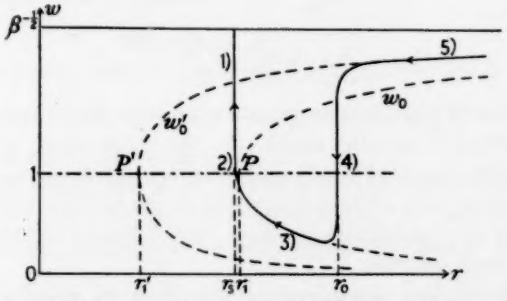

FIG. 4. Sketch of a solution curve for the two-dimensional sink type flow ($a < 0$)

It is worth while noting that equation (26) resembles in many ways van der Pol's equation for relaxation oscillations, viz.

$$a\frac{d^2y}{dt^2} - (1-y^2)\frac{dy}{dt} + y = 0.$$

For example, the rapid transition occurring between two regions (2) and (3) or (3) and (4) in Figs. 2 and 4 is due to the same causes which induce the well-known jerky wave form in relaxation oscillations.

Returning to the present problem of finding the solution of (24) there might be a solution which includes transition regions something like (1), (2), (4) since the regions are so narrow that the factor $2/x$ in (24) has little influence on the solution there, while the solution of (26) near the regions (3), (5) is essentially not so different from the inviscid solution; the same situation is also to be expected in the solution of (24). These points will be clarified in the following sections.

4. Typical solution of equation (24)

Corresponding to the typical solution of (26) which was described in the last section, there is a similar solution of (24). This is derived by subdividing the range of x and finding approximate solutions in the sub-regions.

(2) passes the sonic line $w = 1$, then (3) it goes along the supersonic branch of the inviscid solution w_0' until near $r = r_0$, (4) it falls down to the subsonic branch of another inviscid solution w_0 and finally (5) approaches the stagnation point at infinity along w_0. At the limit of $a \to 0$, parts (3) and (5) approach the corresponding parts of inviscid curves while (4) approaches the shock wave. The parts (1), (2) approach the line $P'r_1'$ ('negative shock'). Since the flow is not isentropic but is affected by viscosity and heat conduction, it is natural that the solution as $a \to 0$ corresponds to different inviscid solutions which have different entropies. There is an infinite number of solutions of this type depending on the different choice of

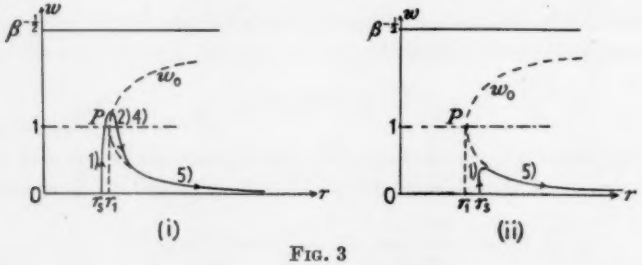

FIG. 3

r_1, r_1', r_0. Two of them are, however, independent. For example, if r_1, r_0 are given, then r_1' must be determined so as to satisfy the shock condition at r_0.

Now, if we move r_0 towards r_1 which is fixed, r_1' moves also towards r_1, and part (3) of the curves becomes smaller and finally disappears.

Special consideration must be given to this case, or more precisely, to the case where $(r_0/r_1)-1 \leqslant O(a^{\frac{1}{2}})$, and the curve illustrating the solution is as shown in Fig. 3 (i).

The solution in the transition regions (2), (4) is described by a kind of transonic equation. But such a region is small ($O(a^{\frac{1}{2}})$) and becomes zero when $a \to 0$ and then the solution at the limit consists of two parts: (1) negative shock, and (5) the subsonic branch of the inviscid solution w_0. It must be remarked that the limit of this solution corresponds to a single inviscid solution.

Solutions of the same type which consist of the two parts (1), (5) shown in Fig. 3 (ii), are possible, though the transition from (1) to (5) is different from that in the solution shown in Fig. 3 (i).

These main properties of the solution for $a > 0$ appear also in the case of $a < 0$ (sink type flow) except for the fact that the roles of the subsonic and supersonic branches of the inviscid solution are interchanged. A typical solution corresponding to that for $a > 0$ in Fig. 2 is illustrated in Fig. 4.

The curve starts from maximum velocity $\beta^{-\frac{1}{2}}$ as $r \to \infty$ on the supersonic

branch of the inviscid solution w_0', goes down to (3) (the subsonic branch of w_0) through (4) and thereafter passes parts (2), (1) and finally ends at the maximum velocity $w = \beta^{-\frac{1}{2}}$.

In the limit $a \to 0$, the parts (5), (3) approach to the inviscid solutions and the part (4) approaches the shock wave. Since shock transition takes place from low to higher values of the entropy and w_0 has higher entropy than w_0', the transition must be from w_0' to w_0 as was true for the case $a > 0$. Solutions of a special type similar to that shown for the case $a > 0$ in Fig. 3 also exist.

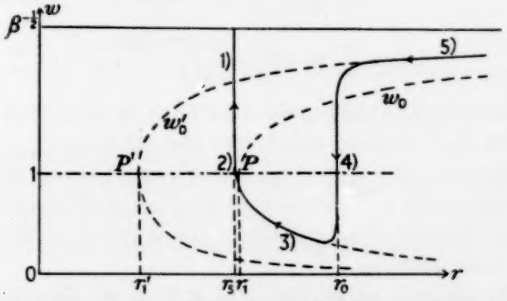

FIG. 4. Sketch of a solution curve for the two-dimensional sink type flow ($a < 0$)

It is worth while noting that equation (26) resembles in many ways van der Pol's equation for relaxation oscillations, viz.

$$a\frac{d^2y}{dt^2} - (1-y^2)\frac{dy}{dt} + y = 0.$$

For example, the rapid transition occurring between two regions (2) and (3) or (3) and (4) in Figs. 2 and 4 is due to the same causes which induce the well-known jerky wave form in relaxation oscillations.

Returning to the present problem of finding the solution of (24) there might be a solution which includes transition regions something like (1), (2), (4) since the regions are so narrow that the factor $2/x$ in (24) has little influence on the solution there, while the solution of (26) near the regions (3), (5) is essentially not so different from the inviscid solution; the same situation is also to be expected in the solution of (24). These points will be clarified in the following sections.

4. Typical solution of equation (24)

Corresponding to the typical solution of (26) which was described in the last section, there is a similar solution of (24). This is derived by sub-dividing the range of x and finding approximate solutions in the sub-regions.

Detailed consideration is given mainly to the case of source type flow ($a > 0$) since the second case ($a < 0$) is similar to the first case, at least qualitatively.

In the regions (3), (5), the solutions of (26) are not so different from the inviscid solution and the term $aw^2(d^2w/dt^2)$ can be considered to be small there, since for the inviscid solution d^2w/dt^2 remains of the same order as the other terms except in the neighbourhood of $t = 0$. In equation (24), too, the inviscid solution w_0, satisfying the equation

$$-(1-w_0^2)\frac{dw_0}{dx}+\frac{2}{x}w_0(1-\beta w_0^2) = 0, \tag{27}$$

and given by

$$x = \frac{r_1}{r} = w_0^{\frac{1}{2}}\left(\frac{1-\beta w_0^2}{1-\beta}\right)^{(1-\beta)/4\beta}, \tag{28}$$

is considered to be a good approximation for w in (24) when a is small so long as $aw^2(d^2w/dx^2)$ remains small. On the other hand, in the regions (1), (2), (4) the term $aw^2(d^2w/dx^2)$ cannot be neglected and w_0 ceases to be an approximation to w; different approximations are then needed. Fitting together these approximate solutions in the different regions, we finally obtain the overall solution.

We begin by finding the deviation of w from w_0, necessary to fit the approximate solution in (3), (5) (from now on, for convenience, we shall use these notations also for the corresponding regions in the solution of (24)) to the approximate solutions in the neighbouring regions (1), (2), (4). For this purpose, we put

$$w = w_0+f \tag{29}$$

where we suppose

$$f \ll w_0.$$

Substituting from (29) to (24) and neglecting small quantities of order higher than f^2, we get

$$f''-\frac{1}{a}\left(\frac{1}{w_0^2}-1\right)f'+2\left(\frac{w_0''}{w_0}+\frac{1}{a}\frac{w_0'}{w_0}+\frac{1}{ax}\frac{1-3\beta w_0^2}{w_0^2}\right)f = -w_0'', \tag{30}$$

where primes denote differentiation with respect to x. By a transformation

$$f = e^{z/a}g,$$

where

$$z = \frac{1}{2}\int^x\left(\frac{1}{w_0^2}-1\right)dx, \tag{31}$$

equation (30) is transformed into the standard form

$$g''-a^{-2}\chi(x)g = -w_0''e^{-z/a}, \tag{32}$$

where

$$\chi(x) \equiv \chi_0(x)+a\chi_1(x)+a^2\chi_2(x),$$

$$\chi_0(x) = \frac{1}{4}\left(\frac{1}{w_0^2}-1\right)^2, \qquad \chi_1(x) = -\left(\frac{w_0'}{w_0}-\frac{4\beta}{x}\right), \qquad \chi_2(x) = -2\frac{w_0''}{w_0}. \tag{33}$$

Since equation (32) is of Green's type, its asymptotic solution for small values of a can be obtained by Jeffreys's method (6). In the region where χ_0, χ_1, χ_2 remain of comparable orders of magnitude, two independent solutions g_1, g_2 of the homogeneous part of (32) are, to a first approximation, given by

$$g_1, g_2 \sim \chi^{-\frac{1}{4}} e^{\pm\xi/a},$$

where

$$\eta = \int^x \chi^{\frac{1}{2}}\, dx. \tag{34}$$

Using the fact that the Wronskian $g_1' g_2 - g_1 g_2'$ is equal to $2/a$, the approximate expression for f becomes

$$\begin{aligned} f &= e^{z/a\beta} \\ &\sim \chi^{-\frac{1}{4}}\Big\{A e^{(z+\eta)/a} + B e^{(z-\eta)/a} - \tfrac{1}{2}a\, e^{(z+\eta)/a}\int w_0''\chi^{-\frac{1}{4}} e^{-(z+\eta)/a}\, dx + \\ &\qquad + \tfrac{1}{2}a\, e^{(z-\eta)/a}\int w_0''\chi^{-\frac{1}{4}} e^{-(z-\eta)/a}\, dx\Big\}, \end{aligned} \tag{35}$$

where A, B are arbitrary constants.

We consider firstly the case $a > 0$ (source type flow). Since w_0 consists of two branches, $w_0 < 1$ (subsonic branch) and $w_0 > 1$ (supersonic branch), we must consider the solution for each branch separately. For $w_0 < 1$ we have

$$\begin{aligned} \eta &= \int^x \chi^{\frac{1}{2}}\, dx = \int^x \left\{\frac{1}{2}\left(\frac{1}{w_0^2} - 1\right) - \frac{a w_0}{1-w_0^2}\left(w_0' - \frac{4\beta w_0}{x}\right) + \ldots\right\} dx \\ &= z - a\log(1-w_0^2)^{-\frac{1}{4}}(1-\beta w_0^2) + \ldots, \\ \chi^{-\frac{1}{4}} &= \left\{\frac{1}{2}\left(\frac{1}{w_0^2} - 1\right)\right\}^{-\frac{1}{2}}\left\{1 + a\left(\frac{w_0'}{w_0} - \frac{4\beta}{x}\right)\left(\frac{1}{w_0^2} - 1\right)^{-2} + \ldots\right\}, \end{aligned} \tag{36}$$

and (35) reduces to

$$\begin{aligned} f \sim w_0\Big\{&\sqrt{2}\, A(1-\beta w_0^2)^{-1} e^{2z/a} + \sqrt{2}\, B(1-w_0^2)^{-1}(1-\beta w_0^2) - \\ &- a(1-\beta w_0^2)^{-1} e^{2z/a}\int w_0'' w_0 (1-w_0^2)^{-1}(1-\beta w_0^2) e^{-2z/a}\, dx + \\ &+ a(1-w_0^2)^{-1}(1-\beta w_0^2)\int w_0'' w_0 (1-\beta w_0^2)^{-1}\, dx + \ldots\Big\}. \end{aligned} \tag{37}$$

The third term can be shown to be small by integrating by parts:

$$\begin{aligned} &a(1-\beta w_0^2)^{-1} e^{2z/a}\int w_0'' w_0 (1-w_0^2)^{-1}(1-\beta w_0^2) e^{-2z/a}\, dx \\ &\quad = -a^2 w_0'' w_0^3 (1-w_0^2)^{-2} + a^2(1-\beta w_0^2)^{-1} e^{2z/a} \times \\ &\qquad \times \int e^{-2z/a}\frac{d}{dz}\{w_0'' w_0^3 (1-w_0^2)^{-2}(1-\beta w_0^2)\}\, dz. \end{aligned} \tag{38}$$

The behaviours of w_0 and z for small x are

$$w_0 \sim kx^2, \qquad 2z \sim -\frac{1}{3k^2}\frac{1}{x^3},$$

where

$$k = (1-\beta)^{(1-\beta)/2\beta},$$

so that behaviour of f/w for small x becomes, from (37),

$$f/w_0 \sim \sqrt{2}\,Ae^{-1/(3ak^2x^3)}+\sqrt{2}\,B+\tfrac{2}{3}ak^2x^3.$$

Now f must tend to zero as $a \to 0$ at a fixed x (say x_1), and so $B \to 0$ as $a \to 0$. Finally, we get

$$f/w_0 \sim \sqrt{2}\,A(1-\beta w_0^2)^{-1}e^{2z/a}+a(1-w_0^2)^{-1}(1-\beta w_0^2)\int w_0''\,w_0(1-\beta w_0^2)^{-1}\,dx + \\ +\sqrt{2}\,B(1-w_0^2)^{-1}(1-\beta w_0^2)+\ldots. \quad (39)$$

In the first term $e^{2z/a}$ is of a higher order of small quantities than any finite power of a and thus the first term will be quite small. Accordingly, for the limiting case when a is small, the deviation, f, of w from w_0 is also small ($f = O(a)$) in the region (5) ($a > 0$, $w_0 < 1$). But it is possible that the term $Ae^{2z/a}$ may become large at a certain point. Introducing z_0 instead of A, where z_0 is given by

$$\sqrt{2}\,A = e^{-2z_0/a}, \quad (40)$$

the first term becomes $(1-\beta w_0^2)^{-1}e^{2(z-z_0)/a}$.

Now, if it happens that $z = z_0$ at $x = x_0$ (say), the magnitude of this term will vary suddenly from a small to a very large value, as x passes through x_0 (r decreasing), since a is assumed to be a very small number. This feature may be incorporated in the following approximate formula valid near $x = x_0$ for (39). From (31) we have

$$2(z-z_0) = \int_{x_0}^{x}\left(\frac{1}{w_0}-1\right)dx \sim \left(\frac{1}{w_{01}^2}-1\right)(x-x_0),$$

assuming that $x-x_0$ is small and denoting by w_{01} the value of w_0 at x_0. Thus, (39) becomes

$$f \sim w_{01}(1-\beta w_{01}^2)^{-1}e^{\{(1/w_{01}^2)-1\}(x-x_0)/a} \quad (x < x_0), \quad (41)$$

neglecting small quantities.

If we change the variable x to ξ according to the relation

$$x = x_0+a\xi, \quad (42)$$

(41) gives $$f \sim w_{01}(1-\beta w_{01}^2)^{-1}e^{\{(1/w_{01}^2)-1\}\xi} \quad (\xi < 0). \quad (43)$$

The choice of z_0 or x_0 (which corresponds to r_0 in Fig. 2) is completely arbitrary so long as $\chi_0(x_0)$, $\chi_1(x_0)$, $\chi_2(x_0)$ in (33) are of order unity. This means that such a sudden change can happen anywhere in the region $1 > x_0 > x_1$ excluding $x_0 \sim 1$.

Having now determined a position of sudden change $x = x_0$, we proceed to find an approximate solution which is valid in a narrow region (4) near $x = x_0$. Changing the variable from x to ξ by (42), equation (24) becomes

$$w^2\frac{d^2w}{d\xi^2}-(1-w^2)\frac{dw}{d\xi}+\frac{2a}{x_0+a\xi}w(1-\beta w^2) = 0.$$

Neglecting the last term since it is multiplied by a and is small provided $a\xi$ remains small, we have the approximate equation

$$w^2\frac{d^2w}{d\xi^2}-(1-w^2)\frac{dw}{d\xi}=0, \tag{44}$$

which on integration gives

$$\frac{dw}{d\xi}+\frac{1}{w}+w=c, \tag{45}$$

where c is a constant of integration. Choosing c so that (45) assumes the form

$$\frac{dw}{d\xi}=\frac{1}{w}(w-w_1)(w_2-w), \tag{46}$$

where
$$w_1+w_2=c, \qquad w_1w_2=1 \quad (w_1<1), \tag{47}$$

and integrating (46) in the region $w_2 \geqslant w \geqslant w_1$, we have

$$\frac{w_1}{w_2-w_1}\log(w-w_1)-\frac{w_2}{w_2-w_1}\log(w_2-w)=\xi+c', \tag{48}$$

where c' is an integration constant. The integration constants c, c' (or w_1, c') can be determined by comparing equation (48) at large negative ξ (where $a\xi$ remains of order unity) with equation (43).

Considering the behaviour of (48) as $\xi \to -\infty$, we have

$$\begin{aligned} w &\sim w_1+(w_2-w_1)^{w_1/w_1}e^{(w_1-w_1)c'/w_1}e^{(w_2-w_1)\xi/w_1} \\ &= w_1+\left(\frac{1-w_1^2}{w_1}\right)^{1/w_1^2}e^{(1-w_1^2)c'/w_1^2}e^{(1-w_1^2)\xi/w_1^2}. \end{aligned} \tag{49}$$

Comparing (43) and (49), we obtain the values of w_1 and c', viz.

$$w_1=w_{01}, \tag{50}$$

$$\left(\frac{1-w_1^2}{w_1}\right)^{1/w_1^2}e^{(1-w_1^2)c'/w_1^2}=w_{01}(1-\beta w_{01}^2)^{-1}. \tag{51}$$

It is worth noting that (46), (47), (48) are the same as the equations for the velocity distribution deduced from the Navier–Stokes equation for the case of plane shock waves and that the second condition in (47) corresponds to Prandtl's relation. Thus, the transition near $x=x_0$ is seen to have the same feature as that in plane shock waves. In the case of two-dimensional source type flow, the presence of such a shock wave was derived by Levey (2) using quite a different method.

Now the solution (48) must be fitted to a supersonic branch of another inviscid solution for large positive values of ξ. At large $\xi>0$, (48) becomes

$$w \sim \frac{1}{w_{01}}-\frac{1-w_{01}^2}{w_{01}}\left(\frac{1-w_{01}^2}{1-\beta w_{01}^2}\right)^{w_{01}^2}e^{-(1-w_{01}^2)\xi}, \tag{52}$$

where we have used (50), (51). On the supersonic branch ($w_0 > 1$) equation (35) for f reduces to a slightly different form of (39) and

$$f/w_0 \sim \sqrt{2}\,A'(1-\beta w_0^2)(w_0^2-1)^{-1}+\sqrt{2}\,B'(1-\beta w_0^2)^{-1}e^{2z/a}- \\ -a(w_0^2-1)(1-\beta w_0^2)\int w_0''\,w_0(1-\beta w_0^2)^{-1}\,dx, \qquad (53)$$

with arbitrary constants A', B'. Putting

$$\sqrt{2}\,B' = B''e^{-2z_0/a} \qquad (54)$$

and denoting by w_{02} the value of w_0 (supersonic branch) at $x = x_0$, we get an expression for f valid near $x = x_0$ ($x > x_0$):

$$f \sim \sqrt{2}\,A'w_{02}(1-\beta w_{02}^2)(w_{02}^2-1)^{-1}+B''w_{02}(1-\beta w_{02}^2)^{-1}e^{-(1-w_{02}^{-2})(x-x_0)/a}, \qquad (55)$$

neglecting small quantities. Comparing the expression (55) with (52) we get

$$w_{02} = w_2 = \frac{1}{w_{01}}, \qquad B'' = -\left(\frac{1-w_{01}^2}{1-\beta w_{01}^2}\right)^{w_{01}^2+1}, \qquad A' = o(1). \qquad (56)$$

Since the term $B'e^{2z/a}$ becomes quite small when $O(x-x_0)$ becomes larger than a, the solution w in the region (3) is again approximated by the inviscid solution w_0, but this function w_0 does not correspond to the same inviscid solution used before (which was of the form given by (28)), but has a different form given by

$$xk = w_0^{\frac{1}{2}}\left(\frac{1-\beta w_0^2}{1-\beta}\right)^{(1-\beta)/4\beta}, \qquad k = \frac{r_1'}{r_1}, \qquad (57)$$

corresponding to a different entropy. Since at $x = x_0$, w_0 in (28) is w_{01} (< 1) and w_0 in (57) is w_{02} (> 1), we can determine k by using the first condition of (56), whence

$$k = \frac{r_1'}{r_1} = \frac{1}{w_{01}}\left(\frac{1-\beta/w_{01}^2}{1-\beta w_{01}^2}\right)^{(1-\beta)/4\beta}. \qquad (58)$$

It should be noted that the factor k appears only in the explicit relation between x and w_0, (57), and thus the derivation of equation (53) is not affected by the presence of k, although in this case w_0 in (29) must be given by (57). It is convenient to introduce a new variable x' defined by

$$x' = kx = r_1'/r; \qquad (59)$$

then (57) becomes

$$x' = w_0^{\frac{1}{2}}\left(\frac{1-\beta w_0^2}{1-\beta}\right)^{(1-\beta)/4\beta}. \qquad (60)$$

Equation (60) gives an approximation to w in region (3) which ceases to be valid when x' approaches 1. Putting

$$x'-1 = t \qquad (61)$$

and assuming $t \ll 1$, we get an approximate expression for the supersonic branch of (60) near $t = 0$:

$$w_0 \sim 1+\{-2(1-\beta)t\}^{\frac{1}{2}} \quad (t < 0). \qquad (62)$$

Near $x' = 1$, we can use an approximation to (24) already used by Wu (3) in the same region in the two-dimensional case. This approximation is also the same, in principle, as that used by Carrier (5) for finding an approximate solution to the relaxation oscillation problem. Using the transformation

$$w = 1+a^{\frac{1}{3}}v^*(\eta^*), \qquad t = a^{\frac{1}{3}}\eta^*, \tag{63}$$

equation (24) reduces to

$$v^{*\prime\prime}+2v^*v^{*\prime}+2(1-\beta) = O(a^{\frac{1}{3}}). \tag{64}$$

Integrating and omitting the $a^{\frac{1}{3}}$ term, we find

$$v^{*\prime}+v^{*2}+2(1-\beta)\eta^* = 0. \tag{65}$$

Putting $$v^* = \{2(1-\beta)\}^{\frac{1}{3}}v, \qquad \eta^* = \{2(1-\beta)\}^{-\frac{1}{3}}\eta, \tag{66}$$

equation (65) becomes $$v'+v^2+\eta = 0, \tag{67}$$

and its solution is of the form

$$v = Z'(\eta)/Z(\eta), \tag{68}$$

where $$Z = (-\xi)^{\frac{1}{2}}[K_{\frac{1}{3}}(s)+BK_{-\frac{1}{3}}(-s)], \qquad s = \tfrac{2}{3}(-\eta)^{\frac{3}{2}}, \tag{69}$$

and K_ν is the modified Hankel function. Considering the boundary layer, where $-\xi \gg 1$ and $-t \ll 1$, we can determine B by (62) which is valid in $-t \ll 1$. For large values of $-\xi$, $v \sim -(-\eta)^{\frac{1}{2}}$ if $B \neq 0$ whereas $v \sim (-\eta)^{\frac{1}{2}}$ if $B = 0$ and

$$Z = (-\eta)^{\frac{1}{2}}K_{\frac{1}{3}}(s) = (\pi\eta^{\frac{1}{2}}/\sqrt{3})[J_{\frac{1}{3}}(s')+J_{-\frac{1}{3}}(s')] \tag{70}$$

with $$s' = \tfrac{2}{3}\eta^{\frac{3}{2}}.$$

This approximate solution, v^*, in region (2) ceases to be valid when η approaches η_1, which is associated with the smallest zero of the function in the square brackets in (70). Near $\eta = \eta_1$,

$$v \sim \frac{1}{\eta-\eta_1} \quad \text{and} \quad w \sim 1+\frac{a}{x'-x_1'}, \tag{71}$$

where x_1' is $$1+\{2(1-\beta)\}^{-\frac{1}{3}}a^{\frac{1}{3}}\eta_1.$$

In the adjacent region (1), w varies rapidly from the value near 1 to 0 in a narrow region and the approximate equation (45)

$$\frac{dw}{d\xi}+\frac{1}{w}+w = c \tag{72}$$

can be used again, where ξ is defined by

$$x' = x_1'+a\xi. \tag{73}$$

The arbitrary constant c is determined by comparing (72) with (65) near $x' = x_1'$; this gives

$$c = 2-2(1-\beta)t_1 = 2-(ka)^{\frac{1}{3}}, \tag{74}$$

where $t_1 = \{2(1-\beta)\}^{-\frac{1}{4}}a^{\frac{1}{4}}\eta_1$ and we put $k^{\frac{1}{4}} = \{2(1-\beta)\}^{\frac{1}{4}}\eta_1$. With the value of c in (74), (72) is transformed into

$$\frac{dw}{d\xi}+\frac{w^2-\{2-(ka)^{\frac{1}{2}}\}w+1}{w} = 0,$$

which gives on integration

$$\xi+c' = (ka)^{-\frac{1}{4}}\tan^{-1}\{(ka)^{-\frac{1}{4}}(1-w)\}-\log(1-w), \tag{75}$$

neglecting small quantities. Considering a region where $(1-w)^{-1}a^{\frac{1}{4}} = o(1)$, (75) reduces to

$$\xi+c' \sim (ka)^{-\frac{1}{4}}(\tfrac{1}{2}\pi)-\frac{1}{1-w}-\log(1-w).$$

Comparing this with (71), which gives $1-w \sim -\xi^{-1}$, we get

$$c' = (ka)^{-\frac{1}{4}}\tfrac{1}{2}\pi$$

and $$\xi = (ka)^{-\frac{1}{4}}[\tan^{-1}\{(ka)^{-\frac{1}{4}}(1-w)\}-\tfrac{1}{2}\pi]-\log(1-w).$$

Using x' instead of ξ, we have

$$x'-x'_1 = k^{-\frac{1}{4}}a^{\frac{1}{4}}[\tan^{-1}\{(ka)^{-\frac{1}{4}}(1-w)\}-\tfrac{1}{2}\pi]-a\log(1-w). \tag{76}$$

When $w = 0$, $\qquad x' \sim x'_1 = 1+\{2(1-\beta)\}^{-\frac{1}{4}}a^{\frac{1}{4}}\eta_1.$

The typical solution terminates at a distance of order $a^{\frac{1}{4}}$ from $x' = 1$. This agrees with the result obtained by Wu (**3**) for the case of two-dimensional sink type flow. When a becomes zero the typical solution is as follows: w in $x_1 < x < x_0$ (region 5), approaches $w_0(x)$ (subsonic branch) with $|w-w_0| = O(a)$; in $|x_0-x| = O(a)$ (region 4), w approaches the straight line from $w_{01}\,(= w_0(x_0))$ to $w_{02}\,(w_{01}w_{02} = 1)$. In $x_0 < x < k$ or $x_0/k < x' < 1$ (region 3) w approaches $w_0(x')$ (supersonic branch) with $|w-w_0| = O(a)$; in $|x'-1| = O(a^{\frac{1}{2}})$ (regions (2), (1)) w approaches the straight line from 1 to 0.

The typical solution for the case of $a < 0$ (sink type flow) can be found in the same way as above. Qualitatively, there is little difference between these two cases except for the fact that the roles of subsonic and supersonic branches in the inviscid solution are interchanged as we have seen in section 3.

5. Other solutions

When x_0 in (40) approaches 1, the approximate solution (35) for f is no longer valid, since χ_0, χ_1, χ_2 in (33) become of smaller order than 1. Instead, we have an approximate equation (63) with (66), (68), (69), valid near $x = 1$. Since the subsonic branch of w_0 near $x = 1$ is expressed by

$$w_0 \sim 1-\{-2(1-\beta)t\}^{\frac{1}{2}} \quad \text{where } x-1 = t,$$

the arbitrary constant B in (69) must be chosen as non-zero in this case

and the solution curves near $x = 1$ become approximately as shown in Fig. 5, the exact shape depending on the value of B.

For a more accurate determination of the values of B, we need a more precise approximation for w than w_0 near $x = 1$. In the case of two-dimensional sink type flow, Wu (**3**) used Lighthill's method for the purpose and this seems likely to be the case in the present problem also.

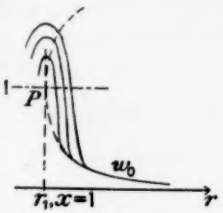

FIG. 5

For $x > 1$ the solutions approach a solution which is the continuation of the supersonic branch. At the limit of $a \to 0$, this type of solution becomes the subsonic branch of the inviscid solution and the straight line.

The special type of solution which corresponds to that in Fig. 3 (ii) is obtained if we take $\sqrt{2}\,A = -e^{-2z_0/a}$ instead of

$$\sqrt{2}\,A = e^{-2z_0/a}. \tag{40}$$

Acknowledgement

The author wishes to express his thanks to Professor C. L. Pekeris for an opportunity to work at the Weizmann Institute of Science.

REFERENCES

1. A. SAKURAI, *J. Phys. Soc. Japan*, **4–6** (1949) 199.
2. H. C. LEVEY, *Quart. Appl. Math.* **12** (1954) 25.
3. T. Y. WU, ibid. **13** (1955) 393.
4. W. PROSNAK, *Arch. Mech. Stos.* **8** (1956) 615.
5. C. F. CARRIER, *Advances in Applied Mechanics*, vol. III (1953), p. 1.
6. H. JEFFREYS and B. S. JEFFREYS, *Methods of Mathematical Physics* (Cambridge, 1956).

AN APPROXIMATION TO THE BOUNDARY LAYER FLOW ALONG AN EDGE

By L. SOWERBY

(*Department of Theoretical Mechanics, University of Bristol*)

[Received 31 May 1957]

SUMMARY

The steady flow of viscous incompressible fluid past an infinite flat quarter plate is considered, one edge of the plate being parallel to the main stream. Boundary layer equations are derived in a system of parabolic coordinates, and expansions in series provide a set of ordinary differential equations to determine the flow near this edge of the plate. An iterative procedure is described to solve these equations; the approximations thus obtained indicate a decrease from the normal flat-plate value in the thickness of the boundary layer at the edge, and there is a singularity in the density of the skin friction at the edge. Both of these effects were predicted in previous investigations on a related problem.

1. Introduction

HITHERTO the study of the effects of corners and edges on boundary layers has been concerned mainly with the Rayleigh problem. In this problem a viscous incompressible fluid bounded by two infinite half plates which intersect to form an edge (or corner) is set in motion by the sudden uniform motion of both plates parallel to their line of intersection; the determination of the velocity of the fluid depends on the appropriate solution of the heat conduction equation. Howarth (**1**) and Sowerby and Cooke (**2**, **3**) have considered various cases, and have made use of a hypothesis due to Rayleigh to deduce qualitative information about the related steady flow problems.

In this paper a direct attempt is made to consider certain features of the boundary layer for the steady flow of fluid past an infinite flat quarter plate, the main stream flow being parallel to one edge of the plate. The presence of an edge or corner leads to considerable complication in the form of the boundary layer equations, and the determination of the whole flow in the layer would be difficult. The results of the following investigation are therefore restricted; we consider an approximation to the flow in the layer at the edge, in the plane of the plate, and hence determine the singularity in the skin friction at this edge. This singularity, and a certain decrease in the thickness of the layer at the edge, have been predicted by Howarth (**1**), and the results obtained here are in accordance with Howarth's predictions.

2. Equations of motion in parabolic coordinates

The flat quarter plate is taken to occupy the quarter plane $z = 0, x, y \geqslant 0$, in a system of cartesian coordinates (x, y, z), the main stream velocity of the fluid being constant with cartesian components $(U, 0, 0)$. It is convenient to replace y and z by parabolic coordinates α, β, defined by the relations

$$y = \alpha^2 - \beta^2, \qquad z = 2\alpha\beta \tag{2.1}$$

since the coordinate system (x, α, β) will later allow the formulation of

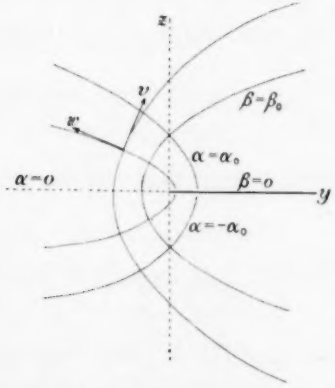

FIG. 1. Diagram showing the system of coordinates; the section is at right angles to the direction of the main stream. The coordinates ξ, η are given by the relations $\xi = \alpha(U/\nu x)^{\frac{1}{2}}$ and $\eta = \beta(U/\nu x)^{\frac{1}{2}}$, so that in the diagram the curves $\alpha = \text{const}$, $\beta = \text{const}$ are also curves $\xi = \text{const}$, $\eta = \text{const}$, respectively

boundary conditions in terms of a single coordinate. This system is an orthogonal system of coordinates, the surfaces $\alpha = \text{const}$, $\beta = \text{const}$ being parabolic cylinders as shown in Fig. 1.

In this system of coordinates, let the components of the velocity $\mathbf{v}$ in the fluid be (u, v, w). The equation of motion for a viscous incompressible fluid in steady motion is

$$\tfrac{1}{2}\operatorname{grad}\mathbf{v}^2 - \mathbf{v} \wedge \operatorname{curl}\mathbf{v} = -\frac{1}{\rho}\operatorname{grad} p - \nu \operatorname{curl}\operatorname{curl}\mathbf{v}, \tag{2.2}$$

while the equation of continuity is

$$\operatorname{div}\mathbf{v} = 0.$$

In the coordinate system (x, α, β) this last equation becomes

$$\frac{\partial}{\partial x}(h_1^2 u) + \frac{\partial}{\partial \alpha}(h_1 v) + \frac{\partial}{\partial \beta}(h_1 w) = 0,$$

where
$$h_1 = 2(\alpha^2+\beta^2)^{\frac{1}{2}}, \tag{2.3}$$

and hence, with the introduction of functions $f(x, \alpha, \beta)$, $\psi(x, \alpha, \beta)$, the general solution of the equation of continuity is

$$h_1^2 u = f_\beta, \qquad h_1 v = -\psi_\beta, \qquad h_1 w = \psi_\alpha - f_x, \tag{2.4}$$

a suffix, as usual, denoting differentiation with respect to the variable indicated. The vector equation (2.2) then gives the following equations of motion:

$$uu_x - \frac{1}{h_1^2}\psi_\beta u_\alpha + \frac{1}{h_1^2}u_\beta(\psi_\alpha - f_x) = -\frac{1}{\rho}\frac{\partial p}{\partial x} + \frac{\nu}{h_1^2}(u_{\alpha\alpha}+u_{\beta\beta}+f_{x\alpha\beta}), \tag{2.5}$$

$$\begin{aligned} &-u\psi_{\beta x} + \frac{1}{h_1^2}\psi_\beta\psi_{\beta\alpha} - \frac{1}{h_1^2}(\psi_\alpha - f_x)\psi_{\beta\beta} - \frac{4\alpha}{h_1^4}\{\psi_\beta^2+(\psi_\alpha - f_x)^2\} \\ &\quad = -\frac{1}{\rho}\frac{\partial p}{\partial \alpha} - \nu\left\{\frac{1}{h_1^2}(\psi_{\alpha\alpha\beta}+\psi_{\beta\beta\beta} - f_{x\alpha\beta}) - \frac{8\beta}{h_1^4}(\psi_{\alpha\alpha}+\psi_{\beta\beta} - f_{x\alpha}) + \psi_{\beta xx} + u_{x\alpha}\right\}, \end{aligned} \tag{2.6}$$

$$\begin{aligned} &u(\psi_{x\alpha} - f_{xx}) - \frac{1}{h_1^2}\psi_\beta(\psi_{\alpha\alpha} - f_{x\alpha}) + \frac{1}{h_1^2}(\psi_\alpha - f_x)(\psi_{\alpha\beta} - f_{x\beta}) - \frac{4\beta}{h_1^4}\{\psi_\beta^2+(\psi_\alpha - f_x)^2\} \\ &\quad = -\frac{1}{\rho}\frac{\partial p}{\partial \beta} + \nu\left\{\frac{1}{h_1^2}(\psi_{\alpha\alpha\alpha}+\psi_{\beta\beta\alpha} - f_{x\alpha\alpha}) - \frac{8\alpha}{h_1^4}(\psi_{\alpha\alpha}+\psi_{\beta\beta} - f_{x\alpha}) - u_{\beta x} + \psi_{\alpha xx} - f_{xxx}\right\}. \end{aligned} \tag{2.7}$$

3. The boundary layer equations and boundary conditions

The above are the complete equations of motion, and we could proceed from these to deduce boundary layer equations in the usual way. However, a solution of the problem in which y and z appear only in the combination $y/x^{\frac{1}{2}}$ and $z/x^{\frac{1}{2}}$ may be expected; accordingly Carrier's method (**4**) may be used to deduce the particular forms of the boundary layer equations which are required. That is, we now write

$$\left.\begin{aligned} X = \left(\frac{\nu}{Ux}\right)^{\frac{1}{2}}, \qquad \xi = \left(\frac{U}{\nu x}\right)^{\frac{1}{4}}\alpha, \qquad \eta = \left(\frac{U}{\nu x}\right)^{\frac{1}{4}}\beta \\ h = 2(\xi^2+\eta^2)^{\frac{1}{2}} = \left(\frac{U}{\nu x}\right)^{\frac{1}{4}}h_1 \end{aligned}\right\}, \tag{3.1}$$

and

$$\left.\begin{aligned} f &= (U\nu^3x^3)^{\frac{1}{4}}\{g(\xi,\eta)+Xg_1(\xi,\eta)+X^2g_2(\xi,\eta)+\ldots\} \\ \psi &= \nu\{\phi(\xi,\eta)+X\phi_1(\xi,\eta)+X^2\phi_2(\xi,\eta)+\ldots\} \\ p &= \rho U^2\{p_0(\xi,\eta)+Xp_1(\xi,\eta)+X^2p_2(\xi,\eta)+\ldots\} \end{aligned}\right\}. \tag{3.2}$$

It is also convenient to write

$$u = U\{q(\xi,\eta)+Xq_1(\xi,\eta)+X^2q_2(\xi,\eta)+\ldots\}, \tag{3.3}$$

so that, from (2.4), (3.1), and (3.2) we have

$$4(\xi^2+\eta^2)q = \frac{\partial g}{\partial \eta}, \quad \text{etc.} \tag{3.4}$$

If these expressions are substituted in the equations (2.5)–(2.7), and the coefficients of the various powers of X are then equated to zero, we obtain the following equations. From (2.6) and (2.7),

$$\frac{\partial p_0}{\partial \xi} = \frac{\partial p_0}{\partial \eta} = \frac{\partial p_1}{\partial \xi} = \frac{\partial p_1}{\partial \eta} = 0, \tag{3.5}$$

$$\begin{aligned}(\xi^2+\eta^2)^2 q \frac{\partial}{\partial \eta}(\xi\phi_\xi+\eta\phi_\eta)+(\xi^2+\eta^2)\phi_\eta\phi_{\xi\eta}- \\ -(\xi^2+\eta^2)\phi_{\eta\eta}(\phi_\xi-k)-\xi\{\phi_\eta^2+(\phi_\xi-k)^2\} \\ = -(\xi^2+\eta^2)^2 P_\xi-(\xi^2+\eta^2)(\phi_{\xi\xi\eta}+\phi_{\eta\eta\eta}-k_{\xi\eta})+2\eta(\phi_{\xi\xi}+\phi_{\eta\eta}-k_\xi),\end{aligned} \tag{3.6}$$

$$\begin{aligned}(\xi^2+\eta^2)^2 q\left\{\frac{\partial}{\partial \xi}(\xi\phi_\xi+\eta\phi_\eta)-(k+\xi k_\xi+\eta k_\eta)\right\}+(\xi^2+\eta^2)\phi_\eta(\phi_{\xi\xi}-k_\xi)- \\ -(\xi^2+\eta^2)(\phi_\xi-k)(\phi_{\xi\eta}-k_\eta)+\eta\{\phi_\eta^2+(\phi_\xi-k)^2\} \\ = (\xi^2+\eta^2)^2 P_\eta-(\xi^2+\eta^2)(\phi_{\xi\xi\xi}+\phi_{\xi\eta\eta}-k_{\xi\xi})+2\xi(\phi_{\xi\xi}+\phi_{\eta\eta}-k_\xi),\end{aligned} \tag{3.7}$$

where
$$P = 4p_2-\xi q_\xi-\eta q_\eta$$
and
$$4k = 3g-\xi g_\xi-\eta g_\eta \Bigg\}. \tag{3.8}$$

From (2.5), using the results of (3.5), we have

$$-(\xi^2+\eta^2)\xi q q_\xi+q_\eta(\phi_\xi-\tfrac{3}{4}g+\tfrac{1}{4}\xi g_\xi)-\phi_\eta q_\xi = q_{\xi\xi}+q_{\eta\eta}. \tag{3.9}$$

There are further equations for g_1, ϕ_1, etc., which will be neglected. The above equations, therefore, will describe the flow over the plate provided X is small; that is, at sufficiently large distances downstream from the leading edge of the plate. Equations (3.6)–(3.9), together with equation (3.4), are thus appropriate boundary layer equations for this problem.

The expressions for the velocity components are, from relations (2.4), (3.1), and (3.4),

$$\left.\begin{aligned}4(\xi^2+\eta^2)u &= Ug_\eta \quad (u = Uq) \\ 2(\xi^2+\eta^2)^{\frac{1}{2}}v &= -\left(\frac{\nu U}{x}\right)^{\frac{1}{2}}\phi_\eta \\ 2(\xi^2+\eta^2)^{\frac{1}{2}}w &= \left(\frac{\nu U}{x}\right)^{\frac{1}{2}}(\phi_\xi-k)\end{aligned}\right\}. \tag{3.10}$$

It is clear that the above equations of motion are much more involved than the boundary layer equations for two-dimensional flow past a flat plate, even when allowance is made for the complications introduced by the choice of coordinate system. In particular, in the two-dimensional problem the component of velocity normal to the plate is obtained by simple integration

of the equation of continuity; in this problem, however, the transverse components of velocity depend on the determination of ϕ, which satisfies the fourth order partial differential equation obtained by eliminating P between equations (3.6) and (3.7).

It remains to formulate boundary conditions for u, v, and w. The surface of the plate is defined completely by the single condition $\eta = 0$; further, as $\eta \to \infty$ (for any fixed value of x) we move everywhere away from the plate into the main stream of the fluid. The surface $\xi = 0$ is the plane extending away from the edge of the plate into the fluid, and coplanar with the plate. As $\xi \to \pm\infty$ we move away from this edge across the plate along its upper and lower sides respectively. This is illustrated in Fig. 1. The boundary conditions are therefore

$$u = v = w = 0, \quad \text{when } \eta = 0,$$

and

$$u \to U, \quad \text{as } \eta \to \infty.$$

Since ϕ satisfies a fourth order differential equation it should be possible also to specify boundary conditions on v and w as $\eta \to \infty$, namely

$$v, w \to 0, \quad \text{as } \eta \to \infty.$$

For the reason given above, it is not possible to impose this type of boundary condition in the two-dimensional problem. From the expressions (3.10), the boundary conditions will be satisfied provided

$$\left.\begin{aligned} q = \phi_\eta = \phi_\xi - k = 0 \quad &\text{when } \eta = 0 \\ q \to 1, \qquad \phi_\eta, \phi_\xi - k \to 0 \quad &\text{as } \eta \to \infty \end{aligned}\right\}. \tag{3.11}$$

4. The flow near the edge of the plate

The feature of special interest in this problem is the flow in the vicinity of the edge of the plate, where ξ is small. We seek therefore a solution of the boundary layer equations in the form of a series of powers of ξ, the coefficients being functions of η. It is clear that q, g, and P must be even functions, and ϕ an odd function, of ξ.

At this stage it is convenient to introduce a change of scale in the coordinate system by writing

$$\left.\begin{aligned} c\xi &= \xi_1 \\ c\eta &= \eta_1 \end{aligned}\right\}, \tag{4.1}$$

where the constant c will be determined at a later stage. Hence, if P is eliminated between the equations (3.6) and (3.7), and we write

$$\left.\begin{aligned} q &= \tfrac{1}{3}c^4\{u_0(\eta_1)+\xi_1^2 u_2(\eta_1)+\xi_1^4 u_4(\eta_1)+\ldots\} \\ g &= \tfrac{1}{3}c\{f_0(\eta_1)+\xi_1^2 f_2(\eta_1)+\xi_1^4 f_4(\eta_1)+\ldots\} \\ \phi &= \xi_1\psi_1(\eta_1)+\xi_1^3\psi_3(\eta_1)+\xi_1^5\psi_5(\eta_1)+\ldots \end{aligned}\right\}, \tag{4.2}$$

we obtain a set of equations to determine the functions which appear as coefficients of powers of ξ_1. The conditions (3.11) give the following boundary conditions on these functions

$$\left.\begin{aligned} &\left.\begin{aligned} u_0 = u_2 = u_4 = \ldots = 0 \\ \psi_1' = \psi_3' = \ldots = 0 \\ \psi_1 - f_0 = \psi_3 - \tfrac{1}{9} f_2 = \ldots = 0 \end{aligned}\right\} \quad \text{when } \eta_1 = 0 \\ &\left.\begin{aligned} u_0 \to 3/c^4, \qquad u_2, u_4, \ldots \to 0 \\ \psi_1', \psi_3', \ldots \to 0 \\ \psi_1 - f_0 + \tfrac{1}{3}\eta_1 f_0', \qquad \psi_3 + \tfrac{1}{9}(\eta_1 f_2' - f_2) \to 0 \end{aligned}\right\} \quad \text{as } \eta_1 \to \infty \end{aligned}\right\} \tag{4.3}$$

and we may complete the definition of g by taking $f_r(0) = 0$ $(r = 0, 2, \ldots)$. The first pair of equations is

$$u_0'' + (f_0 - \psi_1) u_0' + 2u_2 = 0, \tag{4.4}$$

$$f_0' = \eta_1^2 u_0, \tag{4.5}$$

and although u_0 may be eliminated easily to provide a single differential equation it is preferable, for numerical calculation, to retain the equations as they stand. The remaining equations become progressively more complicated.

It is clear that the process of solving such equations is complicated by the appearance of higher order terms in the equations. For example, equation (4.4) contains the terms $\psi_1 u_0'$ and $2u_2$. The proposed method of solution, therefore, amounts to an iterative procedure, in which the expansions (4.2) are first developed in stages. The higher order terms are thus neglected in the first place in the equations, which are then solved to give approximate values of the various functions; these approximate values are then used in the complete equations to give second approximations for the functions. Thus we begin with

$$\left.\begin{aligned} q &= \tfrac{1}{3} c^4 u_0(\eta_1) \\ g &= \tfrac{4}{3} c f_0(\eta_1) \\ \phi &= 0 \end{aligned}\right\}, \tag{4.6}$$

so that the terms which are independent of ξ_1 in equations (3.4) and (3.9) are zero provided

$$u_0'' + u_0' f_0 = 0, \tag{4.7}$$

$$f_0' = \eta_1^2 u_0, \tag{4.8}$$

and the boundary conditions are

$$\left.\begin{aligned} u_0(0) = 0, \qquad f_0(0) = 0 \\ u_0 \to 3/c^4 \quad \text{as } \eta_1 \to \infty \end{aligned}\right\}. \tag{4.9}$$

The reason for the change of scale in the coordinates ξ, η is now clear.

Following Töpfer's method (5) for the solution of the Blasius equation, the numerical solution of the above equations may be simplified by replacing the last boundary condition by the condition

$$u_0'(0) = 1, \tag{4.10}$$

and the scale factor c is then determined by writing

$$ac^4 = 3, \tag{4.11}$$

where a is the asymptotic value assumed by u_0 for large values of η_1.

Equations (4.7) and (4.8) were solved numerically by the Adams–Bashforth method, and the results of this first approximation for u_0 and f_0 are shown in Table 1. This table may be extended by use of the asymptotic solution of the equations, which is found to be

$$\left.\begin{aligned} u_0 &= a - A\int_{\eta_1}^{\infty} \exp(-\tfrac{1}{12}ax^4+bx)\,dx \\ f_0 &= \tfrac{1}{3}a\eta_1^3 - b + \tfrac{1}{3}A\int_{\eta_1}^{\infty} (x^3-\eta_1^3)\exp(-\tfrac{1}{12}ax^4+bx)\,dx \end{aligned}\right\}, \tag{4.12}$$

in which the values of the constants are

$$a = 1{\cdot}68465, \qquad b = 0{\cdot}8922, \qquad A = 0{\cdot}345. \tag{4.13}$$

The relation (4.11) now gives $c = 1{\cdot}15519$.

With these first approximations for u_0 and f_0, the next stage is to extend the expansion (4.6) by introducing ψ_1, so that

$$q = \tfrac{1}{3}c^4u_0(\eta_1), \qquad g = \tfrac{4}{3}cf_0(\eta_1), \qquad \phi = \xi_1\psi_1(\eta_1), \tag{4.14}$$

where u_0, f_0 are now regarded as already determined. The coefficient of ξ_1 in the equation for ϕ is then zero provided

$$\psi_1^{\mathrm{iv}} + \left(f_0 - \psi_1 - \frac{4}{\eta_1}\right)\psi_1''' + \left(\tfrac{5}{3}u_0\eta_1^2 + \psi_1' - \frac{2}{\eta_1}(f_0-\psi_1)\right)\psi_1'' + \tfrac{2}{3}\eta_1^2u_0'\psi_1' = 0, \tag{4.15}$$

and the boundary conditions for ψ_1, from (4.3) and (4.12), are now clearly

$$\left.\begin{aligned} \psi_1(0) = \psi_1'(0) &= 0 \\ \psi_1' \to 0, \qquad \psi_1 \to -b = -0{\cdot}8922 &\quad \text{as } \eta_1 \to \infty \end{aligned}\right\}. \tag{4.16}$$

Equation (4.15) is, of course, non-linear in ψ_1. But it should be remembered that this method can yield approximations only for the various functions. In fact the first approximations for u_0 and f_0 have been derived by neglecting ψ_1 in the coefficient $\psi_1 - f_0$; further, the full equation for ψ_1 (which involves the higher order terms) introduces further terms on the right-hand side of the equation. It is consistent with the iterative procedure,

TABLE 1

Values of the functions u_0, f_0, ψ_1, u_2, and f_2

(see equations 4.7, 4.8, 4.17, 4.19, 4.20, 4.4, 4.5)

	First approximation			*Second approximation*		*First approximation*	
η_1	u_0	u_0'	f_0	u_0	f_0	$-\psi_1$	$-\psi_1'$
0	0	1·00000	0	0	0	0	0
0·05	0·05000	1·00000	0	0·0500	0	0·0003	0·0107
0·10	0·10000	1·00000	0·00003	0·1000	0	0·0011	0·0213
0·15	0·15000	1·00000	0·00013	0·1499	0·0001	0·0024	0·0320
0·20	0·20000	0·99998	0·00040	0·1997	0·0004	0·0043	0·0427
0·25	0·25000	0·99995	0·00098	0·2494	0·0009	0·0067	0·0534
0·30	0·29999	0·99988	0·00203	0·2989	0·0019	0·0096	0·0641
0·35	0·34999	0·99974	0·00375	0·3482	0·0036	0·0131	0·0747
0·40	0·39997	0·99949	0·00640	0·3973	0·0062	0·0171	0·0855
0·45	0·44993	0·99908	0·01025	0·4461	0·0100	0·0216	0·0963
0·50	0·49987	0·99844	0·01562	0·4945	0·0152	0·0267	0·1071
0·55	0·54977	0·99749	0·02287	0·5426	0·0223	0·0323	0·1180
0·60	0·59961	0·99612	0·03239	0·5903	0·0316	0·0385	0·1289
0·65	0·64937	0·99422	0·04461	0·6374	0·0436	0·0452	0·1400
0·70	0·69902	0·99163	0·05999	0·6840	0·0586	0·0525	0·1512
0·75	0·74852	0·98821	0·07903	0·7300	0·0771	0·0604	0·1625
0·80	0·79783	0·98376	0·10228	0·7752	0·0996	0·0688	0·1739
0·85	0·84688	0·97808	0·13029	0·8196	0·1267	0·0777	0·1855
0·90	0·89561	0·97094	0·16367	0·8631	0·1588	0·0873	0·1974
0·95	0·94394	0·96210	0·20305	0·9056	0·1966	0·0975	0·2095
1·00	0·99179	0·95131	0·24908	0·9470	0·2406	0·1083	0·2218
1·05	1·03904	0·93832	0·30246	0·9872	0·2913	0·1197	0·2342
1·10	1·08558	0·92285	0·36387	1·0260	0·3494	0·1317	0·2468
1·15	1·13128	0·90466	0·43405	1·0634	0·4155	0·1443	0·2594
1·20	1·17599	0·88351	0·51373	1·0993	0·4900	0·1576	0·2719
1·25	1·21958	0·85921	0·60365	1·1335	0·5738	0·1715	0·2843
1·30	1·26186	0·83160	0·70454	1·1659	0·6671	0·1861	0·2962
1·35	1·30268	0·80060	0·81714	1·1964	0·7708	0·2012	0·3075
1·40	1·34186	0·76619	0·94219	1·2250	0·8852	0·2168	0·3181
1·45	1·37924	0·72846	1·08038	1·2516	1·0109	0·2330	0·3276
1·50	1·41466	0·68757	1·23240	1·2761	1·1483	0·2496	0·3359
1·55	1·44795	0·64384	1·39889	1·2985	1·2980	0·2666	0·3429
1·60	1·47900	0·59766	1·58046	1·3187	1·4603	0·2839	0·3481
1·65	1·50769	0·54957	1·77769	1·3369	1·6356	0·3014	0·3515
1·70	1·53393	0·50019	1·99110	1·3530	1·8243	0·3190	0·3529
1·75	1·55769	0·45023	2·22115	1·3672	2·0266	0·3367	0·3522
1·80	1·57896	0·40045	2·46827	1·3795	2·2430	0·3542	0·3493
1·85	1·59775	0·35165	2·73285	1·3900	2·4736	0·3716	0·3441
1·90	1·61415	0·30460	3·01521	1·3988	2·7187	0·3886	0·3370
1·95	1·62826	0·26003	3·31565	1·4062	2·9785	0·4053	0·3279
2·00	1·64021	0·21858	3·63444	1·4123	3·2534	0·4214	0·3171
2·05	1·65017	0·18074	3·97181	1·4172	3·5434	0·4370	0·3050
2·10	1·65835	0·14688	4·32800	1·4211	3·8489	0·4519	0·2917
2·15	1·66493	0·11721	4·70322	1·4241	4·1701	0·4662	0·2776
2·20	1·67014	0·09174	5·09769	1·4264	4·5072	0·4797	0·2631
2·25	1·67418	0·07038	5·51164	1·4282	4·8605	0·4925	0·2485
2·30	1·67724	0·05285	5·94532	1·4295	5·2303	0·5045	0·2339
2·35	1·67952	0·03882	6·39900	1·4304	5·6167	0·5159	0·2196
2·40	1·68117	0·02786	6·87293	1·4311	6·0202	0·5265	0·2061

TABLE 1 (*continued*)

	First approximation			*Second approximation*		*First approximation*	
η_1	u_0	u_0'	f_0	u_0	f_0	$-\psi_1$	$-\psi_1'$
2·45	1·68235	0·01952	7·36745	1·4316	6·4410	0·5365	0·1934
2·50	1·68316	0·01333	7·88287	1·4319	6·8795	0·5458	0·1815
2·55	1·68371	0·00887	8·41955	1·4321	7·3360	0·5546	0·1705
2·60	1·68407	0·00574	8·97783	1·4322	7·8107	0·5629	0·1604
2·65	1·68431	0·00361	9·55811	1·4323	8·3041	0·5707	0·1513
2·70	1·68445	0·00221	10·16077	1·4323	8·8165	0·5780	0·1429
2·75	1·68453	0·00131	10·78621	1·4324	9·3483	0·5850	0·1351
2·80	1·68458	0·00075	11·43483	1·4324	9·8997	0·5915	0·1281
2·85				1·4324	10·4713	0·5978	0·1218
2·90				1·4324	11·0632	0·6037	0·1159
2·95				1·4324	11·6759	0·6094	0·1105
3·00				1·4324	12·3098	0·6148	0·1057
3·10						0·6249	0·0970
3·20						0·6342	0·0896
3·30						0·6428	0·0829
3·40						0·6508	0·0768
3·50						0·6582	0·0710
3·60						0·6650	0·0658
3·70						0·6714	0·0618
3·80						0·6774	0·0584
3·90						0·6831	0·0552
4·00						0·6884	0·0524

TABLE 1 (*continued*)

First approximation

η_1	u_2	f_2	η_1	u_2	f_2	η_1	u_2	f_2
0	0	0	1·00	0·1008	0·5255	2·00	0·0317	2·0822
0·05	0·0058	0·0013	1·05	0·1032	0·5817	2·05	0·0262	2·1704
0·10	0·0115	0·0050	1·10	0·1050	0·6408	2·10	0·0213	2·2582
0·15	0·0172	0·0113	1·15	0·1062	0·7029	2·15	0·0169	2·3456
0·20	0·0230	0·0200	1·20	0·1067	0·7680	2·20	0·0132	2·4325
0·25	0·0287	0·0314	1·25	0·1065	0·8359	2·25	0·0101	2·5190
0·30	0·0344	0·0452	1·30	0·1055	0·9066	2·30	0·0075	2·6050
0·35	0·0401	0·0617	1·35	0·1037	0·9799	2·35	0·0055	2·6907
0·40	0·0457	0·0807	1·40	0·1012	1·0557	2·40	0·0039	2·7760
0·45	0·0512	0·1024	1·45	0·0978	1·1339	2·45	0·0027	2·8610
0·50	0·0567	0·1267	1·50	0·0937	1·2142	2·50	0·0018	2·9459
0·55	0·0621	0·1538	1·55	0·0889	1·2965	2·55	0·0012	3·0305
0·60	0·0674	0·1836	1·60	0·0835	1·3804	2·60	0·0008	3·1150
0·65	0·0725	0·2162	1·65	0·0776	1·4657	2·65	0·0005	3·1994
0·70	0·0774	0·2516	1·70	0·0712	1·5523	2·70	0·0003	3·2838
0·75	0·0821	0·2899	1·75	0·0645	1·6397	2·75	0·0002	3·3681
0·80	0·0866	0·3311	1·80	0·0577	1·7278	2·80	0·0001	3·4524
0·85	0·0907	0·3752	1·85	0·0509	1·8163	2·85	0·0001	
0·90	0·0945	0·4223	1·90	0·0442	1·9050	2·90	0·0000	
0·95	0·0978	0·4724	1·95	0·0378	1·9937			

therefore, to neglect the non-linear terms in (4.15) in deriving a first approximation for ψ_1. The equation then becomes

$$\psi_1^{iv}+\left(f_0-\frac{4}{\eta_1}\right)\psi_1'''+\left(\tfrac{5}{3}u_0\,\eta_1^2-\frac{2}{\eta_1}f_0\right)\psi_1''+\tfrac{2}{3}\eta_1^2 u_0'\psi_1'=0. \qquad (4.17)$$

This equation, with boundary conditions (4.16), was solved by use of the finite difference form of the equation, with an interval of 0·05 in η_1 (this method was used for the solution of all the remaining equations). The values of ψ_1 and ψ_1' are shown in Table 1; it will be seen that ψ_1 does not tend rapidly to its limiting value, and this may be expected since an asymptotic solution of equation (4.17) yields a complementary function which behaves like η^{-1} for large values of η_1.

The next stage is the introduction of the functions u_2 and f_2, for which we take

$$q=\tfrac{1}{3}c^4(u_0+\xi_1^2 u_2), \qquad g=\tfrac{4}{3}c(f_0+\xi_1^2 f_2), \qquad \phi=\xi_1\psi_1, \qquad (4.18)$$

so that

$$u_2''+(f_0-\psi_1)u_2'+(\tfrac{2}{3}\eta_1^2 u_0+2\psi_1')u_2+\tfrac{1}{3}u_0'f_2=0, \qquad (4.19)$$

$$f_2'=u_0+\eta_1^2 u_2, \qquad (4.20)$$

with boundary conditions $u_2(0)=f_2(0)=0$, $u_2\to 0$ as $\eta_1\to\infty$. The calculation showed that these boundary conditions are not sufficient to define a unique solution for u_2 and f_2—the condition at infinity appeared to be automatically satisfied by any solution which satisfied the conditions at $\eta_1=0$. A unique solution was obtained by making u_2 tend to zero exponentially, in the same way that u_0 tends to the constant value a, and it is reasonable to suppose that u_2 must also behave in this way. Table 1 shows the values of u_2 and f_2.

The next stages in the calculation would be the determination of approximations for ψ_3, u_4, f_4, etc., but the functions already calculated are sufficient to provide a second approximation for u_0 and f_0, which is the main purpose of this paper. We return now to equations (4.4) and (4.5), and solve them with the same boundary conditions as before, using for ψ_1 and u_2 the approximations which have been derived; the results are shown in Table 1.

In this second approximation, the new values of the constants a, b, c are

$$a=1{\cdot}4324, \qquad b=0{\cdot}5819, \qquad c=1{\cdot}2030, \qquad (4.21)$$

so that a shows a 15% decrease from its original value, b a 35% decrease, and c a 4% increase. The change in b is substantial, so that the tabulated values of ψ_1 are probably too large numerically. However, an initial change of this order in ψ_1 (and also, probably, a similar decrease in u_2) might well be expected, since we began by taking $\psi_1=u_2=0$ in the calculation of

the original value of a, where the change is now only 15%. The evidence suggests that further stages in the iteration would yield a slightly lower change in a than this. Table 1 shows that the percentage changes in u_0 and f_0, for all values of η_1, vary from zero to a maximum of 15.

It is clear that it would be desirable to continue the calculations, both to improve the approximations and to obtain some information about the convergence of the iterative process, but the work becomes progressively heavier. For example, in order to complete the next cycle in the process, which is to obtain a third approximation for u_0 and f_0 (and thus a new limiting value for ψ_1), it would be necessary to solve six further differential equations of which three would be of the fourth order. This and further work, indeed, might well require the use of an electronic computer. As far as can be judged there is no difficulty in extending the calculations, other than the considerable labour which is involved.

5. Discussion of results

The above approximations give an indication of certain features of the boundary layer. If the coordinates

$$Y = \left(\frac{U}{\nu x}\right)^{\frac{1}{2}} y, \qquad Z = \left(\frac{U}{\nu x}\right)^{\frac{1}{2}} z, \tag{5.1}$$

are now introduced, then in the plane $z = 0, y \leqslant 0$ (so that $\xi_1 = 0$) u attains a value within 1% of its main stream value when $\eta_1 = 2{\cdot}15$ (first approximation) and $\eta_1 = 2{\cdot}1$ (second approximation); the corresponding values of Y are $-3{\cdot}46$ and $-3{\cdot}06$ respectively. If we regard the 1% criterion as defining the thickness of the boundary layer, then the corresponding value in the flow over an infinite flat half plate (the Blasius problem) is $Z = 5{\cdot}0$, the coordinate z being measured along a normal to the plate. The ratio of the two thicknesses is therefore 0·69 for the first approximation, and 0·61 for the second approximation. It is probable that the true value of the ratio lies between these values, and is close to 0·61. The results agree with Howarth's prediction (**1**) that a certain decrease in the boundary layer thickness is to be expected in the vicinity of the edge.

The behaviour of the skin friction on the plate near the edge is of chief interest here. If τ denotes the component, measured in the direction of the main stream, of skin friction per unit area, then

$$\tau = \mu\left(\frac{\partial u}{\partial z}\right)_{z=0} = \tfrac{1}{6}\mu U\left(\frac{U}{\nu x}\right)^{\frac{1}{2}} \frac{c^5}{Y^{\frac{1}{2}}}\{u_0'(0)+c^2 Y u_2'(0)+\ldots\}$$

$$= \tfrac{1}{6}\mu U\left(\frac{U}{\nu x}\right)^{\frac{1}{2}} \frac{c^5}{Y^{\frac{1}{2}}}\{1+c^2 Y u_2'(0)+\ldots\} \quad (Y > 0), \tag{5.2}$$

where the prime denotes differentiation with respect to η_1. This expression

indicates a singularity in the density of skin friction at the edge of the plate. The order of the singularity is that predicted by the use of Rayleigh's hypothesis (Howarth (1)) which gives, as the leading terms in τ,

$$\tau = \frac{2\sqrt{2}}{\pi^{\frac{1}{2}}}\mu U\left(\frac{U}{\nu x}\right)^{\frac{1}{2}}\frac{\Gamma(\frac{5}{4})}{Y^{\frac{1}{4}}}\{1+0{\cdot}33773Y+\ldots\} \tag{5.3}$$

where $\Gamma(\frac{5}{4}) = 0{\cdot}9064$.

The limit of the ratio of the value given by result (5.2) to the value given by (5.3), as $Y \to +0$, is 0·7447 with the first approximation for c, and 0·9120 with the second approximation. This last ratio is probably slightly higher than the true value. The second approximation also provides an estimate of the coefficient of $Y^{\frac{1}{4}}$ in (5.2); the value of $u_2'(0)$ is 0·1150, so that

$$c^2u_2'(0) = 0{\cdot}1664.$$

This is about one-half the corresponding coefficient in (5.3).

REFERENCES

1. L. Howarth, *Proc. Camb. Phil. Soc.* **46** (1950) 127.
2. L. Sowerby, *Phil. Mag.* (7) **42** (1951) 176.
3. —— and J. C. Cooke, *Quart. J. Mech. App. Math.* **6** (1953) 50.
4. G. F. Carrier, *Quart. Appl. Math.* **4** (1946) 367.
5. C. Töpfer, *Z. f. Math. u. Phys.* **60** (1912) 397.

A SOLUTION OF THE NAVIER–STOKES EQUATIONS ILLUSTRATING THE RESPONSE OF A LAMINAR BOUNDARY LAYER TO A GIVEN CHANGE IN THE EXTERNAL STREAM VELOCITY

By J. WATSON (*National Physical Laboratory, Teddington, Middlesex*)

[Received 5 September 1957]

SUMMARY

Exact solutions of the Navier–Stokes equations are derived by a Laplace-transform technique for two-dimensional, incompressible flow past an infinite plane porous wall. It is assumed that the flow is independent of the distance parallel to the wall and that the velocity component normal to the wall is constant. A general formula is derived for the velocity distribution as a function of the given free-stream velocity and, from this, general formulae for the skin friction and displacement thickness are obtained.

Among the particular cases considered are (i) flow in which the free-stream velocity is changed impulsively from one value to another, (ii) uniform acceleration of the main stream from a given value of the velocity, and (iii) flow in which the free-stream velocity consists of a mean value with a superimposed decaying oscillation. In the first case a secondary boundary layer of a Rayleigh impulsive flow type is created immediately after the impulsive increase in free-stream velocity and this secondary layer increases in thickness with time until the final steady state is reached. In the second case also, a secondary boundary layer is formed at the instant when the free-stream velocity begins to accelerate and ultimately the skin friction consists of a quasi-steady part and a part proportional to the product of the free-stream acceleration and a 'virtual mass' equal to the mass of fluid in the displacement area. In the final case the fluctuating skin friction is found to have a phase advance over the fluctuating free-stream velocity. For sufficiently large frequencies this phase advance is $\frac{1}{4}\pi$ and the amplitude of the skin friction fluctuation is proportional to the square root of the frequency and to the amplitude of the free-stream velocity fluctuation.

1. Introduction

LIGHTHILL (1) has investigated the effect of fluctuations of the external stream on the boundary layer of a two-dimensional body. In addition, Stuart (2) has obtained an exact solution of the Navier–Stokes equations for the case of fluctuating flow past an infinite plane wall with constant suction, and has compared some of his results with Lighthill's. This paper is an extension of Stuart's work to the case of general unsteady flows past the wall, but with the suction still held constant.

The generalization of the velocity field is effected by means of a Laplace-transform technique; many forms of the time-dependent external stream

velocity can be considered, since the mathematical conditions which the velocity must satisfy are only very weak. General formulae are given for the boundary-layer velocity distribution and for the skin friction. Among the particular cases considered are (i) flows in which the external stream velocity goes from one value to another, either impulsively or with acceleration, (ii) the case of a uniform acceleration from a given value of the velocity, and (iii) the case of an external stream which consists of a mean value with a superimposed decaying oscillation.

Immediately after an impulsive increase of velocity at time $t = 0$, a secondary boundary layer is created whose thickness is of order $\sqrt{(\nu t)}$, where ν is the kinematic viscosity. Outside this thin layer the main boundary layer behaves as if it were inviscid, and at each point has its initial value plus the same impulse as is given to the external flow. As time progresses the secondary layer increases in thickness and gradually distorts the flow until the ultimate steady-state boundary layer is reached. It follows that because of the presence of the very thin secondary layer, the skin friction at first rises to a large value, and then decays to its ultimate steady value as the secondary layer increases in thickness. The initial thin secondary layer is of the form of a Rayleigh impulsive flow, and it can be inferred that when any boundary layer is given an impulsive shift from one velocity to another, the flow will react as though it were inviscid except within a thin secondary layer. In a separating boundary-layer flow it can further be inferred that the large rise in skin friction would have an appreciable effect on the transient position of the point of separation.

In the case of a boundary layer with an external stream accelerating uniformly from a given value at $t = 0$, a secondary boundary layer is formed at small times whose thickness is of order $\sqrt{(\nu t)}$, and for a free stream $U_0(1+kt)$ the skin friction initially grows like $t^{\frac{1}{2}}$. This result follows because outside the thin secondary layer the fluid behaves as though it were inviscid and has its velocity increased by $U_0 kt$; thus the *increase* in velocity rises from zero at the wall to $U_0 kt$ in a distance of order $\sqrt{(\nu t)}$, leading to the above skin-friction growth. The skin friction at large times is found to consist of two parts, the first of which is the same as if the skin friction were steady at the instantaneous free-stream speed. Together with this quasi-steady skin friction is a part which is proportional to the product of the free-stream acceleration and a 'virtual mass' equal to the mass of fluid in the displacement area; this second part of the skin friction arises because, through the action of viscosity, the pressure gradient does not accelerate the fluid in the boundary layer as much as the free-stream and consequently there is a virtual acceleration in the negative direction, corresponding to a drag. By combining two accelerations at different

times, the case of a fluid accelerating from one velocity to another is considered.

The final case dealt with is that in which the free-stream velocity is constant for $t < 0$ and has a superimposed decaying oscillation for $t > 0$. The skin friction is found to have a phase advance over the velocity fluctuation. For sufficiently large frequencies or, in other words, for a small logarithmic decrement, the skin friction behaves as though the free-stream oscillation were a non-decaying one with its instantaneous amplitude. Then the amplitude of the skin friction fluctuation is proportional to the product of the square root of the frequency and the instantaneous amplitude of the free-stream velocity fluctuation; moreover, the phase advance is $\frac{1}{4}\pi$. In this quasi-harmonic state, conditions are analogous to those for pure oscillatory flows of high frequency (Lighthill (**1**)).

A final point is that the velocity distributions obtained by E. J. Watson (**3**) for the flow past an infinite flat plate without suction are particular cases of the general solution given in this paper.

2. List of symbols

x	coordinate parallel to wall.
y	coordinate normal to wall.
t	time.
t_c	characteristic time.
p	pressure.
u	velocity in x-direction.
v	velocity in y-direction.
$U(t)$	free-stream velocity.
U_0	constant reference velocity.
v_w	(constant) velocity component normal to wall.
ρ	density of fluid.
μ	viscosity of fluid.
ν	kinematic viscosity of fluid (μ/ρ).
$\zeta_0(y)$	defined by equation (3.4).
$f(t), g(y,t)$	defined by equation (3.5).
T	non-dimensional time ($tv_w^2/4\nu$).
T_c	non-dimensional characteristic time.
η	non-dimensional distance normal to wall ($y\lvert v_w\rvert/\nu$).
Ω	non-dimensional frequency.
δ_{10}	steady displacement thickness ($\nu/\lvert v_w\rvert$).
δ_1	displacement thickness, defined by equation (3.13).
τ_w	skin friction.

$\operatorname{erf} x$ error function $\left(\dfrac{2}{\pi^{\frac{1}{2}}}\displaystyle\int_0^x e^{-x^2}\,dx\right)$.

$\operatorname{erfc} x$ $1-\operatorname{erf} x$.

$C(x)$ Fresnel integral $\left[\dfrac{1}{(2\pi)^{\frac{1}{2}}}\displaystyle\int_0^x \frac{\cos x\,dx}{x^{\frac{1}{2}}}\right]$.

$S(x)$ Fresnel integral $\left[\dfrac{1}{(2\pi)^{\frac{1}{2}}}\displaystyle\int_0^x \frac{\sin x\,dx}{x^{\frac{1}{2}}}\right]$.

3. General theory

Let x denote the distance along a two-dimensional, infinite, plane porous wall, y the distance normal to it, u and v the corresponding components of velocity, t the time, p the pressure, ρ the density, and ν the kinematic viscosity. For two-dimensional incompressible flow which is independent of x, the Navier–Stokes equations and the equation of continuity are

$$\left.\begin{aligned} \frac{\partial u}{\partial t}+v\frac{\partial u}{\partial y} &= -\frac{1}{\rho}\left(\frac{\partial p}{\partial x}\right)+\nu\frac{\partial^2 u}{\partial y^2} \\ \frac{\partial v}{\partial t} &= -\frac{1}{\rho}\left(\frac{\partial p}{\partial y}\right) \\ \frac{\partial v}{\partial y} &= 0 \end{aligned}\right\}, \tag{3.1}$$

subject to the boundary conditions $u = 0$ at $y = 0$ and $u \to U(t)$ as $y \to \infty$, $U(t)$ being the free-stream velocity. In order to obtain a *steady* solution of the boundary-layer type it is known that v must be a negative, non-zero constant (v_w). In the unsteady case also we shall make this restriction (Stuart (**2**)); then p is independent of y, $-(1/\rho)\,\partial p/\partial x$ equals dU/dt, and the first equation (3.1) becomes

$$\frac{\partial u}{\partial t}+v_w\frac{\partial u}{\partial y}=\frac{dU}{dt}+\nu\frac{\partial^2 u}{\partial y^2}. \tag{3.2}$$

Stuart (**2**) considered a periodic velocity field of the form

$$\left.\begin{aligned} U(t) &= U_0[1+\epsilon e^{i\omega t}] \\ u &= U_0[\zeta_0(y)+\epsilon\zeta_1(y)e^{i\omega t}] \\ v &= v_w \end{aligned}\right\}, \tag{3.3}$$

where ϵ is a constant, and found that

$$\zeta_0(y) = 1-\exp(-y|v_w|/\nu)$$

and

$$\zeta_1(y) = 1-\exp(-hy|v_w|/\nu), \tag{3.4}$$

where $h = \frac{1}{2}\{1+\sqrt{(1+4i\omega\nu/v_w^2)}\}$. He also pointed out the existence of an exact solution of (3.1) of the form†

$$\left.\begin{aligned} U(t) &= U_0[1+f(t)] \\ u &= U_0[\zeta_0(y)+g(y,t)] \\ v &= v_w \end{aligned}\right\}, \tag{3.5}$$

where $\zeta_0(y)$ is given by (3.4) and where $f(t)$ is a given arbitrary function and $g(y,t)$ is a function to be determined. The present paper deals with an investigation of this generalized case.‡

Let us first make the transformation

$$T = tv_w^2/4\nu = \nu t/4\delta_{10}^2, \qquad \eta = y|v_w|/\nu, \tag{3.6}$$

where δ_{10} is the steady displacement thickness $(\nu/|v_w|)$. Substituting (3.5) in (3.2) and utilizing the fact that ζ_0 is given by (3.4) we obtain

$$\frac{\partial g(\eta,T)}{\partial T} - 4\frac{\partial g(\eta,T)}{\partial \eta} = f'(T)+4\frac{\partial^2 g(\eta,T)}{\partial \eta^2} \tag{3.7}$$

with the boundary conditions $g = 0$ at $\eta = 0$ and $g \to f(T)$ as $\eta \to \infty$.

In solving (3.7) we use the two-sided Laplace transform, which eliminates the independent variable T. It is defined by van der Pol and Bremmer (6) (with a change of notation) as

$$\bar{x}(p) = p\int_{-\infty}^{\infty} e^{-pT}x(T)\,dT.$$

The inverse is

$$x(T) = \frac{1}{2\pi i}\int_{c-i\infty}^{c+i\infty} e^{pT}\frac{\bar{x}(p)}{p}\,dp.$$

A formal solution of (3.7) by the Laplace transform technique will now be derived. To do this we note that the transform of the first term on the left-hand side of (3.7) is

$$p\int_{-\infty}^{\infty} e^{-pT}\frac{\partial g(\eta,T)}{\partial T}\,dT = p^2\int_{-\infty}^{\infty} e^{-pT}g\,dT = p\bar{g}(\eta,p),$$

provided that $e^{-pT}g(\eta,T) \to 0$ as $T \to \pm\infty$, where $\bar{g}(\eta,p)$ is the transform of g. Similarly, the transform of $f'(T)$ is $p\bar{f}(p)$, provided that $e^{-pT}f(T) \to 0$ as $T \to \pm\infty$. The Laplace transform of (3.7) is therefore

$$\frac{d^2\bar{g}}{d\eta^2}+\frac{d\bar{g}}{d\eta}-\frac{p}{4}\bar{g} = -\frac{p}{4}\bar{f} \tag{3.8}$$

† After this work was completed, the author found that the solution when $U(t) = 0$ for $t < 0$ has been given by Hasimoto (4).

‡ There is also a solution of (3.1) in which the steady part of the free stream has a uniform shear. The unsteady part g of the velocity profile u is independent of the shear (Curle (5)) and so is given by the solution of this paper for zero shear.

with the boundary conditions

$$\left.\begin{aligned} \bar{g} &= 0 \quad \text{at } \eta = 0 \\ \bar{g} &\to \bar{f} \quad \text{as } \eta \to \infty \end{aligned}\right\}. \tag{3.9}$$

If $k = \frac{1}{2}\{1+\sqrt{(1+p)}\}$ and that branch of the square root is chosen which makes $\sqrt{(1+p)} = +1$ when $p = 0$, then the function $\bar{f}(1-e^{-k\eta})$ satisfies (3.8) and the boundary conditions (3.9); the real part of k is positive for all values of p with this choice of the square root. It follows that

$$\bar{g} = \bar{f}(1-e^{-k\eta}) \tag{3.10}$$

is the unique solution of (3.8) subject to (3.9).

It is now necessary to determine g. We first note that (3.10) is the product of two functions of p one of which, $\bar{f}(p)$, has a known inverse, $f(T)$. Thus the function g is best obtained by using the composition-product rule, namely that the inverse of

$$\frac{1}{p}\bar{x}_1(p)\bar{x}_2(p) \quad \text{is} \quad \int_{-\infty}^{\infty} x_1(\lambda)x_2(T-\lambda)\,d\lambda.$$

We identify $\bar{f}$ with $\bar{x}_2$, f with x_2, and $p(1-e^{-k\eta})$ with $\bar{x}_1$. We now need the inverse of the transform $p(1-e^{-k\eta})$. Using two standard results we find that this inverse is given by

$$\begin{aligned}
&\delta(T)-e^{-\frac{1}{2}\eta}\frac{1}{2\pi i}\int_{c-i\infty}^{c+i\infty} e^{pT}e^{-\frac{1}{2}\eta\sqrt{(1+p)}}\,dp \\
&\quad = \delta(T)-e^{-\frac{1}{2}\eta}e^{-T}\frac{1}{2\pi i}\int_{c^*-i\infty}^{c^*+i\infty} e^{pT}pe^{-\frac{1}{2}\eta\sqrt{p}}\frac{dp}{p} \quad (c^* = c+1) \\
&\quad = \delta(T)-\frac{4}{\eta^2}e^{-\frac{1}{2}\eta}e^{-T}\frac{1}{2\pi i}\int_{c'-i\infty}^{c'+i\infty} e^{p(4T/\eta^2)}pe^{-\sqrt{p}}\frac{dp}{p} \quad \left(c' = \frac{c^*\eta^2}{4}\right) \\
&\quad = \delta(T)-\frac{4}{\eta^2}e^{-\frac{1}{2}\eta}e^{-T}H\left(\frac{4T}{\eta^2}\right)\frac{e^{-\eta^2/16T}}{2\pi^{\frac{1}{2}}T^{\frac{1}{2}}}\frac{\eta^3}{8} \\
&\quad = \delta(T)-\frac{\eta H(4T/\eta^2)}{4\pi^{\frac{1}{2}}T^{\frac{1}{2}}}e^{-\frac{1}{2}\eta}e^{-T}e^{-\eta^2/16T},
\end{aligned}$$

where $\delta(T)$ is the delta function and $H(T)$ is the unit function. The composition-product rule then gives

$$\begin{aligned}
g(\eta, T) &= \int_{-\infty}^{\infty} f(T-\lambda)\left[\delta(\lambda)-\frac{\eta H(4\lambda/\eta^2)}{4\pi^{\frac{1}{2}}\lambda^{\frac{1}{2}}}e^{-\frac{1}{2}\eta}e^{-\lambda}e^{-\eta^2/16\lambda}\right]d\lambda \\
&= f(T)-\frac{\eta e^{-\frac{1}{2}\eta}}{4\pi^{\frac{1}{2}}}\int_0^{\infty}\lambda^{-\frac{1}{2}}f(T-\lambda)\exp\left\{-\left(\lambda+\frac{\eta^2}{16\lambda}\right)\right\}d\lambda.
\end{aligned} \tag{3.11}$$

It is assumed that $f(T)$ is bounded in and integrable over any finite range and the integral $\int_A^\infty \lambda^{-\frac{1}{2}} f(T-\lambda)e^{-\lambda}\,d\lambda$ $(A > 0)$ is absolutely convergent for finite T. In such a case, it can be shown that $g(\eta, T)$ as given by (3.11) satisfies (3.7) and, at points where $f(T)$ is continuous, that it satisfies the boundary conditions. Consequently (3.5), where $g(y, t)$ is given by (3.11) and (3.6), satisfies (3.1) and the corresponding boundary conditions at points of continuity of $f(T)$; on physical grounds the solution is unique. Functions, $f(T)$, which do not satisfy the above conditions may, however, lead to a solution; in such cases it must be checked that (3.11) satisfies (3.7) and the boundary conditions. From equations (3.4) and (3.11) the velocity distribution, (3.5), is given by

$$\left.\begin{aligned} U(T)/U_0 &= 1+f(T) \\ u/U_0 &= 1-e^{-\eta}+f(T)-\frac{\eta e^{-\frac{1}{4}\eta}}{4\pi^{\frac{1}{2}}}\int_0^\infty \lambda^{-\frac{1}{2}} f(T-\lambda)\exp\left\{-\left(\lambda+\frac{\eta^2}{16\lambda}\right)\right\} d\lambda \\ v &= v_w \end{aligned}\right\}, \tag{3.12}$$

where T, η are related to t, y by (3.6). It can be shown that if the free-stream velocity ultimately becomes steady, then the velocity distribution reaches a form similar to the undisturbed velocity distribution; that is if $\lim_{T\to\infty} U(T) = U(\infty)$, where $U(\infty)$ is a finite constant, then

$$\lim_{T\to\infty} u(\eta, T) = \zeta_0(\eta)U(\infty).$$

Similarly if $\lim_{T\to-\infty} U(T) = U(-\infty)$, then

$$\lim_{T\to-\infty} u(\eta, T) = \zeta_0(\eta)U(-\infty)$$

under similar conditions. These results are proved in Appendix A. Particular cases of the general velocity distribution are discussed in the following sections.

The displacement thickness, δ_1, may be defined by

$$\delta_1|v_w|/\nu = \int_0^\infty \left[1-\frac{u(\eta, T)}{U(T)}\right] d\eta, \tag{3.13}$$

which will now be evaluated from (3.12) under the assumption that the integral

$$\int_0^\infty \lambda^{-\frac{1}{2}} f(T-\lambda)e^{-\lambda}\,d\lambda$$

is absolutely convergent for finite T. From (3.13)

$$\delta_1|v_w|/\nu = \frac{U_0}{U(T)}\int_0^\infty \left[\frac{U(T)}{U_0}-\frac{u(\eta, T)}{U_0}\right] d\eta,$$

which yields, after a little algebra and use of (3.12),

$$\delta_1|v_w|/\nu = \frac{1}{[1+f(T)]}\left[1+\frac{2}{\pi^{\frac{1}{2}}}\int_0^\infty \lambda^{-\frac{1}{2}} f(T-\lambda)e^{-\lambda}\,d\lambda - 2\int_0^\infty f(T-\lambda)\operatorname{erfc}\lambda^{\frac{1}{2}}\,d\lambda\right], \tag{3.14}$$

It now remains to derive a formula for the skin friction, τ_w, which is given by

$$\tau_w/\rho U_0|v_w| = \left[\partial\left(\frac{u(\eta,T)}{U_0}\right)\Big/\partial\eta\right]_{\eta=0} = \lim_{\eta\to 0}\frac{u(\eta,T)}{\eta U_0} \tag{3.15}$$

since $u\to 0$ as $\eta\to 0$. From (3.12) and by making use of equation (B,2), this becomes

$$\tau_w/\rho U_0|v_w| = 1+f(T)+\frac{1}{4\pi^{\frac{1}{2}}}\int_0^\infty \lambda^{-\frac{1}{2}}\{f(T)-f(T-\lambda)\}e^{-\lambda}\,d\lambda, \tag{3.16}$$

provided that the integral in (3.16) is absolutely convergent. This is so if at the point T

$$|f(T)-f(T-\lambda)| < C|\lambda|^k \quad \text{for } |\lambda|\leqslant\delta, \tag{3.17}$$

where C is a positive constant and $k>\frac{1}{2}$. We note that a function which satisfies (3.17) is necessarily continuous at the point T; while a function which has a finite derivative at T satisfies (3.17) and the skin friction is given by (3.16).

4. Applications of general theory

In the following examples all the conditions on $f(T)\equiv U(T)/U_0-1$ are satisfied in order that the velocity distribution, the displacement thickness and the skin friction be given by (3.12), (3.14), and (3.16) respectively.

4.1. *Periodic velocity field*

Application is made to the case $f(T)\equiv \epsilon e^{i\Omega T}$, where $\Omega = 4\nu\omega/v_w^2$, in order to demonstrate that certain results given by Stuart (2) can be derived from the results given in section 3. The second equation in (3.12) becomes

$$\frac{u}{U_0} = 1-e^{-\eta}+\epsilon e^{i\Omega T}-\epsilon e^{i\Omega T}\frac{\eta e^{-\frac{1}{4}\eta}}{4\pi^{\frac{1}{2}}}\int_0^\infty \lambda^{-\frac{1}{2}}e^{-i\Omega\lambda}\exp\left\{-\left(\lambda+\frac{\eta^2}{16\lambda}\right)\right\}d\lambda$$

$$= 1-e^{-\eta}+\epsilon e^{i\Omega T}-\epsilon e^{i\Omega T}\frac{\eta e^{-\frac{1}{4}\eta}}{4\pi^{\frac{1}{2}}}\int_0^\infty \lambda^{-\frac{1}{2}}e^{-(a^2\lambda+b^2/\lambda)}\,d\lambda,$$

where $a=(1+i\Omega)^{\frac{1}{2}}$ with $\operatorname{re}(a)>0$ and $b=\frac{1}{4}\eta$. Using the evaluation of the integral given in Appendix B, equation (B, 4), we obtain

$$u/U_0 = 1-e^{-\eta}+\epsilon e^{i\Omega T}-\epsilon e^{i\Omega T}\frac{4\pi^{\frac{1}{2}}\eta e^{-\frac{1}{4}\eta}}{4\pi^{\frac{1}{2}}\eta}e^{-\frac{1}{4}\eta(1+i\Omega)^{\frac{1}{2}}}$$

$$= 1-e^{-\eta}+\epsilon e^{i\Omega T}(1-e^{-h\eta}), \tag{4.1}$$

where $h = \frac{1}{2}\{1+(1+i\Omega)^{\frac{1}{2}}\}$ and $\Omega = 4\nu\omega/v_w^2$, which is a result given by Stuart.

From (3.16) the skin friction is given by

$$\tau_w/\rho U_0|v_w| = 1+\epsilon e^{i\Omega T}+\frac{\epsilon e^{i\Omega T}}{4\pi^{\frac{1}{2}}}\int_0^\infty \lambda^{-\frac{1}{2}}(1-e^{-i\Omega\lambda})e^{-\lambda}\,d\lambda.$$

The integral in this equation may be integrated by parts to give

$$\begin{aligned}\tau_w/\rho U_0|v_w| &= 1+\epsilon e^{i\Omega T}-\frac{\epsilon e^{i\Omega T}}{2\pi^{\frac{1}{2}}}\int_0^\infty \lambda^{-\frac{1}{2}}\{e^{-\lambda}-(1+i\Omega)e^{-(1+i\Omega)\lambda}\}\,d\lambda\\ &= 1+\epsilon e^{i\Omega T}-\epsilon e^{i\Omega T}\{\tfrac{1}{2}-\tfrac{1}{2}(1+i\Omega)^{\frac{1}{2}}\}\\ &= 1+\epsilon e^{i\Omega T}h, \qquad (4.2)\end{aligned}$$

where $h = \frac{1}{2}\{1+(1+i\Omega)^{\frac{1}{2}}\}$, by use of equation (B, 6) of Appendix B. This agrees with Stuart's result.

4.2. *Impulsive velocity fields*

(*a*) *Single impulse*

The case of a single impulse at $T = 0$, namely

$$U(T) = U_0 \quad \text{for } T < 0; \qquad U(T) = U_0(1+\Delta) \quad \text{for } T > 0$$

where Δ is a constant, is now considered. This corresponds to

$$f(T) \equiv \Delta H(T),$$

where Δ is constant and $H(T)$ is the unit function. The velocity is given by (3.12) and, because of the factor $H(T-\lambda)$, the integrand is zero for $\lambda > T$. Consequently it is only necessary to integrate from 0 to T when T is positive; for negative values of T the integrand is identically zero. Thus, provided $T \neq 0$ the velocity has the form

$$\begin{aligned}\frac{u}{U_0} &= 1-e^{-\eta}+\Delta H(T)-\frac{\Delta\eta e^{-\frac{1}{2}\eta}H(T)}{4\pi^{\frac{1}{2}}}\int_0^T \lambda^{-\frac{1}{2}}\exp\left\{-\left(\lambda+\frac{\eta^2}{16\lambda}\right)\right\}d\lambda\\ &= 1-e^{-\eta}+\Delta H(T)-\Delta H(T)\frac{2\pi^{\frac{1}{2}}\eta e^{-\frac{1}{2}\eta}}{4\pi^{\frac{1}{2}}\eta}e^{\frac{1}{2}\eta}\times\\ &\qquad\times\left[e^{-\eta}\operatorname{erfc}\left(\frac{\eta}{4T^{\frac{1}{2}}}-T^{\frac{1}{2}}\right)+\operatorname{erfc}\left(\frac{\eta}{4T^{\frac{1}{2}}}+T^{\frac{1}{2}}\right)\right]\end{aligned}$$

from equation (B, 2) of Appendix B. Hence

$$\frac{u}{U_0} = 1-e^{-\eta}+\Delta H(T)\left[1-\tfrac{1}{2}e^{-\eta}\operatorname{erfc}\left(\frac{\eta}{4T^{\frac{1}{2}}}-T^{\frac{1}{2}}\right)-\tfrac{1}{2}\operatorname{erfc}\left(\frac{\eta}{4T^{\frac{1}{2}}}+T^{\frac{1}{2}}\right)\right] \qquad (4.3)$$

for $T \neq 0$. It is easily seen from this that, as $T \to \infty$, $u/U_0 \to (1-e^{-\eta})(1+\Delta)$ as we would expect from Appendix A with $U(\infty) = U_0(1+\Delta)$.

The displacement thickness, δ_1, as defined by (3.13), is given by (3.14) for $T \neq 0$. Thus

$$\delta_1|v_w|/\nu = \frac{1}{\{1+\Delta H(T)\}}\left[1+\frac{2\Delta H(T)}{\pi^{\frac{1}{2}}}\int_0^T \frac{e^{-\lambda}\,d\lambda}{\lambda^{\frac{1}{2}}} - 2\Delta H(T)\int_0^T \operatorname{erfc}\lambda^{\frac{1}{2}}\,d\lambda\right]. \quad (4.4)$$

From Appendix B, equation (B, 5) gives

$$\int_0^T \frac{e^{-\lambda}\,d\lambda}{\lambda^{\frac{1}{2}}} = \pi^{\frac{1}{2}}\operatorname{erf} T^{\frac{1}{2}}. \quad (4.5)$$

Together with this result, a double integration by parts of the second integral leads to

$$\int_0^T \operatorname{erfc}\lambda^{\frac{1}{2}}\,d\lambda = T\operatorname{erfc} T^{\frac{1}{2}} - (T^{\frac{1}{2}}/\pi^{\frac{1}{2}})e^{-T} + \tfrac{1}{2}\operatorname{erf} T^{\frac{1}{2}} \quad (4.6)$$

so that (4.4) becomes

$$\delta_1|v_w|/\nu = \frac{1}{\{1+\Delta H(T)\}}[1+\Delta H(T)\{(2T^{\frac{1}{2}}/\pi^{\frac{1}{2}})e^{-T}+\operatorname{erf} T^{\frac{1}{2}} - 2T\operatorname{erfc} T^{\frac{1}{2}}\}] \quad (4.7)$$

for $T \neq 0$.

Finally, the skin friction, τ_w, given by (3.16) is, for $T \neq 0$,

$$\begin{aligned}\tau_w/\rho U_0|v_w| &= 1+\Delta H(T)+\frac{\Delta H(T)}{4\pi^{\frac{1}{2}}}\int_T^\infty \frac{e^{-\lambda}\,d\lambda}{\lambda^{\frac{1}{2}}} \\ &= 1+\Delta H(T)+\frac{\Delta H(T)}{4\pi^{\frac{1}{2}}}\left[\frac{2e^{-T}}{T^{\frac{1}{2}}} - 2\int_T^\infty \frac{e^{-\lambda}\,d\lambda}{\lambda^{\frac{1}{2}}}\right].\end{aligned}$$

But

$$\int_T^\infty \frac{e^{-\lambda}\,d\lambda}{\lambda^{\frac{1}{2}}} = \int_0^\infty \frac{e^{-\lambda}\,d\lambda}{\lambda^{\frac{1}{2}}} - \int_0^T \frac{e^{-\lambda}\,d\lambda}{\lambda^{\frac{1}{2}}} = \pi^{\frac{1}{2}} - \pi^{\frac{1}{2}}\operatorname{erf} T^{\frac{1}{2}} \quad (4.8)$$

from (4.5). Hence

$$\begin{aligned}\tau_w/\rho U_0|v_w| &= 1+\Delta H(T)+\frac{\Delta H(T)}{4\pi^{\frac{1}{2}}}\left[\frac{2e^{-T}}{T^{\frac{1}{2}}} - 2\pi^{\frac{1}{2}} + 2\pi^{\frac{1}{2}}\operatorname{erf} T^{\frac{1}{2}}\right] \\ &= 1+\frac{\Delta H(T)}{2}\left[1+\operatorname{erf} T^{\frac{1}{2}}+\frac{e^{-T}}{(\pi T)^{\frac{1}{2}}}\right] \quad (4.9)\end{aligned}$$

for $T \neq 0$.

A graph of the skin friction, τ_w, for $\Delta = 0{\cdot}2$ is given in Fig. 1. Eventually τ_w reaches the steady value τ_s which, from (4.9), is given by

$$\tau_s/\rho U_0|v_w| = 1+\Delta. \quad (4.10)$$

It can be seen from Fig. 1 that at $T = 0$ the skin friction initially goes to plus infinity and then decreases to its limiting value as T increases. The reason for these properties of the skin friction can be seen as follows. Just

before the main stream velocity is changed impulsively from U_0 to $U_0(1+\Delta)$ the velocity distribution in the boundary layer is $U_0(1-e^{-\eta})$. Just after the application of the impulse, that is for very small values of the time, it can be seen from (4.3) that the velocity distribution is of the form

$$u/U_0 = 1-e^{-\eta}+\Delta-\tfrac{1}{2}\Delta(1+e^{-\eta})\operatorname{erfc}(\eta/4T^{\frac{1}{2}})$$

which depends on the parameter $\eta/T^{\frac{1}{2}}$. From (3.6) this parameter corresponds to the parameter $y/(\nu t)^{\frac{1}{2}}$. For values of y such that $y \gg (\nu t)^{\frac{1}{2}}$ the

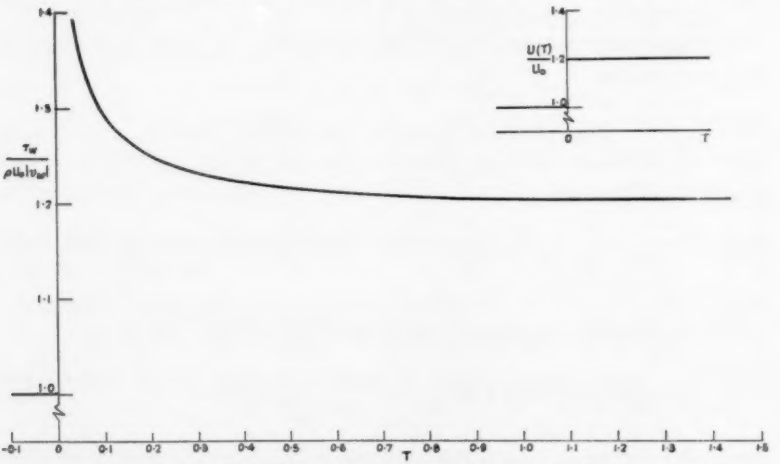

FIG. 1. Behaviour of skin friction in impulsive flow

velocity distribution is $U_0(1-e^{-\eta}+\Delta)$, whereas for values of y of order $(\nu t)^{\frac{1}{2}}$, that is when η is very small, the velocity varies from zero velocity at the wall to the approximate value $U_0\Delta$ in a distance y of order $(\nu t)^{\frac{1}{2}}$. In physical terms, for very small times there is a secondary boundary layer on the wall, whose thickness is of order $(\nu t)^{\frac{1}{2}}$. As $t \to 0$ the same velocity change, $U_0\Delta$, must take place in an ever decreasing distance; thus the skin friction becomes infinite as $t \to 0$ like $1/t^{\frac{1}{2}}$. As time progresses the secondary boundary layer increases in thickness and distorts the flow in such a way that the initial velocity $U_0(1-e^{-\eta}+\Delta)$ approaches more and more closely the ultimate form $U_0(1+\Delta)(1-e^{-\eta})$. A further fact worth noting is that the viscous effects of the impulse are confined to the secondary boundary layer; so that the flow outside the secondary layer may be regarded as inviscid *as far as the impulse is concerned*† and the velocity there increased,

† A similar phenomenon is noted by Lighthill (7) in his work on shock boundary-layer interaction. He points out that it is only in 'an "inner viscous sublayer" . . . that the disturbances to the viscous forces are comparable with the disturbances to the inertial

for $T > 0$, by $U_0\Delta$, the impulsive increase in the free-stream velocity. Consequently, by letting $T \to 0$, we see that, for $\eta > 0$, the velocity is impulsively increased by $U_0\Delta$ at $T = 0$. It should be noted that, for small values of η and T, the secondary boundary layer is of the form

$$u = U_0\Delta \operatorname{erf}(\eta/4T^{\frac{1}{2}}),$$

and is thus like the Rayleigh boundary layer for impulsive flow from rest.

It is of some interest to define a non-dimensional time, T_c, which is characteristic of the time taken for the skin friction to change from one steady value to another. In the case under consideration this can be defined as follows. Let τ_1 be the undisturbed skin friction, namely,

$$\tau_1 = \rho U_0 |v_w|. \tag{4.11}$$

Then the characteristic time T_c is defined by

$$T_c = \int_0^\infty \left(\frac{\tau_w - \tau_1}{\tau_s - \tau_1} - 1\right) dT, \tag{4.12}$$

where τ_s is given by (4.10). From equation (4.9) this is

$$T_c = \int_0^\infty \left[\frac{1}{2}\left(1 + \operatorname{erf} T^{\frac{1}{2}} + \frac{e^{-T}}{(\pi T)^{\frac{1}{2}}}\right) - 1\right] dT.$$

On performing the integration we obtain

$$T_c = \tfrac{1}{4}. \tag{4.13}$$

From (3.6) this gives

$$t_c = \delta_{10}^2/\nu, \tag{4.14}$$

and for a boundary layer of displacement thickness 0·1 cm this is $t_c \simeq 0{\cdot}07$ sec. The time taken for the flow to settle down to its ultimate state will be about three times this. It can be seen that the characteristic time, in a sense, is analogous to a displacement thickness.

(*b*) *Multiple impulse*

From section 4.2 (*a*) it is a simple matter to derive the velocity distribution for the case when the free-stream velocity is given a series of impulses. In particular consider the case

$$U(T) = \begin{cases} U_0 & (T < 0) \\ U_0(1+\Delta) & (0 < T < T_0) \\ U_0 & (T_0 < T) \end{cases}$$

forces'. Hence outside this layer, though still in the boundary layer, the disturbances to the viscous forces are negligible, and the interaction is quasi-inviscid.

so that

$$f(T) = \begin{cases} 0 & (T < 0) \\ \Delta & (0 < T < T_0 \\ 0 & (T_0 < T) \end{cases}$$

or

$$f(T) = f^*(T) - f^*(T - T_0), \tag{4.15}$$

where

$$f^*(T) \equiv \Delta H(T).$$

From (3.12) it is seen that the part of the velocity distribution which depends on T is linear in f so that by (4.15) it is composed of the part arising from $f^*(T)$ together with the part arising from $-f^*(T-T_0)$. But, from (4.3), the part arising from $f^*(T)$ is

$$\phi(\eta, T) = \Delta H(T)\left[1 - \tfrac{1}{2}e^{-\eta}\operatorname{erfc}\left(\frac{\eta}{4T^{\frac{1}{2}}} - T^{\frac{1}{2}}\right) - \tfrac{1}{2}\operatorname{erfc}\left(\frac{\eta}{4T^{\frac{1}{2}}} + T^{\frac{1}{2}}\right)\right] \tag{4.16}$$

for $T \neq 0$. Similarly the part arising from $-f^*(T-T_0)$ is $-\phi(\eta, T-T_0)$ for $T \neq T_0$. Thus the velocity distribution is given by

$$u/U_0 = 1 - e^{-\eta} + \phi(\eta, T) - \phi(\eta, T-T_0) \tag{4.17}$$

for $T \neq 0$ and $T \neq T_0$, and where $\phi(\eta, T)$ is defined by (4.16). Since $\phi(\eta, T) \to \Delta(1-e^{-\eta})$ as $T \to \infty$ then, from (4.17), $u/U_0 \to (1-e^{-\eta})$ as $T \to \infty$ [$U(\infty) = U_0$ in Appendix A]. By similar reasoning the skin friction, τ_w, is given by

$$\tau_w/\rho U_0|v_w| = 1 + \psi(T) - \psi(T-T_0) \tag{4.18}$$

for $T \neq 0$ and $T \neq T_0$, and where $\psi(T)$ is defined by

$$\psi(T) = \frac{\Delta H(T)}{2}\left[1 + \operatorname{erf} T^{\frac{1}{2}} + \frac{e^{-T}}{(\pi T)^{\frac{1}{2}}}\right]. \tag{4.19}$$

Finally, the displacement thickness, δ_1, is given by

$$\delta_1|v_w|/\nu = [1 + \chi(T) - \chi(T-T_0)]/[1 + \Delta H(T) - \Delta H(T-T_0)] \tag{4.20}$$

for $T \neq 0$ and $T \neq T_0$, and where $\chi(T)$ is defined by

$$\chi(T) = \Delta H(T)\left[\frac{2T^{\frac{1}{2}}e^{-T}}{\pi^{\frac{1}{2}}} + \operatorname{erf} T^{\frac{1}{2}} - 2T\operatorname{erfc} T^{\frac{1}{2}}\right]. \tag{4.21}$$

A graph of the skin friction, τ_w, for $\Delta = 0{\cdot}2$ and $T_0 = 0{\cdot}04$ is given in Fig. 2. For $T < T_0$, $\psi(T-T_0) = 0$ from (4.19), and (4.18) and (4.9) are identical so that, for $T < 0{\cdot}04$, Fig. 2 represents the same skin friction as Fig. 1. By the same reasoning as in section 4.2 (*a*), a *decrease* in free-stream velocity from $U_0(1+\Delta)$ to U_0 at $T = T_0$ causes the skin friction to go to *minus* infinity and then to increase to its limiting value. From (4.18) and (4.19) this steady limiting value, τ_s, is

$$\tau_s/\rho U_0|v_w| = 1. \tag{4.22}$$

Again, as in section 4.2 (*a*), a new secondary boundary layer is created at $T = T_0$ the thickness of which is of order $\nu^{\frac{1}{2}}(T-T_0)^{\frac{1}{2}}$ for small positive $(T-T_0)$ and as time progresses it increases in thickness and modifies the flow to the ultimate steady velocity $U_0(1-e^{-\eta})$. By the same reasoning as

in section 4.2 (*a*), the flow outside this new boundary layer may be regarded as inviscid as far as the impulse at $T = T_0$ is concerned and for $T \geqslant T_0$ the velocity there is decreased by $U_0\Delta$ so that at $T = T_0$ the velocity for $\eta > 0$ is impulsively decreased by this amount.

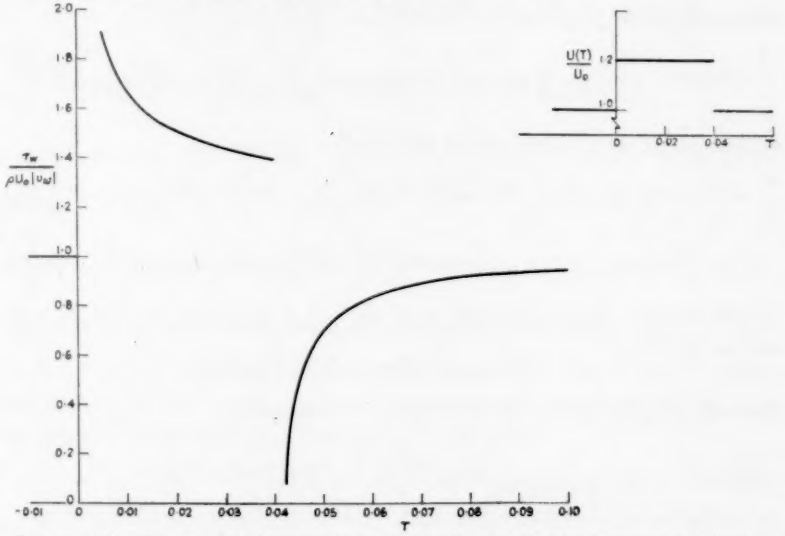

FIG. 2. Behaviour of skin friction in flow with two impulsive changes of velocity

4.3. *Accelerated velocity fields*

(*a*) *Single acceleration*

Consider now an accelerated free stream with velocity of the form

$$U(T) = U_0 \quad \text{for } T < 0, \qquad U(T) = U_0[1+KT] \quad \text{for } T \geqslant 0$$

where K is a constant. This corresponds to

$$f(T) = KT\,H(T), \tag{4.23}$$

where $H(T)$ is the unit function. Note that, although $f(T)$ is not differentiable at $T = 0$, it satisfies (3.17) there. Equations (3.12) and (4.23) yield

$$\frac{u}{U_0} = 1-e^{-\eta}+KT\,H(T)-\frac{K\eta e^{-\frac{1}{4}\eta}H(T)}{4\pi^{\frac{1}{2}}}\int_0^T \lambda^{-\frac{3}{2}}(T-\lambda)\exp\left\{-\left(\lambda+\frac{\eta^2}{16\lambda}\right)\right\}d\lambda$$

$$= 1-e^{-\eta}+KT\,H(T)-\frac{KT\,H(T)\eta e^{-\frac{1}{4}\eta}}{4\pi^{\frac{1}{2}}}\int_0^T \lambda^{-\frac{3}{2}}\exp\left\{-\left(\lambda+\frac{\eta^2}{16\lambda}\right)\right\}d\lambda +$$

$$+\frac{KH(T)\eta e^{-\frac{1}{4}\eta}}{4\pi^{\frac{1}{2}}}\int_0^T \lambda^{-\frac{3}{2}}\exp\left\{-\left(\lambda+\frac{\eta^2}{16\lambda}\right)\right\}d\lambda. \tag{4.24}$$

But from Appendix B, equation (B, 2) gives

$$\int_0^T \lambda^{-\frac{1}{2}} \exp\left\{-\left(\lambda+\frac{\eta^2}{16\lambda}\right)\right\} d\lambda = \frac{2\pi^{\frac{1}{2}}}{\eta} e^{\frac{1}{2}\eta}\left[e^{-\eta}\operatorname{erfc}\left(\frac{\eta}{4T^{\frac{1}{2}}}-T^{\frac{1}{2}}\right)+\operatorname{erfc}\left(\frac{\eta}{4T^{\frac{1}{2}}}+T^{\frac{1}{2}}\right)\right]$$

and equation (B, 1) gives

$$\int_0^T \lambda^{-\frac{1}{2}} \exp\left\{-\left(\lambda+\frac{\eta^2}{16\lambda}\right)\right\} d\lambda = \tfrac{1}{2}\pi^{\frac{1}{2}} e^{\frac{1}{2}\eta}\left[e^{-\eta}\operatorname{erfc}\left(\frac{\eta}{4T^{\frac{1}{2}}}-T^{\frac{1}{2}}\right)-\operatorname{erfc}\left(\frac{\eta}{4T^{\frac{1}{2}}}+T^{\frac{1}{2}}\right)\right]$$

so that (4.24) may be written in the form

$$\frac{u}{U_0} = 1-e^{-\eta}+\tfrac{1}{8}K\,H(T)\left[8T-4T\left\{e^{-\eta}\operatorname{erfc}\left(\frac{\eta}{4T^{\frac{1}{2}}}-T^{\frac{1}{2}}\right)+\operatorname{erfc}\left(\frac{\eta}{4T^{\frac{1}{2}}}+T^{\frac{1}{2}}\right)\right\}+\right.$$
$$\left.+\eta\left\{e^{-\eta}\operatorname{erfc}\left(\frac{\eta}{4T^{\frac{1}{2}}}-T^{\frac{1}{2}}\right)-\operatorname{erfc}\left(\frac{\eta}{4T^{\frac{1}{2}}}+T^{\frac{1}{2}}\right)\right\}\right] \quad (4.25)$$

for all finite T. It is easily seen that, for $\eta > 0$, as $T \to 0$, $u \to U_0(1-e^{-\eta})$ and as $T \to \infty$,

$$u \sim U_0\{1-e^{-\eta}+K[T(1-e^{-\eta})+\tfrac{1}{4}\eta e^{-\eta}]\}.$$

From (3.14) and (4.23) the displacement thickness is

$$\delta_1|v_w|/\nu = \frac{1}{\{1+KT\,H(T)\}}\left[1+\frac{2K\,H(T)}{\pi^{\frac{1}{2}}}\int_0^T \lambda^{-\frac{1}{2}}(T-\lambda)e^{-\lambda}\,d\lambda-\right.$$
$$\left.-2K\,H(T)\int_0^T (T-\lambda)\operatorname{erfc}\lambda^{\frac{1}{2}}\,d\lambda\right]$$
$$= \frac{1}{\{1+KT\,H(T)\}}\left[1+\frac{2KT\,H(T)}{\pi^{\frac{1}{2}}}\int_0^T \lambda^{-\frac{1}{2}}e^{-\lambda}\,d\lambda-\right.$$
$$-\frac{2K\,H(T)}{\pi^{\frac{1}{2}}}\int_0^T \lambda^{\frac{1}{2}}e^{-\lambda}\,d\lambda-2KT\,H(T)\int_0^T \operatorname{erfc}\lambda^{\frac{1}{2}}\,d\lambda+$$
$$\left.+2K\,H(T)\int_0^T \lambda\operatorname{erfc}\lambda^{\frac{1}{2}}\,d\lambda\right]. \quad (4.26)$$

Of the integrals on the right-hand side of (4.26), the first is given by (4.5), the second can be derived from (4.5) and is

$$\int_0^T \lambda^{\frac{1}{2}}e^{-\lambda}\,d\lambda = \tfrac{1}{2}\pi^{\frac{1}{2}}\operatorname{erf}T^{\frac{1}{2}}-T^{\frac{1}{2}}e^{-T}, \quad (4.27)$$

the third is given by (4.6), and the fourth can be obtained by a double integration by parts which, after using (4.27), gives

$$\int_0^T \lambda\operatorname{erfc}\lambda^{\frac{1}{2}}\,d\lambda = \tfrac{1}{2}T^2\operatorname{erfc}T^{\frac{1}{2}}+\tfrac{3}{8}\operatorname{erf}T^{\frac{1}{2}}-\frac{T^{\frac{1}{2}}e^{-T}}{2\pi^{\frac{1}{2}}}-\frac{3T^{\frac{1}{2}}e^{-T}}{4\pi^{\frac{1}{2}}}. \quad (4.28)$$

Substituting in (4.26) and simplifying, we obtain

$$\delta_1|v_w|/\nu = \frac{1}{\{1+KT\,H(T)\}}\Big[1+K\,H(T)\times$$
$$\times\left\{\frac{T^{\frac{1}{2}}e^{-T}}{\pi^{\frac{1}{2}}}+\frac{T^{\frac{1}{2}}e^{-T}}{2\pi^{\frac{1}{2}}}-T^2\operatorname{erfc}T^{\frac{1}{2}}+T\operatorname{erf}T^{\frac{1}{2}}-\tfrac{1}{4}\operatorname{erf}T^{\frac{1}{2}}\right\}\Big] \quad (4.29)$$

for all T.

Finally, from (3.16) the skin friction, τ_w, is, for finite T,

$$\tau_w/\rho U_0|v_w| = 1+KT\,H(T)+\frac{K\,H(T)}{4\pi^{\frac{1}{2}}}\left(\int_0^T \lambda^{-\frac{1}{2}}e^{-\lambda}\,d\lambda+T\int_T^\infty \lambda^{-\frac{1}{2}}e^{-\lambda}\,d\lambda\right). \quad (4.30)$$

But

$$\int_T^\infty \lambda^{-\frac{1}{2}}e^{-\lambda}\,d\lambda = [-2\lambda^{-\frac{1}{2}}e^{-\lambda}]_T^\infty-2\int_T^\infty \lambda^{-\frac{1}{2}}e^{-\lambda}\,d\lambda = 2e^{-T}T^{-\frac{1}{2}}-2\pi^{\frac{1}{2}}+2\pi^{\frac{1}{2}}\operatorname{erf}T^{\frac{1}{2}},$$

by (4.8), while the first integral in (4.30) is given by (4.5). Thus

$$\tau_w/\rho U_0|v_w| = 1+K\,H(T)[\tfrac{1}{2}T+\tfrac{1}{4}\operatorname{erf}T^{\frac{1}{2}}+\tfrac{1}{2}\pi^{-\frac{1}{2}}T^{\frac{1}{2}}e^{-T}+\tfrac{1}{2}T\operatorname{erf}T^{\frac{1}{2}}] \quad (4.31)$$

for all finite T. A graph of $\tau_w/\rho U_0|v_w|$ is given for $K = 4$ (Fig. 3). Eventually τ_w reaches the form which, from (4.31), is given by

$$\tau_w/\rho U_0|v_w| = 1+K(T+\tfrac{1}{4}). \quad (4.32)$$

In Fig. 3 the gradient of the skin friction curve is seen to be infinite at $T = 0$ and then it steadily decreases to a limiting value as the time increases. The reason for this behaviour of the skin friction at $T = 0$ is similar to the reason for infinite skin friction in the impulse case (section 4.2 (a)). In this case, for small positive T, the velocity changes from zero at the wall to $U_0\{(1-e^{-\eta})+KT\}$ in a distance η of order $T^{\frac{1}{2}}$; so that $\tau_w/\rho U_0|v_w| = 1+CT^{\frac{1}{2}}$ where C is a constant. That is, the skin friction grows parabolically for small positive T. As time progresses the secondary boundary layer, with thickness of order $T^{\frac{1}{2}}$, continues to grow and, as it does so, the skin friction changes. Ultimately the skin friction attains the form (4.32). If the term $\frac{1}{4}K$ were not present, this skin friction formula would be that appropriate to a *steady* free-stream velocity $U_0(1+KT)$. The presence of the term $\frac{1}{4}K$ means that the skin friction anticipates the free-stream velocity, since at time T_∞ the skin friction has attained a state which, if the flow were exactly quasi-steady, would be appropriate at $T_\infty+\frac{1}{4}$. This anticipation arises because the pressure gradient which is accelerating the fluid has a greater effect on the more slowly moving fluid near the wall than on the fluid at greater distances from the wall.

For steady flow with free-stream velocity U_0 the skin friction is

$$\tau_w = \rho U_0|v_w|$$

but for large T with free-stream velocity $U_0(1+KT)$ the skin friction from (4.32) is

$$\tau_w = \rho U_0|v_w|(1+KT)+\tfrac{1}{4}\rho U_0|v_w|K$$
$$= \rho|v_w|U(T)+\tfrac{1}{4}\rho|v_w|\frac{dU}{dT}.$$

From (3.6) this may be written in the form

$$\tau_w = \rho|v_w|U(t)+\rho\delta_{10}\frac{dU}{dt} = \tau_q+\rho\delta_{10}\frac{dU}{dt}, \tag{4.33}$$

where δ_{10} is the displacement thickness for a steady free-stream velocity

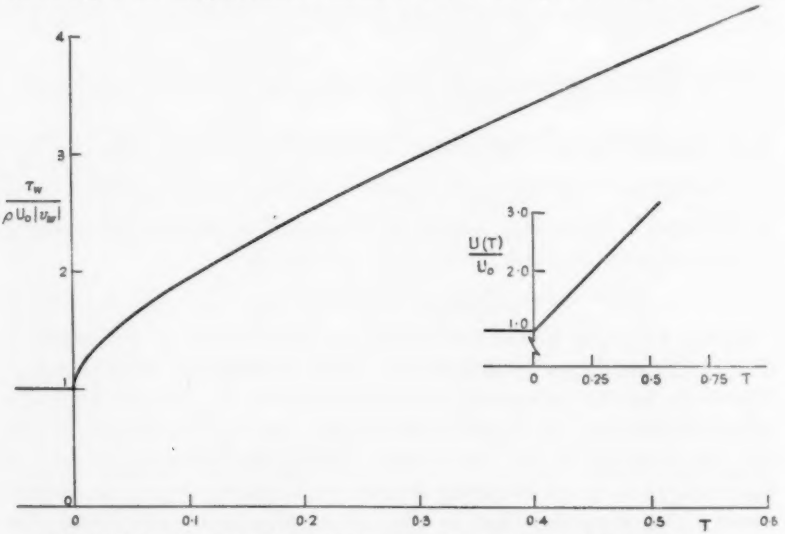

FIG. 3. Behaviour of skin friction in flow with a change of acceleration

and τ_q is the skin friction if the main stream were constant at $U(t)$. It should be noted from (4.29) that as $T \to \infty$, $\delta_1|v_w|/\nu$ tends to the steady form, namely unity; thus $\delta_1 \to \delta_{10}$. Consequently the displacement thickness approaches a quasi-steady state in which, although the fluid is accelerating, the steady displacement thickness applies.

If the outer stream is at rest and the *wall* is moving then the force required to move the wall is given by the drag. The force required for a length l and unit breadth is thus

$$F = F_q+\rho l\delta_{10}\frac{dU}{dt} = F_q+\rho\Delta_{10}\frac{dU}{dt}, \tag{4.34}$$

where Δ_{10} is the 'displacement area' (cf. Lighthill (1)). The term F_q repre-

sents the drag which would arise if the flow were *steady* at the instantaneous velocity $U(t)$. We can thus call it the quasi-steady drag. The second term, however, is the product of a 'virtual mass', $\rho\Delta_{10}$, with the acceleration, dU/dt. This 'virtual mass' arises because, as the wall is accelerating, fluid is accelerated as well through the action of viscosity (cf. Lighthill (**1**)).

(*b*) *Multiple accelerations*

From the results of section 4.3 (*a*) the velocity distribution can be easily derived for the case when the free-stream velocity is given a series of uniform accelerations. Consider, for example, the case in which the fluid accelerates from one velocity, U_0, to another, $U_0(1+KT_0)$, between $T=0$ and $T=T_0$, namely

$$U(T)=\begin{cases} U_0 & (T\leqslant 0)\\ U_0(1+KT) & (0\leqslant T\leqslant T_0)\\ U_0(1+KT_0) & (T_0\leqslant T)\end{cases}$$

or
$$f(T)=KT\,H(T)-K(T-T_0)H(T-T_0)$$

so that $f(T)$ may be written in the same form as (4.15) where here

$$f^*(T)\equiv KT\,H(T).$$

Precisely the same argument can be applied as in section 4.2 (*b*) to determine the velocity distribution, skin friction, and displacement thickness; these are, respectively,

$$u/U_0=1-e^{-\eta}+\alpha(\eta,T)-\alpha(\eta,T-T_0), \tag{4.35}$$

where

$$\alpha(\eta,T)=\tfrac{1}{8}K\,H(T)\Big[8T-4T\Big\{e^{-\eta}\operatorname{erfc}\Big(\frac{\eta}{4T^{\frac{1}{2}}}-T^{\frac{1}{2}}\Big)+\operatorname{erfc}\Big(\frac{\eta}{4T^{\frac{1}{2}}}+T^{\frac{1}{2}}\Big)\Big\}+$$
$$+\eta\Big\{e^{-\eta}\operatorname{erfc}\Big(\frac{\eta}{4T^{\frac{1}{2}}}-T^{\frac{1}{2}}\Big)-\operatorname{erfc}\Big(\frac{\eta}{4T^{\frac{1}{2}}}+T^{\frac{1}{2}}\Big)\Big\}\Big], \tag{4.36}$$

$$\tau_w/\rho U_0|v_w|=1+\beta(T)-\beta(T-T_0), \tag{4.37}$$

where
$$\beta(T)=\tfrac{1}{2}K\,H(T)[T+\tfrac{1}{2}\operatorname{erf}T^{\frac{1}{2}}+\pi^{-\frac{1}{2}}T^{\frac{1}{2}}e^{-T}+T\operatorname{erf}T^{\frac{1}{2}}] \tag{4.38}$$

and

$$\delta_1|v_w|/\nu=[1+\gamma(T)-\gamma(T-T_0)]/[1+KT\,H(T)-K(T-T_0)H(T-T_0)], \tag{4.39}$$

where

$$\gamma(T)=K\,H(T)[\pi^{-\frac{1}{2}}T^{\frac{1}{2}}e^{-T}+\tfrac{1}{2}\pi^{-\frac{1}{2}}T^{\frac{1}{2}}e^{-T}-T^2\operatorname{erfc}T^{\frac{1}{2}}+T\operatorname{erf}T^{\frac{1}{2}}-\tfrac{1}{4}\operatorname{erf}T^{\frac{1}{2}}] \tag{4.40}$$

for all finite T.

A graph of τ_w for $K=4$ and $T_0=\frac{1}{4}$ is given in Fig. 4. For $T<T_0$, $\beta(T-T_0)=0$ from (4.38), and (4.37) and (4.31) are identical so that, for $T<\frac{1}{4}$, Fig. 4 represents the same skin friction as Fig. 3. As in section 4.3 (*a*) it can be shown that the skin friction *decreases* parabolically for small positive values of $(T-T_0)$. For $T>T_0$ there is no pressure gradient so

that the flow will ultimately become steady; it can readily be shown that the ultimate velocity distribution and skin friction are given by

$$u = U_0(1+KT_0)(1-e^{-\eta}) = U(\infty)(1-e^{-\eta})$$

and $\tau_w/\rho U_0|v_w| = 1+KT_0$ respectively. For $K = 4$, $T_0 = \frac{1}{4}$ these are

$$u = 2U_0(1-e^{-\eta}) \quad \text{and} \quad \tau_w/\rho U_0|v_w| = 2.$$

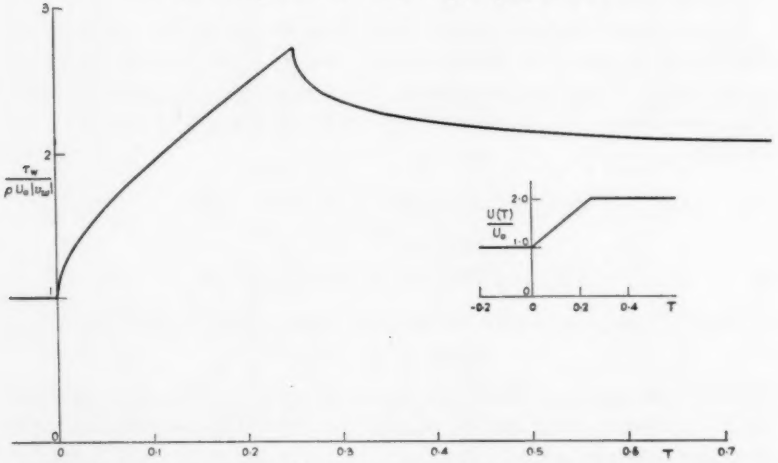

FIG. 4. Behaviour of skin friction in flow with two changes of acceleration

4.4. *Decaying oscillatory velocity field*

Consider the case when the free-stream velocity is given by the real part of

$$U(T) = U_0[1-iA\,H(T)e^{-(K^2-i\Omega)T}],$$

where A, K, and Ω are real constants. Consequently

$$f(T) = -iA\,H(T)e^{-(K^2-i\Omega)T}. \tag{4.41}$$

When $K^2 < 1$, $f(T)$ satisfies the conditions of section 3 so that, from (3.12) the complex form of the velocity distribution is

$$\frac{u}{U_0} = 1-e^{-\eta}-iA\,H(T)e^{-(K^2-i\Omega)T}+$$

$$+iA\,H(T)e^{-(K^2-i\Omega)T}\frac{\eta e^{-\frac{1}{4}\eta}}{4\pi^{\frac{1}{2}}}\int_0^T e^{(K^2-i\Omega)\lambda}\exp\left\{-\left(\lambda+\frac{\eta^2}{16\lambda}\right)\right\}\lambda^{-\frac{1}{2}}\,d\lambda$$

$$= 1-e^{-\eta}-iA\,H(T)e^{-(K^2-i\Omega)T}\left[1-\frac{\eta e^{-\frac{1}{4}\eta}}{4\pi^{\frac{1}{2}}}\int_0^T e^{-(a^2\lambda+b^2/\lambda)}\lambda^{-\frac{1}{2}}\,d\lambda\right],$$

where $a = (1-K^2+i\Omega)^{\frac{1}{2}}$ with the square root chosen so that $\mathrm{re}(a) > 0$,

and where $b = \frac{1}{4}\eta$. By use of equation (B, 2) of Appendix B, the complex velocity becomes

$$\frac{u}{U_0} = 1-e^{-\eta}-iA\,H(T)e^{-(K^2-i\Omega)T}\Big[1-\tfrac{1}{2}e^{-\frac{1}{2}\eta}e^{\frac{1}{2}\eta(1-K^2+i\Omega)^{\frac{1}{2}}}\times$$
$$\times\Big\{e^{-\eta(1-K^2+i\Omega)^{\frac{1}{2}}}\operatorname{erfc}\Big(\frac{\eta}{4T^{\frac{1}{2}}}-(1-K^2+i\Omega)^{\frac{1}{2}}T^{\frac{1}{2}}\Big)+$$
$$+\operatorname{erfc}\Big(\frac{\eta}{4T^{\frac{1}{2}}}+(1-K^2+i\Omega)^{\frac{1}{2}}T^{\frac{1}{2}}\Big)\Big\}\Big] \qquad (4.42)$$

for $T \neq 0$. Equation (4.42) has been derived on the assumption that $K^2 < 1$ but it can readily be shown that u, as given by (4.42), satisfies (3.1) and the corresponding boundary conditions for all K^2 and Ω, provided that $T \neq 0$; so that, exce[illegible] at $T = 0$, the velocity distribution corresponding to (4.41) is given by (4.42) for any real K and Ω. The complex skin friction, τ_w, may be obtained from (4.42) by differentiation with respect to η (cf. equation (3.15)); thus we obtain, for $T \neq 0$,

$$\tau_w/\rho U_0|v_w| = 1-\tfrac{1}{2}iAH(T)[e^{-(K^2-i\Omega)T}+(\pi T)^{-\frac{1}{2}}e^{-T}+$$
$$+e^{-(K^2-i\Omega)T}(1-K^2+i\Omega)^{\frac{1}{2}}\operatorname{erf}\{T^{\frac{1}{2}}(1-K^2+i\Omega)^{\frac{1}{2}}\}]. \qquad (4.43)$$

Consider firstly the particular case $K^2 = 1$. Then the free-stream velocity is
$$U(T) = U_0[1+A\,H(T)e^{-T}\sin\Omega T], \qquad (4.44)$$
and the complex skin friction is deduced from (4.43) as

$$\tau_w/\rho U_0|v_w| = 1-\tfrac{1}{2}iA\,H(T)\,e^{-T}[(\pi T)^{-\frac{1}{2}}+e^{i\Omega T}+e^{i\Omega T}(i\Omega)^{\frac{1}{2}}\operatorname{erf}\{(i\Omega T)^{\frac{1}{2}}\}].$$

But Jahnke and Emde (**8**) give the result, with a change of notation,

$$\operatorname{erf}\{(ix)^{\frac{1}{2}}\} = (2i)^{\frac{1}{2}}[C(x)-i\,S(x)],$$

where C, S are Fresnel's integrals, so that

$$(i\Omega)^{\frac{1}{2}}\operatorname{erf}\{(i\Omega T)^{\frac{1}{2}}\} = (2\Omega)^{\frac{1}{2}}[S(\Omega T)+i\,C(\Omega T)].$$

Consequently, when $K^2 = 1$ the skin friction is

$$\tau_w/\rho U_0|v_w|$$
$$= 1+\tfrac{1}{2}A\,H(T)e^{-T}[\sin\Omega T+(2\Omega)^{\frac{1}{2}}\{S(\Omega T)\sin\Omega T+C(\Omega T)\cos\Omega T\}]. \qquad (4.45)$$

Consider now the case $K^2 \neq 1$. When $\Omega \gg |1-K^2|$ the complex skin friction given by (4.43) is

$$\tau_w/\rho U_0|v_w|$$
$$= 1-\tfrac{1}{2}iA\,H(T)[(\pi T)^{-\frac{1}{2}}e^{-T}+e^{-(K^2-i\Omega)T}+e^{-(K^2-i\Omega)T}(i\Omega)^{\frac{1}{2}}\operatorname{erf}\{(i\Omega T)^{\frac{1}{2}}\}]$$

of which the real part is

$$\tau_w/\rho U_0|v_w|$$
$$= 1+\tfrac{1}{2}A\,H(T)e^{-K^2T}[\sin\Omega T+(2\Omega)^{\frac{1}{2}}\{S(\Omega T)\sin\Omega T+C(\Omega T)\cos\Omega T\}]. \qquad (4.46)$$

This is identical with (4.45) when $K^2 = 1$. Equation (4.46) may be written in the form

$$\tau_w/\rho U_0|v_w| = 1+\tfrac{1}{2}Ae^{-K^2T}H(T)\,B(\Omega,\Omega T)\sin\{\Omega T+\alpha(\Omega,\Omega T)\}, \tag{4.47}$$

where

$$\left.\begin{aligned} B(\Omega,\Omega T) &= [2\Omega\,C^2(\Omega T)+\{1+(2\Omega)^{\frac{1}{2}}\,S(\Omega T)\}^2]^{\frac{1}{2}} \\ \alpha(\Omega,\Omega T) &= \tan^{-1}\frac{(2\Omega)^{\frac{1}{2}}\,C(\Omega T)}{1+(2\Omega)^{\frac{1}{2}}\,S(\Omega T)} \end{aligned}\right\}. \tag{4.48}$$

Thus (4.47) represents the skin friction exactly when $K^2 = 1$ and for $\Omega \gg |1-K^2|$ when $K^2 \neq 1$. Since α is positive, the skin friction has a phase lead over the free-stream velocity fluctuation. Note that, since $C(x)$, $S(x) \to \frac{1}{2}$ as $x \to \infty$, for large ΩT, (4.48) may be replaced by

$$\left.\begin{aligned} B(\Omega) &= [\Omega+(2\Omega)^{\frac{1}{2}}+1]^{\frac{1}{2}} \\ \alpha(\Omega) &= \tan^{-1}\frac{\Omega^{\frac{1}{2}}}{2^{\frac{1}{2}}+\Omega^{\frac{1}{2}}} \end{aligned}\right\} \tag{4.49}$$

and, if both ΩT and Ω are large, (4.48) may be replaced by

$$B = \Omega^{\frac{1}{2}}, \qquad \alpha = \tfrac{1}{4}\pi. \tag{4.50}$$

For any value of K^2, the free-stream velocity is $U_0[1+A\,\Omega T\,H(T)]$ for very small T so that the skin friction grows parabolically for small positive T (cf. section 4.3 (a)). As time increases the skin friction starts to fluctuate due to the fluctuating free-stream velocity and is given by (4.47). For sufficiently large values of the time, ΩT is large for any non-zero value of Ω, and then B and α are given by (4.49) if $K^2 = 1$ or if $\Omega \gg |1-K^2|$. If, furthermore, $\Omega \gg 1$, B and α are given by (4.50). In the latter case, the free-stream velocity and skin friction are given, for $T > 0$, by

$$\left.\begin{aligned} U(T) &= U_0[1+Ae^{-K^2T}\sin\Omega T] \\ \tau_w/\rho U_0|v_w| &= 1+\tfrac{1}{2}Ae^{-K^2T}\,2^{\frac{1}{2}}\sin(\Omega T+\tfrac{1}{4}\pi) \end{aligned}\right\}. \tag{4.51}$$

But Stuart's (2) result for high frequency may be written in the form

$$\left.\begin{aligned} U(T) &= U_0[1+\epsilon\sin\Omega T] \\ \tau_w/\rho U_0|v_w| &= 1+\tfrac{1}{2}\epsilon\Omega^{\frac{1}{2}}\sin(\Omega T+\tfrac{1}{4}\pi) \end{aligned}\right\} \tag{4.52}$$

which formally corresponds to (4.51) if $\epsilon = Ae^{-K^2T}$. Thus the skin friction (4.51) behaves as though the main stream were a pure oscillation about a mean, with amplitude factor Ae^{-K^2T}. By comparison with quasi-steady analogies obtained for other cases, we may refer to this case as quasi-harmonic. In other words this quasi-harmonic property follows from the fact that, for large Ω, the logarithmic decrement of the second term of the skin friction (4.51),

$$\frac{K^2\pi}{\Omega}\log_{10}e = 0{\cdot}4342\frac{K^2\pi}{\Omega},$$

is small. The skin friction given by (4.51) also formally corresponds to Lighthill's (1) expression for the skin friction at large frequencies if

$$\epsilon = Ae^{-K^2T}.$$

A graph of the (exact) skin friction for $K = A = 1$ and $\Omega = 10$ is given in Fig. 5. The properties of the skin friction discussed above are exhibited in this graph. For large ΩT, from equation (4.49), $B = 3{\cdot}93$ and $\alpha = 0{\cdot}605$. It can be shown from the graph that B and α approach these limiting

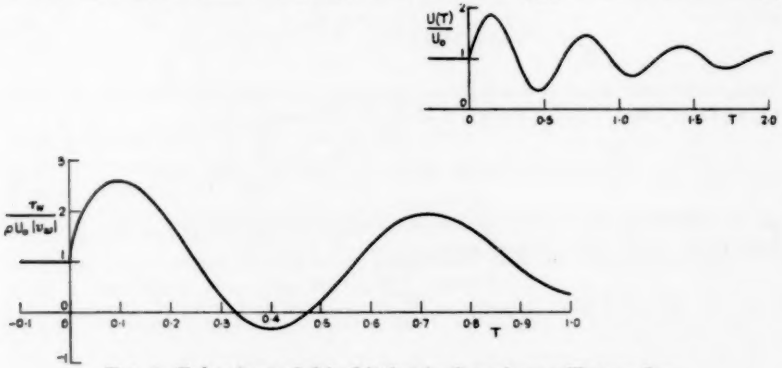

FIG. 5. Behaviour of skin friction in decaying oscillatory flow

values more and more closely as T approaches 1, so that the limiting values of B and α are attained for quite small values of T. This is due to the large value of Ω considered. The values of B and α which result from using the more approximate form (4.50) are $B = 3{\cdot}16$ and $\alpha = 0{\cdot}785$, and these do not differ greatly from the values $B = 3{\cdot}93$, $\alpha = 0{\cdot}605$.

5. Acknowledgements

The author is greatly indebted to his colleague, Dr. J. T. Stuart, at whose suggestion the work was undertaken, for much valuable advice and criticism. The work described above was carried out in the Aerodynamics Division of the National Physical Laboratory, and this paper is published on the recommendation of the Aeronautical Research Council and by permission of the Director of the Laboratory.

APPENDIX A

Suppose that the free-stream velocity ultimately becomes steady, that is,

$$\lim_{T\to\infty} U(T) = U(\infty) \quad \text{or} \quad \lim_{T\to\infty} f(T) = f(\infty),$$

where $U(\infty), f(\infty)$ are finite constants. Then, from (3.12),

$$\lim_{T\to\infty}\left(\frac{u}{U_0}\right) = 1 - e^{-\eta} + f(\infty) - \frac{\eta e^{-\frac{1}{4}\eta}}{4\pi^{\frac{1}{2}}} \lim_{T\to\infty} \int_0^\infty \lambda^{-\frac{1}{2}} f(T-\lambda) \exp\left\{-\left(\lambda + \frac{\eta^2}{16\lambda}\right)\right\} d\lambda \quad \text{(A, 1)}$$

Let
$$\chi(\lambda,\eta) = \lambda^{-\frac{1}{2}}\exp\left\{-\left(\lambda+\frac{\eta^2}{16\lambda}\right)\right\}. \tag{A,2}$$

Then the integral in (A, 1) may be written in the form

$$\int_0^\infty f(T-\lambda)\chi\,d\lambda = \int_0^\infty f(\infty)\chi\,d\lambda + \int_0^{\lambda_0}\{f(T-\lambda)-f(\infty)\}\chi\,d\lambda + \int_{\lambda_0}^\infty\{f(T-\lambda)-f(\infty)\}\chi\,d\lambda. \tag{A,3}$$

The suppositions that $f(\infty)$ is finite and $f(T)$ is bounded in any finite interval imply that $f(T)$ is bounded in $-\infty \leqslant T \leqslant \infty$ so that

$$\left|\int_{\lambda_0}^\infty\{f(T-\lambda)-f(\infty)\}\chi\,d\lambda\right| \leqslant A\int_{\lambda_0}^\infty \lambda^{-\frac{1}{2}}e^{-\lambda}\,d\lambda < \epsilon \tag{A,4}$$

for λ_0 sufficiently large (A is a positive constant). Having chosen some λ_0 to satisfy (A, 4), then, since $|f(T-\lambda)-f(\infty)| < \epsilon$ for T sufficiently large,

$$\left|\int_0^{\lambda_0}\{f(T-\lambda)-f(\infty)\}\chi\,d\lambda\right| \leqslant \epsilon\int_0^{\lambda_0}\chi\,d\lambda < \epsilon\int_0^\infty\chi\,d\lambda = K\epsilon \tag{A,5}$$

for T sufficiently large, where K is a finite positive constant for $0 < \eta < \infty$. Thus from (A, 1), (A, 2), (A, 3), (A, 4), and (A, 5) for $0 < \eta < \infty$

$$\lim_{T\to\infty}\left(\frac{u}{U_0}\right) = 1-e^{-\eta}+f(\infty)-\frac{\eta e^{-\frac{1}{4}\eta}}{4\pi^{\frac{1}{2}}}f(\infty)\int_0^\infty\lambda^{-\frac{1}{2}}\exp\left\{-\left(\lambda+\frac{\eta^2}{16\lambda}\right)\right\}d\lambda$$

$$= 1-e^{-\eta}+f(\infty)-e^{-\eta}f(\infty) = (1-e^{-\eta})[1+f(\infty)]$$

by equation (B, 4), Appendix B.

Thus, from (3.12),
$$\lim_{T\to\infty} u = (1-e^{-\eta})U(\infty). \tag{A,6}$$

Similarly, if $\lim_{T\to-\infty} U(T) = U(-\infty)$, where $U(-\infty)$ is finite then

$$\lim_{T\to-\infty} U(T) = (1-e^{-\eta})U(-\infty). \tag{A,7}$$

APPENDIX B

Some integrals used in the text

For $\mathrm{re}(a) > 0$, $b > 0$, $x \geqslant 0$,

$$I(x,a,b) = \int_0^x \exp\left\{-\left(a^2\lambda+\frac{b^2}{\lambda}\right)\right\}\lambda^{-\frac{1}{2}}\,d\lambda$$

$$= \frac{\pi^{\frac{1}{2}}}{2a}e^{2ab}\left[e^{-4ab}\,\mathrm{erfc}\left(\frac{b}{x^{\frac{1}{2}}}-ax^{\frac{1}{2}}\right)-\mathrm{erfc}\left(\frac{b}{x^{\frac{1}{2}}}+ax^{\frac{1}{2}}\right)\right], \tag{B,1}$$

$$J(x,a,b) = \int_0^x \exp\left\{-\left(a^2\lambda+\frac{b^2}{\lambda}\right)\right\}\lambda^{-\frac{1}{2}}\,d\lambda$$

$$= \frac{\pi^{\frac{1}{2}}}{2b}e^{2ab}\left[e^{-4ab}\,\mathrm{erfc}\left(\frac{b}{x^{\frac{1}{2}}}-ax^{\frac{1}{2}}\right)+\mathrm{erfc}\left(\frac{b}{x^{\frac{1}{2}}}+ax^{\frac{1}{2}}\right)\right]. \tag{B,2}$$

Particular cases of (B, 1) and (B, 2) are

$$I(\infty, a, b) = \frac{\pi^{\frac{1}{2}}}{a} e^{-2ab}, \tag{B, 3}$$

$$J(\infty, a, b) = \frac{\pi^{\frac{1}{2}}}{b} e^{-2ab}. \tag{B, 4}$$

Furthermore, (B, 1) is valid when $b = 0$ so that

$$I(x, a, 0) = \frac{\pi^{\frac{1}{2}}}{a} \operatorname{erf} ax^{\frac{1}{2}} \tag{B, 5}$$

and

$$I(\infty, a, 0) = \frac{\pi^{\frac{1}{2}}}{a}. \tag{B, 6}$$

REFERENCES

1. M. J. Lighthill, *Proc. Roy. Soc.* A, **224** (1954) 1.
2. J. T. Stuart, ibid. **231** (1955) 116.
3. E. J. Watson, ibid. 104.
4. H. Hasimoto, *J. Phys. Soc. Japan*, **12** (1957) 68.
5. N. Curle, Private communication.
6. B. van der Pol and H. Bremmer, *Operational Calculus* (Cambridge, 1955).
7. M. J. Lighthill, *Proc. Roy. Soc.* A, **217** (1953) 478.
8. E. Jahnke and F. Emde, *Tables of Functions* (Dover, 1945).

ON THE VARIATION OF POISSON'S RATIO IN THE SOLUTION OF ELASTIC PROBLEMS

By R. J. KNOPS

(*Department of Mathematics, University of Nottingham*)

[Received 19 September 1957]

SUMMARY

Assuming that the solution is known to a three-dimensional elastic boundary-value problem for a particular Poisson's ratio, equations are established which enable the general solution to be deduced from the known one. The known solution need not necessarily correspond to a real Poisson's ratio; an infinite value, for example, reduces the problem to one in Potential Theory. As illustrations of the method three problems are discussed, one dealing with a semi-infinite body whose plane boundary is rigidly fixed, and two with cones loaded at the vertex. The solutions to the cone problems appear to be new.

1. Introduction

ALTHOUGH the mathematical theory of elasticity was firmly established by the end of the last century the small number of problems which have been completely solved testifies to the difficulty encountered in any practical applications. Even when a general class of boundary-value problems has been integrated the solution usually contains a set of integrals which cannot be exactly evaluated unless the body has some elementary geometrical shape and is loaded in a simple or artificial manner.

These difficulties are increased by the presence in the theory of the elastic moduli as parameters instead of as definite numerical quantities. Retention of the moduli as parameters ensures that the solution to a boundary-value problem is applicable to a general type of medium, but there are many instances where considerable simplifications in the working follow if numerical values for the moduli are inserted at the outset. The resulting solution is then applicable only to a single type of medium and so is strictly limited, but the question then arises whether the general solution to the same problem can be deduced from the known particular one. The answer evidently presents a new method of solving the elastic equations and in the present work the three-dimensional aspects of this topic are discussed.

The two-dimensional case has been partly dealt with by Michell (**1**) (see also (**6**) p. 119), and Coker and Filon (**2**) who investigated solutions only when the boundary conditions were of the stress-type. The three-

dimensional problem was first considered by Westergaard (3) who supposed that, of the two elastic moduli, only Poisson's ratio was varied to give a simplification. We make the same assumption and follow Westergaard's original idea and obtain the general solution from the particular one by the addition of a certain distribution of stresses and displacements. Westergaard's approach made use of the so-called twinned gradient and was only partially successful. The presentation we give leads to a complete development, and suggests that there are several means available for determining the stresses and displacements to be added to the particular solution. The one adopted here employs the Maxwell stress functions and includes Westergaard's results as a special case.

2. Preliminary theory

It was shown by Maxwell (4) that for a medium not subject to body force the Cauchy equilibrium equations

$$\sum_j \frac{\partial \sigma_{ij}}{\partial x_j} = 0 \quad (i,j = 1,2,3), \tag{1}$$

referred to rectangular cartesian coordinates, have a solution

$$\left.\begin{aligned} \sigma_x &= \frac{\partial^2 B}{\partial z^2} + \frac{\partial^2 C}{\partial y^2}, \quad \sigma_y = \frac{\partial^2 C}{\partial x^2} + \frac{\partial^2 A}{\partial z^2}, \quad \sigma_z = \frac{\partial^2 A}{\partial y^2} + \frac{\partial^2 B}{\partial x^2} \\ \sigma_{yz} &= -\frac{\partial^2 A}{\partial y \partial z}, \qquad \sigma_{zx} = -\frac{\partial^2 B}{\partial z \partial x}, \qquad \sigma_{xy} = -\frac{\partial^2 C}{\partial x \partial y} \end{aligned}\right\}, \tag{2}$$

where the σ's are the cartesian components of the stress tensor, and A, B, C are arbitrary functions of x, y, z. The completeness of this solution has been proved by Langhaar and Stippes (5).

If the medium is now assumed homogeneous and isotropic then substituting the stresses (2) into the Beltrami–Michell compatibility equations, viz.

$$\begin{aligned} &\nabla^2\sigma_x + \frac{1}{1+\nu}\frac{\partial^2 \sigma}{\partial x^2} = 0, \quad \nabla^2\sigma_y + \frac{1}{1+\nu}\frac{\partial^2 \sigma}{\partial y^2} = 0, \quad \nabla^2\sigma_z + \frac{1}{1+\nu}\frac{\partial^2 \sigma}{\partial z^2} = 0, \\ &\nabla^2\sigma_{yz} + \frac{1}{1+\nu}\frac{\partial^2 \sigma}{\partial y \partial z} = 0, \quad \nabla^2\sigma_{zx} + \frac{1}{1+\nu}\frac{\partial^2 \sigma}{\partial z \partial x} = 0, \quad \nabla^2\sigma_{xy} + \frac{1}{1+\nu}\frac{\partial^2 \sigma}{\partial x \partial y} = 0, \end{aligned} \tag{3}$$

in which σ is the hydrostatic tension and ν is Poisson's ratio, shows that A, B, C satisfy the compatibility relations

$$\nabla^2 A = \nabla^2 B = \nabla^2 C = \left(\frac{\partial^2 A}{\partial x^2} + \frac{\partial^2 B}{\partial y^2} + \frac{\partial^2 C}{\partial z^2}\right) \Big/ (2-\nu), \tag{4}$$

where ∇^2 denotes the Laplacian operator.

Also, from (2) the hydrostatic tension becomes

$$\sigma = (\sigma_x+\sigma_y+\sigma_z) = \nabla^2(A+B+C)-\left(\frac{\partial^2 A}{\partial x^2}+\frac{\partial^2 B}{\partial y^2}+\frac{\partial^2 C}{\partial z^2}\right)$$

which, with the help of (4) may be expressed as

$$\sigma = \left(\frac{1+\nu}{2-\nu}\right)D, \tag{5}$$

where

$$D = \frac{\partial^2 A}{\partial x^2}+\frac{\partial^2 B}{\partial y^2}+\frac{\partial^2 C}{\partial z^2}.$$

Adding the three Beltrami–Michell equations (3) containing the normal stresses gives

$$\nabla^2\sigma = 0 \tag{6}$$

so that, by (4) and (5),

$$\nabla^4 A = \nabla^4 B = \nabla^4 C = 0; \tag{7}$$

that is, A, B, C *are biharmonic functions.*

The displacements $\mathbf{u} = (u, v, w)$ are found by substituting the stresses (2) into the stress-strain relations

$$2\mu\epsilon_{ij} = \sigma_{ij}-\frac{\nu}{1+\nu}\sigma\delta_{ij},$$

where ϵ_{ij} are the cartesian components of the strain tensor, μ is the shear modulus, and δ_{ij} is the Kronecker delta. The resulting relations are simplified by means of (4) and then integrated to give the displacements. The additional functions introduced by the integration represent a rigid body movement and so can be omitted in the final form of the displacements, which become

$$\left.\begin{aligned} 2\mu u &= \frac{\partial}{\partial x}(A-B-C)\\ 2\mu v &= \frac{\partial}{\partial y}(B-C-A)\\ 2\mu w &= \frac{\partial}{\partial z}(C-A-B)\end{aligned}\right\}. \tag{8}$$

It will be observed that neither of the expressions for the stresses or displacements in terms of Maxwell's stress functions explicitly contain Poisson's ratio. This fact is of importance in the present study.

3. Effect of varying Poisson's ratio

Suppose that a given three-dimensional boundary-value problem without body forces admits of a simple solution when the Poisson's ratio for the medium assumes some particular value ν', so that the Maxwell stress

functions A', B', C' are known. Then in accordance with equations (2) and (8) the stresses and displacements may be expressed in terms of A', B', C', and by equation (4) these functions themselves satisfy the compatibility relations

$$\left.\begin{aligned} \nabla^2 A' = \nabla^2 B' = \nabla^2 C' = D'/(2-\nu') \\ \text{where} \qquad D' = \left(\frac{\partial^2 A'}{\partial x^2} + \frac{\partial^2 B'}{\partial y^2} + \frac{\partial^2 C'}{\partial z^2}\right) \end{aligned}\right\}. \tag{9}$$

Now let Poisson's ratio change to a new value ν, but suppose that the shear modulus and prescribed boundary conditions remain as before. The elastic field is thereby altered, and usually the corresponding field equations must be solved afresh. However, it is proposed to show that the altered field may be determined from that associated with the particular value ν' of Poisson's ratio without any further explicit reference to the field equations. As such it appears to offer a new method for solving elastic problems in three dimensions.

We will call the elastic field associated with the Poisson's ratio ν' the *initial state* and designate with primes all quantities connected with it. The elastic field associated with the new Poisson's ratio ν and which we seek to determine, will be called the *final state*, and the corresponding quantities are left unprimed. This notation is adopted throughout.

We assume that the final value of Poisson's ratio is perfectly general and is only restricted by sufficient conditions for the uniqueness of the final state. For example, ν must be within the range $-1 < \nu < \frac{1}{2}$ in order that the strain-energy function be positive-definite, as required by Kirchhoff's uniqueness theorem. The theorem further requires the strains to be derivable from the displacements according to

$$\epsilon_{ij} = \frac{1}{2}\left(\frac{\partial u_i}{\partial x_j} + \frac{\partial u_j}{\partial x_i}\right)$$

and to be related to stresses by means of the generalized Hooke's law

$$\sigma_{ij} = \frac{2\mu\nu}{(1-2\nu)}\epsilon_{kk}\delta_{ij} + 2\mu\epsilon_{ij} \quad (k = 1, 2, 3) \tag{10}$$

where the summation convention is used; the stresses, moreover, must satisfy the equilibrium equations (1). Besides these field equations, the elastic components must also satisfy the prescribed boundary conditions. Such a state, satisfying all the requirements of the uniqueness theorem, is called a *possible elastic state* and the associated Poisson's ratio is said to be *real*. It should be noted that if the field equations are still satisfied for an unreal Poisson's ratio the only consequence is that their solution is possibly no longer unique and therefore not physically significant.

The final state therefore forms a possible elastic state with a real Poisson's ratio and the same boundary conditions as in the initial problem. A set of Maxwell stress functions A, B, C can thus be associated with the final state, and these unknown functions obey the compatibility relation (4) so that the final stresses and displacements can be derived from them by means of equations (2) and (8) respectively.

Now consider the difference between the final and initial stress functions:

$$A'' = A - A', \quad B'' = B - B', \quad C'' = C - C'. \tag{11}$$

It follows immediately from (7) that A'', B'', C'' *are biharmonic functions.*

By analogy with (2) we may formally define an equilibrium state of stress:

$$\left.\begin{aligned} \sigma''_x &= \frac{\partial^2 B''}{\partial z^2} + \frac{\partial^2 C''}{\partial y^2}, \quad \sigma''_y = \frac{\partial^2 C''}{\partial x^2} + \frac{\partial^2 A''}{\partial z^2}, \quad \sigma''_z = \frac{\partial^2 A''}{\partial y^2} + \frac{\partial^2 B''}{\partial x^2} \\ \sigma''_{yz} &= -\frac{\partial^2 A''}{\partial y \partial z}, \qquad \sigma''_{zx} = -\frac{\partial^2 B''}{\partial z \partial x}, \qquad \sigma''_{xy} = -\frac{\partial^2 C''}{\partial x \partial y} \end{aligned}\right\}, \tag{12}$$

and similarly by analogy with (8) we may formally define a set of displacements to be

$$\left.\begin{aligned} 2\mu u'' &= \frac{\partial}{\partial x}(A'' - B'' - C'') \\ 2\mu v'' &= \frac{\partial}{\partial y}(B'' - C'' - A'') \\ 2\mu w'' &= \frac{\partial}{\partial z}(C'' - A'' - B'') \end{aligned}\right\}. \tag{13}$$

The stresses given in (12) are not in general associated with the displacements given in (13) through stress-strain relations of the type (10), and indeed the precise connexion between them is by no means obvious. However, it is possible to interpret (12) and (13) in a very simple manner. For by the Principle of Superposition and equations (2) and (11) the stress distribution (12) forms the difference between the final and initial stress distributions and thus represents the increment in the stresses which occurs when Poisson's ratio is changed in value. Likewise for the displacements (13); they may be regarded as forming the increments in the displacements of the medium due to a change in Poisson's ratio.

This interpretation provides the key to the present solution of the field equations, because once these increments have been determined the final state is essentially known.

The most suitable way of calculating the *additional state*, as it may be called, is to derive equations for the additional stress functions A'', B'', C'' in terms of the known components of the initial state, solve these equations for the stress functions, and then use equations (12) and (13) to

obtain the additional stresses and displacements. The equations for A'', B'', C'' are established below, but before doing so we briefly mention another approach which although not so convenient in the solution of actual problems is nevertheless useful in the deduction of certain theorems concerning the additional state.† This second method consists in deriving equations for the additional stresses and displacements directly by forming the difference between the appropriate field equations of the final and initial states. For instance, since

$$\sigma''_{ij} = \sigma_{ij} - \sigma'_{ij},$$

$$\mathbf{u}'' = \mathbf{u} - \mathbf{u}'$$

we may take the difference of the respective stress-strain relations (10) and obtain

$$\sigma''_{ij} = 2\mu\left[\frac{\nu}{1-2\nu}\epsilon''_{kk} + \frac{\nu-\nu'}{(1-2\nu)(1-2\nu')}\epsilon'_{kk}\right]\delta_{ij} + 2\mu\epsilon''_{ij}, \tag{14}$$

which relates the additional stresses and strains. Again, those equations which are derived from the Beltrami–Michell and Navier compatibility relations may be identified with those of the classical field theory, but include a body force term whose magnitude depends upon the initial hydrostatic tension and the initial and final Poisson's ratios. The solution to these equations presents no essentially new approach and for this reason we omit a more complete discussion.

Any calculation of the additional state is simplified by the boundary conditions for this state, since these are homogeneous. That is, on those parts of the surface where the tractions are prescribed the additional state has zero tractions; on those parts of the surface where the displacements are prescribed the additional state has zero displacements; and on those parts where the boundary conditions are of the 'mixed' type, the additional state has the corresponding 'mixed' components zero. When dealing with the stress-functions A'', B'', C'' it must be remembered that the boundary conditions involve their first and second derivatives, and not the functions themselves, so that it is appropriate combinations of these derivatives which become zero on the boundary.

Equations for A'', B'', C'' may be derived as follows. Subtracting (9) from (4) and using (11) gives

$$\nabla^2 A'' = \nabla^2 B'' = \nabla^2 C'' \tag{15}$$

and also

$$\nabla^2 C'' = \frac{D}{(2-\nu)} - \frac{D'}{(2-\nu')}. \tag{16}$$

† A full description of these theorems is beyond the scope of the present study.

Substituting

$$D = D' + D'', \qquad D'' = \left(\frac{\partial^2 A''}{\partial x^2} + \frac{\partial^2 B''}{\partial y^2} + \frac{\partial^2 C''}{\partial z^2}\right),$$

in (16) we obtain $$(2-\nu)\nabla^2 C'' - D'' = \left(\frac{\nu-\nu'}{2-\nu'}\right) D',$$

which on using (5) can be rewritten in its final form

$$(2-\nu)\nabla^2 C'' - \left(\frac{\partial^2 A''}{\partial x^2} + \frac{\partial^2 B''}{\partial y^2} + \frac{\partial^2 C''}{\partial z^2}\right) = \left(\frac{\nu-\nu'}{1+\nu'}\right)\sigma'. \tag{17}$$

Equations (15) and (17) together with the boundary conditions enable the biharmonic functions A'', B'', C'' to be determined. This is illustrated later in sections 8 and 9.

4. Axially symmetric states

For many practical applications it is useful to have the results of section 3 reformulated in the special case of axial symmetry. We use cylindrical polar coordinates (r, θ, z) with z as the axis of symmetry. Langhaar and Stippes (**2**) have shown that the complete representation of the stresses now requires just two biharmonic functions F, H, depending only on r, z, namely,

$$\left.\begin{aligned} \sigma_r = \frac{\partial^2 F}{\partial z^2} + \frac{1}{r}\frac{\partial H}{\partial r}, \qquad \sigma_\theta = \frac{\partial^2 F}{\partial z^2} + \frac{\partial^2 H}{\partial r^2}, \qquad \sigma_z = \frac{\partial^2 F}{\partial r^2} + \frac{1}{r}\frac{\partial F}{\partial r} \\ \sigma_{rz} = -\frac{\partial^2 F}{\partial r \partial z}, \qquad \sigma_{r\theta} = \sigma_{z\theta} = 0 \end{aligned}\right\}. \tag{18}$$

The Beltrami–Michell compatibility equations†

$$\left.\begin{aligned} \nabla^2\sigma_r - \frac{2}{r^2}(\sigma_r - \sigma_\theta) + \frac{1}{(1+\nu)}\frac{\partial^2 \sigma}{\partial r^2} = 0 \\ \nabla^2\sigma_\theta + \frac{2}{r^2}(\sigma_r - \sigma_\theta) + \frac{1}{(1+\nu)}\frac{1}{r}\frac{\partial \sigma}{\partial r} = 0 \\ \nabla^2\sigma_z + \frac{1}{(1+\nu)}\frac{\partial^2 \sigma}{\partial z^2} = 0 \\ \nabla^2\sigma_{rz} - \frac{1}{r^2}\sigma_{rz} + \frac{1}{(1+\nu)}\frac{\partial^2 \sigma}{\partial r \partial z} = 0 \end{aligned}\right\} \tag{19}$$

after substitution of (18) lead to

$$\nabla^2 F = \nabla^2 H = \frac{1}{(\nu-1)}\frac{\partial^2}{\partial z^2}(F-H). \tag{20}$$

† The compatibility equations in the axial-symmetric case are derived in (**6**), chap. xiii.

From (18) we have for the hydrostatic tension

$$\sigma = \nabla^2(F+H)+\frac{\partial^2}{\partial z^2}(F-H),$$

so that with (20),

$$\sigma = \left(\frac{\nu+1}{\nu-1}\right)\frac{\partial^2}{\partial z^2}(F-H). \tag{21}$$

The displacements (u_r, u_θ, w) associated with the stresses (19) may now be calculated as in section 2. On integrating the stress-strain relations after these have been reduced by means of (20) the displacements to within a rigid body movement become

$$\left.\begin{aligned} 2\mu u_r &= -\frac{\partial H}{\partial r} \\ u_\theta &= 0 \\ 2\mu w &= \frac{\partial}{\partial z}(H-2F) \end{aligned}\right\}. \tag{22}$$

To calculate the final state from the known initial one we proceed exactly as before and assume that (F', H'), (F, H) are the initial and final sets of the Maxwell stress functions. Then F', H' satisfy

$$\nabla^2 F' = \nabla^2 H' = \frac{1}{(\nu'-1)}\frac{\partial^2}{\partial z^2}(F'-H') \tag{23}$$

with similar relations for F, H. The stresses and displacements corresponding to both states may be derived from equations of type (18) and (22). By taking

$$F'' = F-F', \qquad H'' = H-H'$$

we see that the stresses and displacements defined by equations (18) and (22) in terms of F'', H'' represent the increments in the corresponding components due to a variation of Poisson's ratio, and hence are the stresses and displacements of the additional state. Subtracting (23) from (20) gives

$$\nabla^2 F'' = \nabla^2 H'' \tag{24}$$

and

$$(\nu-1)\nabla^2 F''-\frac{\partial^2}{\partial z^2}(F''-H'') = \left(\frac{\nu'-\nu}{1+\nu'}\right)\sigma' \tag{25}$$

which are analogous to equations (15) and (17) of section 3.

The boundary conditions for the additional state are again homogeneous and similar conclusions follow as in section 3. Using these boundary conditions and (24) and (25) we may determine F'', H'' and thus the additional stresses and displacements, and then complete the problem as previously described.

5. Connexion with Westergaard's method

If in the general case of section 3 we put $A'' = B'' = 0$, and in the axially-symmetric case we put $F'' = 0$, both C'' and H'' become harmonic functions. Also (16) and (25) reduce to

$$\frac{\partial^2 H''}{\partial z^2} = \frac{\partial^2 C''}{\partial z^2} = \left(\frac{\nu' - \nu}{1+\nu'}\right)\sigma'. \tag{26}$$

Moreover, from (16) we have

$$\frac{D}{(2-\nu)} = \frac{D'}{(2-\nu')},$$

which on using (5) becomes

$$\frac{\sigma}{1+\nu} = \frac{\sigma'}{1+\nu'}, \tag{27}$$

and so

$$\sigma'' = \sigma - \sigma' = \left(\frac{\nu - \nu'}{1+\nu'}\right)\sigma'. \tag{28}$$

Similar results hold for the axially symmetric state.

Equations (26), (27), (28) have been previously deduced by Westergaard (**3**) by an allied method which makes use of the so-called twinned gradient. In this method Westergaard restricts the additional displacement field to that which can be expressed as the twinned gradient of some function ϕ to be determined later. That is,

$$2\mu \mathbf{u}'' = \left(-\mathbf{i}\frac{\partial}{\partial x} - \mathbf{j}\frac{\partial}{\partial y} + \mathbf{k}\frac{\partial}{\partial z}\right)\phi, \tag{29}$$

where $\mathbf{i}$, $\mathbf{j}$, $\mathbf{k}$ are the unit cartesian vectors, and the operator on the right side is the twinned gradient. This form of $\mathbf{u}''$ is clearly axially symmetric about the z-axis. The additional strains are derived from the displacements in the usual way and then the stresses are obtained by means of the stress-strain relations (14), although Westergaard deduced these in a less straightforward manner than that given here. The additional stress distribution so obtained is also axially symmetric with the shear components σ_{xz}, σ_{yz} both zero. In order to establish equations which can easily be solved for ϕ, Westergaard had further to restrict this distribution to be planar by taking σ_z zero. Then ϕ becomes a harmonic function identical to C'' and H'', and satisfies equation (26) which can now be solved. The method is applied to the problem of a force at a point of the plane bounding a semi-infinite body and also to the problem of a thick disk rotating about its axis of revolution, but in both these cases it so happens that the additional state is a planar one, otherwise the method would be inapplicable.

Westergaard's approach neglects any mention of boundary conditions for the additional state but inspection shows that he assumed these to be of the 'stress-boundary' type. A further requirement, therefore, is that the additional surface tractions must be zero. This is automatically satisfied in the case where the body is bounded by planes, the additional state of stress occurring parallel to these planes.

The restrictive character of the method is caused by adopting the form (29) for the additional displacement instead of calculating it as we have done. Indeed, although Westergaard includes in his presentation an indication for a generalization,† this artificial step obscures the underlying principles and it is only when we regard the additional state as the difference of two possible elastic ones that an extension becomes possible.

6. Choice of initial state

In choosing the initial state we are not prevented from considering any value whatsoever for the initial Poisson's ratio, since although the field equations remain physically significant only for real values of ν, they are mathematically consistent for all values and hence yield a solution no matter what value of Poisson's ratio is taken. Thus, any boundary-value problem can be solved with an unreal ν, and moreover the same methods can be adopted as for the 'real' theory, except that now the 'stresses', 'strains', and 'displacements' are purely mathematical entities and the solution is possibly no longer unique. The derivation of equations (15) and (17) depends only on the mathematical validity of the field equations and so is true for all values of ν and ν'.

Hence we may solve the given boundary-value problem for an unreal ν and use our method to convert the solution to one corresponding to a real value. The final solution is unique since all the conditions of Kirchhoff's uniqueness theorem are met.

The advantage of extending the choice of initial Poisson's ratio to unreal values lies in being able to select any value which offers a simplification. Apart from values which simplify particular problems, there are also others which when substituted into the field equations effect a significant reduction to the theory as a whole. Examples of these values are 0, $\frac{1}{2}$, ± 1, ∞. The real cases 0, $\frac{1}{2}$ have been dealt with by Sokolnikoff (**7**); we consider in the next section the unreal case $\nu = \infty$, and then use the results in the solution to a particular problem.

† The present extension of Westergaard's original idea was first suggested to me by Professor R. Hill.

7. Field equations for infinite Poisson's ratio

When Poisson's ratio is infinite and provided the shear modulus is held finite, Young's modulus is also infinite, and Lamé's constants λ, μ are connected by the relation

$$\lambda+\mu = 0. \tag{30}$$

The stress-strain relations (10) become

$$\sigma_{ij} = \mu(2\epsilon_{ij}-\epsilon_{kk}\delta_{ij}) \tag{31}$$

and hence by the addition of the normal components of (31) we have

$$\sigma = -\mu\epsilon_{kk}.$$

From (1) and (31) with the strains expressed in terms of the displacements,

$$\nabla^2\mathbf{u} = 0.$$

That is, *the displacements are harmonic functions*; and *therefore so also are the stresses and strains*. Moreover, the equilibrium equations are still identically satisfied by (2) and similar arguments which led to (4) now show that the Maxwell stress functions, instead of being biharmonic, are harmonic.

The solution to Kelvin's problem of a point force inside an extended body becomes particularly simple. Suppose the force is of magnitude P and acts at the origin of coordinates along the positive direction of the z-axis. The specification of a point force requires the stresses to be $O(R^{-2})$ near the origin, where R is the distance from the origin; also, for an infinite medium the stresses must vanish as $O(R^{-2})$ at infinity in order to comply with Kirchhoff's uniqueness theorem. These conditions apply for real values of Poisson's ratio but we assign them to the present problem so that the stresses of any derived elastic state containing a point force have the correct order of magnitude.

To describe completely the stresses we need only two stress-functions as there is symmetry about the z-axis. These functions must be harmonic and give rise to stresses of $O(R^{-2})$ both at the origin and at infinity. Therefore, let

$$H = 0, \qquad F = B\log(R+z),$$

where B is a constant to be determined later.

In accordance with (18) and (22) the stresses and displacements are

$$\left.\begin{aligned} \sigma_r = -B\frac{z}{R^3}, \quad \sigma_\theta = -B\frac{z}{R^3}, \quad \sigma_z = B\frac{z}{R^3}, \quad \sigma_{rz} = B\frac{r}{R^3} \\ u_r = u_\theta = 0, \qquad 2\mu w = -2B/R \end{aligned}\right\}. \tag{32}$$

To find B we observe that the total vertical pressure on any plane

$z =$ a positive constant must be $\frac{1}{2}P$. Hence, for $z > 0$,

$$\tfrac{1}{2}P = -2\pi Bz \int_z^\infty \frac{dR}{R^2}$$

and so

$$B = -\frac{P}{4\pi}.$$

Substituting B in (32) completes the solution.

8. Internal force in semi-infinite medium with plane rigidly-constrained boundary

We now use the solution to Kelvin's problem to solve the problem of a force inside a semi-infinite medium whose plane boundary is held rigidly fixed; that is, all components of the displacement are zero on the boundary. For an infinite Poisson's ratio the derivation from Kelvin's solution corresponds to a problem in Potential Theory, and can therefore be easily accomplished. We thereafter use the results of section 4 to obtain from this particular state that associated with a general value of Poisson's ratio.

Let the medium occupy the space $z \leqslant 0$ and take the force to be of magnitude P acting in the positive direction of the z-axis at the point $(0, 0, -c)$. Due to this force the solution contains a singularity of the Kelvin type found in (32), and further this can be the only singularity since there is only one force acting. Therefore if S_K represents the distribution (32) with a suitable change of axes, we may assume that S_K provides the singular part of the final distribution and so when Poisson's ratio is infinite the problem is reduced to finding a distribution S_1 regular and harmonic in $z \leqslant 0$ such that the displacements belonging to

$$S = S_1 + S_K$$

vanish on the boundary $z = 0$.

Now in (32) the w-displacement is clearly the singular part of the first Green's function for the half-space occupied by the body. This function is harmonic, vanishes over the boundary and is, moreover, known for the region under consideration. Hence it will serve for the w-displacement of S. The u_r-displacement of S_K is identically zero throughout the body so that the corresponding displacement of S_1 must vanish on $z = 0$. Since this component is regular we have from a well-known theorem in Potential Theory that it is identically zero throughout the half-space. Thus we may write for the displacement of S

$$u_r' = 0, \qquad 2\mu w' = \frac{P}{2\pi}\left(\frac{1}{R} - \frac{1}{R_1}\right), \tag{33}$$

where $R^2 = x^2+y^2+(z+c)^2, \qquad R_1^2 = x^2+y^2+(z-c)^2.$

The second displacement component, u_θ, is obviously zero since there is axial symmetry about the z-axis. The strains are

$$\left.\begin{aligned} \epsilon'_z = \frac{P}{4\pi\mu}\frac{\partial}{\partial z}\left(\frac{1}{R}-\frac{1}{R_1}\right), \qquad \epsilon'_{rz} = \frac{P}{8\pi\mu}\frac{\partial}{\partial r}\left(\frac{1}{R}-\frac{1}{R_1}\right) \\ \epsilon'_r = \epsilon'_\theta = 0 \end{aligned}\right\}, \tag{34}$$

and from (31) the stresses are

$$\left.\begin{aligned} \sigma'_r = -\frac{P}{4\pi}\frac{\partial}{\partial z}\left(\frac{1}{R}-\frac{1}{R_1}\right), \qquad \sigma'_\theta = -\frac{P}{4\pi}\frac{\partial}{\partial z}\left(\frac{1}{R}-\frac{1}{R_1}\right) \\ \sigma'_z = \frac{P}{4\pi}\frac{\partial}{\partial z}\left(\frac{1}{R}-\frac{1}{R_1}\right), \qquad \sigma'_{rz} = \frac{P}{4\pi}\frac{\partial}{\partial r}\left(\frac{1}{R}-\frac{1}{R_1}\right) \end{aligned}\right\}. \tag{35}$$

Equations (33), (34), (35) supply the solution to the problem when Poisson's ratio is infinite.

The solution for any other value may now be derived from the theory described in section 4, with the initial state corresponding to one with an infinite Poisson's ratio. Thus, we must find two biharmonic functions F'', H'' which satisfy

$$\nabla^2 F'' = \nabla^2 H'' \tag{36}$$

and

$$(\nu-1)\nabla^2 F'' - \frac{\partial^2}{\partial z^2}(F''-H'') = \sigma', \tag{37}$$

where σ' is given in (35). Furthermore, since the displacements are everywhere prescribed on the surface, the boundary conditions for the additional state are that the displacements vanish everywhere on $z = 0$. That is,

$$u''_r = w'' = 0 \quad \text{on } z = 0,$$

or by (22),

$$\frac{\partial H''}{\partial r} = \frac{\partial}{\partial z}(H''-2F'') = 0 \quad \text{on } z = 0. \tag{38}$$

To calculate F'', H'' we start by integrating (36), giving

$$H'' = F''+\alpha, \tag{39}$$

where α is a regular harmonic function in $z \leqslant 0$, and then substitute for H'' from (39) in (37). This gives

$$\nabla^2 F'' = \left\{\sigma' - \frac{\partial^2 \alpha}{\partial z^2}\right\} \Big/ (\nu-1),$$

which on using (35) for σ' becomes

$$\nabla^2 F'' = \left[-\frac{P}{4\pi}\frac{\partial}{\partial z}\left(\frac{1}{R}-\frac{1}{R_1}\right) - \frac{\partial^2 \alpha}{\partial z^2}\right] \Big/ (\nu-1),$$

and so, by integrating,

$$F'' = \frac{1}{8\pi(1-\nu)}\left[\frac{z+c}{R} - \frac{z}{R_1}\right] + \frac{z}{2(1-\nu)}\frac{\partial \alpha}{\partial z} + \beta, \tag{40}$$

where β is also a regular harmonic function in $z \leqslant 0$. Returning to the boundary conditions (38), we put

$$H'' = 0 \quad \text{on } z = 0 \tag{41}$$

and thus obtain by (39)

$$F'' = -\alpha \quad \text{on } z = 0 \tag{42}$$

and by (38),

$$\frac{\partial F''}{\partial z} = \frac{\partial \alpha}{\partial z} \quad \text{on } z = 0. \tag{43}$$

Then since α is regular we have from (42) and (40)

$$\alpha = -\frac{Pc}{8\pi(1-\nu)}\left(\frac{1}{R_1}\right) - \beta \quad \text{in } z \leqslant 0 \tag{44}$$

and from (43) and (40)

$$\frac{1}{2}\left(\frac{1-2\nu}{1-\nu}\right)\frac{\partial \alpha}{\partial z} = -\frac{Pc}{8\pi(1-\nu)}\frac{\partial}{\partial z}\left(\frac{1}{R_1}\right) + \frac{\partial \beta}{\partial z}$$

which, on integrating once with respect to z, becomes

$$\frac{1}{2}\left(\frac{1-2\nu}{1-\nu}\right)\alpha = -\frac{P}{8\pi(1-\nu)}\left(\frac{c}{R_1}\right) + \beta. \tag{45}$$

No additive arbitrary function of x, y is required since α, β, $1/R_1$ vanish as $z \to -\infty$.

From (44) and (45) we find

$$\alpha = -\frac{P}{2\pi(3-4\nu)}\left(\frac{c}{R_1}\right),$$

$$\beta = \frac{P}{8\pi(3-4\nu)(1-\nu)}\left(\frac{c}{R_1}\right),$$

and these expressions when substituted into (40) and (39) lead to the following final forms of F'' and H'':

$$F'' = P\left[\frac{z+c}{R} - \frac{z}{R_1}\right]\Big/[8\pi(1-\nu)] + Pc\left[\frac{1}{R_1} - 2z\frac{\partial}{\partial z}\left(\frac{x^3}{R_1}\right)\right]\Big/[8\pi(3-4\nu)(1-\nu)],$$

$$H'' = P\left[(z+c)\left(\frac{1}{R} - \frac{1}{R_1}\right)\right]\Big/[8\pi(1-\nu)] - Pcz\frac{\partial}{\partial z}\left(\frac{1}{R_1}\right)\Big/[4\pi(3-4\nu)(1-\nu)]. \tag{46}$$

Calculating the additional state from (46), (18), and (22) and adding this

to the stresses and displacements of (35) and (33) respectively gives the final solution to the problem for any value of Poisson's ratio:

$$\sigma_r = -\frac{P}{4\pi}\frac{\partial}{\partial z}\left(\frac{1}{R}-\frac{1}{R_1}\right)-\frac{P}{8\pi(1-\nu)}\left[\frac{z+c}{R^3}+\frac{3r^2(z+c)}{R^5}-\frac{(z-c)}{R_1^3}-\frac{3r^2z}{R_1^5}\right]-$$
$$-\frac{Pc}{8\pi(3-4\nu)(1-\nu)}\left[3\frac{\partial^2}{\partial z^2}\left(\frac{1}{R_1}\right)-2z\frac{\partial^3}{\partial r^2\partial z}\left(\frac{1}{R_1}\right)\right],$$

$$\sigma_\theta = -\frac{P}{4\pi}\frac{\partial}{\partial z}\left(\frac{1}{R}-\frac{1}{R_1}\right)+\frac{P}{8\pi(1-\nu)}\left[\frac{z-c}{R_1^3}-\frac{z+c}{R^3}-\frac{3cr^2}{R_1^5}\right]-$$
$$-\frac{3Pc}{8\pi(3-4\nu)(1-\nu)}\left[\frac{(z-c)(z-3c)}{R_1^5}-\frac{1}{R_1^3}\right],$$

$$\sigma_z = \frac{P}{4\pi}\frac{\partial}{\partial z}\left(\frac{1}{R}-\frac{1}{R_1}\right)+\frac{P}{8\pi(1-\nu)}\left[\frac{z+c}{R^3}-\frac{z+c}{R_1^3}+\frac{3z^2(z-c)}{R_1^5}-\frac{3(z+c)^3}{R^5}\right]+$$
$$+\frac{Pc}{8\pi(3-4\nu)(1-\nu)}\left[2z\frac{\partial^3}{\partial z^3}\left(\frac{1}{R_1}\right)-\frac{\partial^2}{\partial z^2}\left(\frac{1}{R_1}\right)\right],$$

$$\sigma_{rz} = \frac{P}{4\pi}\frac{\partial}{\partial r}\left(\frac{1}{R}-\frac{1}{R_1}\right)+\frac{P}{8\pi(1-\nu)}\left[r\left(\frac{1}{R^3}-\frac{1}{R_1^3}\right)-\frac{3(z+c)^2r}{R^5}+\frac{3rz(z-c)}{R_1^5}\right]+$$
$$+\frac{Pc}{8\pi(3-4\nu)(1-\nu)}\left[\frac{3r(z-c)}{R_1^5}+\frac{6rz}{R_1^5}-\frac{42rz(z-c)^2}{R^7}\right],$$

$$\sigma = -\frac{P}{4\pi}\left(\frac{1+\nu}{1-\nu}\right)\left(\frac{z+c}{R^3}\right)+\frac{P}{4\pi(1-\nu)}\left[z(1+\nu)-\nu c+\frac{7c}{2(3-4\nu)}\right]-$$
$$-\frac{3Pc}{8\pi(1-\nu)R_1^5}\left[r^2+\frac{7(z+c)^2}{3-4\nu}\right].$$

$$2\mu u_r = \frac{P}{8\pi(1-\nu)}r(z+c)\left[\frac{1}{R^3}-\frac{1}{R_1^3}\right]+\frac{3Pc}{4\pi(3-4\nu)(1-\nu)}\frac{rz(z-c)}{R_1^5},$$

$$2\mu w = \frac{P}{2\pi}\left(\frac{1}{R}-\frac{1}{R_1}\right)+\frac{P}{8\pi(1-\nu)}\left[\frac{(z+c)^2}{R^3}-\frac{(z-c)^2}{R_1^3}\right]+$$
$$+\frac{Pc}{4\pi(3-4\nu)(1-\nu)}z\left[\frac{3(z-c)^2}{R_1^5}-\frac{1}{R_1^3}\right].$$

The solution was first obtained by Rongved (**8**) who used a slight modification of the method adopted by Mindlin for the allied problem of a force inside a semi-infinite body whose plane boundary is traction-free. Both approaches are closely related to Potential Theory and therefore require a knowledge of the Green's functions for the region occupied by the body. They cannot be generally applied and are successful only in those problems where the Green's functions are known. Our method is of course not bound by this restriction since it is only for an infinite Poisson's ratio that Potential Theory is explicitly introduced. However, it is preferable

to use Mindlin's approach since this gives immediately the final solution for any value of ν and does not involve the two subsidiary problems which are an essential part of our method.

9. Two further problems

To illustrate another way of determining the additional stress functions we solve the two problems of a solid bounded by two right circular coaxial cones loaded by a force acting at the common vertex in the directions (i) along the common axis; and (ii) perpendicular to the common axis. We suppose those parts of the solid at great distances are held fixed.

By considering the form of the initial hydrostatic tension it is possible to express the additional stress functions as linear combinations of certain harmonic and biharmonic functions and thereby reduce equation (17) to a relation between the constant coefficients of the linear combinations. These constants are adjusted so that the reduced equation (17) and the boundary conditions for the additional state are satisfied.

Westergaard, amongst others, has mentioned (3) that when Poisson's ratio is $\frac{1}{2}$ the stress distribution in Kelvin's problem is purely radial and hence the stresses, strains, and displacements in this case are the same as those for variously shaped cones loaded by a force at the vertex, and also for an infinite wedge loaded at a point of its edge. Included amongst these general bodies are those considered in (i) and (ii) so that their solution is known for Poisson's ratio $\frac{1}{2}$ and we therefore take this to be the initial state.

(i) *Solid bounded by two coaxial cones loaded at the common vertex by a force acting along the axis*

Let the common vertex be the origin of coordinates and draw the positive z-axis coincident with the common axis of the cones. Take the semi-vertical angles of the outer and inner cones to be α and β respectively, and suppose that P is the magnitude of the force which acts at O in the positive direction of the z-axis (see Fig. 1).

It is convenient to use the spherical polar (R, θ, ϕ) components of the stress tensor and displacement vector and to express these components in terms of the coordinates (r, R, z) where

$$r = R\sin\phi, \qquad z = R\cos\phi.$$

When Poisson's ratio is $\frac{1}{2}$ the solution may be derived from Kelvin's problem and takes the form

$$\sigma'_R = \sigma' = -\frac{3P}{2\pi a}\left(\frac{z}{R^3}\right) \tag{47}$$

with the other stress components vanishing; and

$$2\mu u_R = \frac{P}{2\pi a}\frac{z}{R^2}, \qquad u_\theta = 0, \qquad 2\mu u_\phi = -\frac{P}{2\pi a}\frac{r}{R^2}, \tag{48}$$

where $$a = (\cos^3\beta - \cos^3\alpha).$$

It may be easily verified that the stress-distribution (47) leaves the surfaces of the cones $\phi = \alpha$, $\phi = \beta$ free from tractions and exactly counterbalances the force at the vertex. Any stress distribution which is added

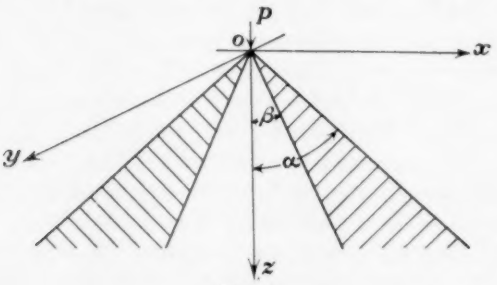

FIG. 1

to allow for a variation in Poisson's ratio must therefore leave the surfaces stress-free and also give rise to no further resultant force at the vertex.

Clearly there is symmetry about the z-axis, so we may use the results of section 4. With

$$\nu' = \tfrac{1}{2}, \qquad \sigma' = -\frac{3P}{2\pi a}\frac{z}{R^3},$$

equations (24) and (25) for the additional stress functions F'', H'' become

$$(\nu-1)\nabla^2 F'' - \frac{\partial^2}{\partial z^2}(F''-H'') = -(1-2\nu)\frac{P}{2\pi a}\frac{z}{R^3}, \tag{49}$$

$$\nabla^2 F'' = \nabla^2 H''. \tag{50}$$

In order to reduce (49) to a relation between constants and also to satisfy (50) it is reasonable to try the following forms for F'' and H'':

$$\left.\begin{aligned} F'' &= k\frac{z}{R} + n\log(R+z) + m\log(R-z) \\ H'' &= k\frac{z}{R} + h\log(R+z) + g\log(R-z) \end{aligned}\right\}, \tag{51}$$

where g, h, k, m, n are constants. Substitution of (51) into (49) gives

$$2(\nu-1)k + (h-g) + p = (1-2\nu)\frac{P}{2\pi a} \tag{52}$$

with $$p = (m-n).$$

The cylindrical polar components of the additional stresses may be obtained from (51) and (18) and then transforming by the tensorial law we find that the stresses in spherical polar coordinates are

$$\left.\begin{aligned}
\sigma''_R &= -(p+2k)\frac{\cos\phi}{R^2}+\left[\frac{h}{1+\cos\phi}+\frac{g}{1-\cos\phi}\right]\frac{\sin^2\phi}{R^2}\\
\sigma''_\theta &= (p-k)\frac{\cos\phi}{R^2}+\frac{h(\cos^2\phi+\cos\phi-1)}{R^2(1+\cos\phi)}+g\,\frac{(\cos^2\phi-\cos\phi-1)}{R^2(1-\cos\phi)}\\
\sigma''_\phi &= (p-k)\frac{\cos\phi}{R^2}+\left[\frac{h}{1+\cos\phi}+\frac{g}{1-\cos\phi}\right]\frac{\cos^2\phi}{R^2}\\
\sigma''_{R\phi} &= (p-k)\frac{\sin\phi}{R^2}+\left[\frac{h}{1+\cos\phi}+\frac{g}{1-\cos\phi}\right]\frac{\sin\phi\cos\phi}{R^2}\\
\sigma''_{R\theta} &= \sigma''_{\phi\theta} = 0
\end{aligned}\right\}. \quad (53)$$

Similarly, the displacements are

$$\left.\begin{aligned}
2\mu u''_R &= (h-g-2p)\frac{\cos\phi}{R}-\left[\frac{h}{1+\cos\phi}+\frac{g}{1-\cos\phi}\right]\frac{\sin^2\phi}{R}\\
u''_\theta &= 0\\
2\mu u''_\phi &= -\left[(h-g-2p-k)+\cos\phi\left(\frac{h}{1+\cos\phi}+\frac{g}{1-\cos\phi}\right)\right]\frac{\sin\phi}{R}
\end{aligned}\right\}. \quad (54)$$

The condition that the additional stress distribution (53) gives rise to no extra resultant force at the vertex is that the tractions in the direction of the axis of the cone taken across any spherical surface, centre the vertex, must be zero. That is

$$\int_\beta^\alpha (\sigma''_{R\phi}\sin^2\phi-\sigma''_R\sin\phi\cos\phi)\,d\phi = 0$$

or from (53), $$k[\cos^2\alpha+\cos\alpha\cos\beta+\cos^2\beta-1]+p = 0. \quad (55)$$

The sides of the body remain stress-free, so that

$$\sigma''_\phi = \sigma''_{R\phi} = 0 \quad \text{for} \quad \phi = \alpha, \beta$$

and so from (53)

$$\left.\begin{aligned}
(p-k)+\frac{h\cos\alpha}{(1+\cos\alpha)}+\frac{g\cos\alpha}{(1-\cos\alpha)} &= 0\\
(p-k)+\frac{h\cos\beta}{(1+\cos\beta)}+\frac{g\cos\beta}{(1-\cos\beta)} &= 0
\end{aligned}\right\}. \quad (56)$$

Solving equations (52), (55), (56) for the four unknown constants g, h, k, p gives

$$\left.\begin{aligned} g &= -\frac{(1-2\nu)P}{4\pi a}\,\frac{L(1-\cos\alpha)(1-\cos\beta)}{M} \\ h &= \frac{(1-2\nu)P}{4\pi a}\,\frac{L(1+\cos\alpha)(1+\cos\beta)}{M} \\ k &= \frac{(1-2\nu)P}{4\pi a}\,\frac{\cos\alpha\cos\beta}{M} \\ p &= -\frac{(1-2\nu)P}{4\pi a}\,\frac{(L-1)\cos\alpha\cos\beta}{M} \end{aligned}\right\} \tag{57}$$

where

$$\left.\begin{aligned} L &= (\cos^2\alpha+\cos\alpha\cos\beta+\cos^2\beta) \\ M &= (\cos^2\alpha+2\nu\cos\alpha\cos\beta+\cos^2\beta) \end{aligned}\right\}$$

Substituting these values in (53) and (54) and adding the resulting system of stresses and displacements to the initial state, (47) and (48) give the final form of the distribution for any value of Poisson's ratio

$$\sigma_R = -\frac{P}{2\pi}\,\frac{[3M+(1-2\nu)(L-3)\cos\alpha\cos\beta]}{LMN}\,\frac{z}{R^3}+$$

$$+\frac{(1-2\nu)P}{4\pi MN}\left[\frac{(1+\cos\alpha)(1+\cos\beta)}{(R+z)}-\frac{(1-\cos\alpha)(1-\cos\beta)}{(R-z)}\right]\frac{r^2}{R^3},$$

$$\sigma_\theta = \frac{(1-2\nu)P}{4\pi MN}\left[(1+\cos\alpha)(1+\cos\beta)\frac{(z^2+zR-R^2)}{R^3(R+z)}-\right.$$

$$\left.-(1-\cos\alpha)(1-\cos\beta)\frac{(z^2-zR-R^2)}{R^3(R-z)}-2\cos\alpha\cos\beta\,\frac{z}{R^3}\right],$$

$$\sigma_\phi = \frac{(1-2\nu)P}{4\pi MN}\left[(1+\cos\alpha)(1+\cos\beta)\frac{z^2}{R^3(R+z)}-\right.$$

$$\left.-(1-\cos\alpha)(1-\cos\beta)\frac{z^2}{R^3(R-z)}-2\cos\alpha\cos\beta\,\frac{z}{R^3}\right],$$

$$\sigma_{R\phi} = \frac{(1-2\nu)P}{4\pi MN}\left[(1+\cos\alpha)(1+\cos\beta)\frac{rz}{R^3(R+z)}-\right.$$

$$\left.-(1-\cos\alpha)(1-\cos\beta)\frac{rz}{R^3(R-z)}-2\cos\alpha\cos\beta\,\frac{r}{R^3}\right],$$

$$\sigma_{R\theta} = \sigma_{\phi\theta} = 0,$$

$$\sigma = -\frac{(1+\nu)P}{\pi MN}\,\frac{z}{R^3}.$$

$$2\mu u_R = \frac{P}{4\pi LMN}[M+2(1-2\nu)\{L+\cos\alpha\cos\beta(3L-2)\}]\frac{z}{R^3}-$$

$$-\frac{(1-2\nu)P}{4\pi MN}\left[\frac{(1+\cos\alpha)(1+\cos\beta)}{(R+z)}-\frac{(1-\cos\alpha)(1-\cos\beta)}{(R-z)}\right],$$

$$u_\theta = 0,$$

$$2\mu u_\phi = -\frac{(1-2\nu)P}{4\pi LMN}\left[2\{L+\cos\alpha\cos\beta(3L-1)\}\frac{r}{R^3}+\right.$$

$$\left.+L\left\{(1+\cos\alpha)(1+\cos\beta)\frac{rz}{R^2(R+z)}-(1-\cos\alpha)(1-\cos\beta)\frac{rz}{R^2(R-z)}\right\}\right],$$

with L and M given by (57), and

$$N = (\cos\beta-\cos\alpha).$$

The solution to the solid cone loaded by a force at the vertex along the axis may be deduced by taking $\beta = 0$. The problem has been previously treated by Michell (**9**),† who combined various simple solutions, all containing a singularity in the stresses of $O(R^{-2})$ at the origin, so as to satisfy the boundary conditions.

By putting $\alpha = \frac{1}{2}\pi$ in the solution to the solid cone we can obtain that for a force acting perpendicular to the plane boundary of a semi-infinite body at a point of the boundary. The solution was first derived by Boussinesq,‡ and later used by Westergaard to illustrate his method of the twinned gradient. Westergaard took as initial state Kelvin's solution when Poisson's ratio is $\frac{1}{2}$, and indeed, had we directly applied our method to the same problem the various steps of the derivation would have been precisely similar, showing that the twinned gradient approach is a particular case of our own. (For details of Westergaard's solution, see (**3**) p. 139.)

(ii) *Solid bounded by two coaxial cones loaded by a force at the common vertex perpendicular to the axis*

We use the same general approach as in (i) with the exception that as there is no axial symmetry we must employ the results of section 3 instead of section 4.

The common vertex of the cones is again taken as the origin of coordinates and the axis of the cones as the positive z-axis. The x-axis is drawn along the line of action of the applied force which is of magnitude P, and α and β are the semi-vertical angles of the outer and inner cones respectively. (See Fig. 2.)

The initial state is chosen as the solution to Kelvin's problem with ν

† See also Love (**10**), 201.
‡ Ibid. 189.

as $\frac{1}{2}$, since then the stress-distribution is entirely radial; in cartesian coordinates this is

$$\left.\begin{aligned} \sigma'_x &= -\frac{3P}{\pi ab}\left(\frac{x^3}{R^5}\right), \quad \sigma'_y = -\frac{3P}{\pi ab}\left(\frac{xy^2}{R^5}\right), \quad \sigma'_z = -\frac{3P}{\pi ab}\left(\frac{xz^2}{R^5}\right) \\ \sigma'_{zy} &= -\frac{3P}{\pi ab}\left(\frac{xyz}{R^5}\right), \quad \sigma'_{xz} = -\frac{3P}{\pi ab}\left(\frac{x^2z}{R^5}\right), \quad \sigma'_{xy} = -\frac{3P}{\pi ab}\left(\frac{x^2y}{R^5}\right) \end{aligned}\right\}, \tag{58}$$

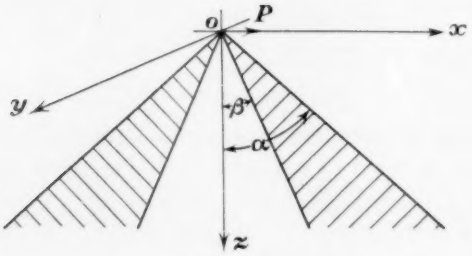

FIG. 2

where

$$a = 3-(\cos^2\alpha+\cos\alpha\cos\beta+\cos^2\beta),$$

$$b = (\cos\beta-\cos\alpha).$$

The initial displacement field is

$$2\mu u' = \frac{P}{\pi ab}\left(1+\frac{x^2}{R^2}\right)\frac{1}{R}, \quad 2\mu v' = \frac{P}{\pi ab}\left(\frac{xy}{R^3}\right), \quad 2\mu w' = \frac{P}{\pi ab}\left(\frac{xz}{R^3}\right). \tag{59}$$

The stresses (58) leave the surfaces of the body $\phi = \alpha$, $\phi = \beta$ free from tractions and counterbalance the applied force. The additional stresses must therefore leave the surfaces stress-free and give rise to zero resultant force at the vertex, and so we adjust accordingly the constants of the linear combinations for A'', B'', C''. On substituting

$$\nu' = \tfrac{1}{2}, \qquad \sigma' = -\frac{3P}{\pi ab}\frac{x}{R^3}$$

in equation (17), the relations for the additional stress functions A'', B'', C'' become

$$(2-\nu)\nabla^2 C''-\left(\frac{\partial^2 A''}{\partial x^2}+\frac{\partial^2 B''}{\partial y^2}+\frac{\partial^2 C''}{\partial z^2}\right) = \frac{(1-2\nu)}{\pi ab}\left(\frac{x}{R^3}\right), \tag{60}$$

$$\nabla^2 A'' = \nabla^2 B'' = \nabla^2 C''. \tag{61}$$

Equation (61) is identically satisfied and equation (60) reduces to a relation between constants if A'', B'', C'' have the form

$$\left.\begin{aligned} A'' &= k\frac{x}{R}+p\left(\frac{x}{R+z}\right)+n\left(\frac{x}{R-z}\right)+q\log(R+x)+g\log(R-x)\\ B'' &= k\frac{x}{R}+p\left(\frac{x}{R+z}\right)+n\left(\frac{x}{R-z}\right)+m\log(R+x)+f\log(R-x)\\ C'' &= k\frac{x}{R}+h\left(\frac{x}{R+z}\right)+d\left(\frac{x}{R-z}\right)+m\log(R+x)+f\log(R-x) \end{aligned}\right\} \quad (62)$$

where $d, f, g, h, k, m, n, p, q$ are constants.

With these expressions the cartesian components of the additional stress-tensor can be obtained from (2) and by transforming into spherical polar components it can be shown that the condition for stress-free boundaries requires the constants to satisfy the following equations:

$$g = q = 0, \quad (63)$$

$$\left.\begin{aligned} (k+p+n+t)+\frac{h\cos^2\alpha}{(1+\cos\alpha)^2}+\frac{d\cos^2\alpha}{(1-\cos\alpha)^2}-\frac{2p\cos\alpha}{(1+\cos\alpha)}+\frac{2n\cos\alpha}{(1-\cos\alpha)} &= 0\\ (k+p+n+t)+\frac{h\cos^2\beta}{(1+\cos\beta)^2}+\frac{d\cos^2\beta}{(1-\cos\beta)^2}-\frac{2p\cos\beta}{(1+\cos\beta)}+\frac{2n\cos\beta}{(1-\cos\beta)} &= 0\\ (k+p+n+t)\cos\alpha-\frac{h\cos\alpha(1-\cos^2\alpha)}{(1+\cos\alpha)^2}-\frac{d\cos\alpha(1-\cos^2\alpha)}{(1-\cos\alpha)^2}- & \\ -\frac{p(2\cos^2\alpha-1)}{(1+\cos\alpha)}+\frac{n(2\cos^2\alpha-1)}{(1-\cos\alpha)} &= 0\\ (k+p+n+t)\cos\beta-\frac{h\cos\beta(1-\cos^2\beta)}{(1+\cos\beta)^2}-\frac{d\cos\beta(1-\cos^2\beta)}{(1-\cos\beta)^2}- & \\ -\frac{p(2\cos^2\beta-1)}{(1+\cos\beta)}+\frac{n(2\cos^2\beta-1)}{(1-\cos\beta)} &= 0 \end{aligned}\right\} \quad (64)$$

where $$t = (m-f).$$

Substitution of (62) and (63) in (60) gives

$$2k(1-\nu)+(h+d)-(p+n)+t = (2\nu-1)\frac{P}{\pi ab}. \quad (65)$$

For the additional stress distribution to have no resultant force at the vertex, the tractions in the x-direction over any plane $z =$ a positive constant must be zero. Thus

$$\int_0^{2\pi}\int_{z\tan\beta}^{z\tan\alpha}\sigma''_{xz}\,r\,dr d\theta = 0$$

or since $$\sigma''_{xz} = -\frac{\partial^2 B''}{\partial x\partial z}, \quad \text{then} \quad (a-2)k-p-n-2t = 0. \quad (66)$$

Solving the six equations (64), (65), (66) for the six unknown constants d, h, k, n, p, t gives:

$$\left.\begin{aligned} d &= -\frac{(1-2\nu)P}{4\pi be}C^2D^2(A\cos\beta+B\cos\alpha) \\ h &= (1-2\nu)\frac{P}{4\pi}\frac{A^2B^2(C\cos\beta+D\cos\alpha)}{be} \\ k &= -(1-2\nu)\frac{P}{\pi}\frac{s}{abe} \\ n &= (1-2\nu)\frac{P}{2\pi}\frac{CDE\cos\alpha\cos\beta}{be} \\ p &= (1-2\nu)\frac{P}{2\pi}\frac{AB(2-E)\cos\alpha\cos\beta}{be} \\ t &= -(1-2\nu)\frac{P}{\pi}\frac{(aE\cos\alpha\cos\beta-s)}{abe} \end{aligned}\right\}, \tag{67}$$

where

$$\left.\begin{aligned} a &= 3-(\cos^2\alpha+\cos\alpha\cos\beta+\cos^2\beta) \\ b &= (\cos\beta-\cos\alpha) \\ l &= \cos^2\alpha+\cos^2\beta-\cos\beta(1+\cos\alpha\cos\beta) \\ s &= \cos\alpha\cos\beta\{1+\cos\alpha\cos\beta(\cos\alpha\cos\beta-2)\} \\ e &= (1-2\nu)s-al \\ A &= (1+\cos\alpha), \qquad C = (1-\cos\alpha) \\ B &= (1+\cos\beta), \qquad D = (1-\cos\beta) \\ E &= (1-\cos\alpha\cos\beta) \end{aligned}\right\}. \tag{68}$$

The final stresses and displacements for any value of Poisson's ratio are then found by adding the additional stresses and displacements found from (12), (13), (62), (63), and (67) to the corresponding initial components in (58) and (59). This leads to

$$\sigma_x = \frac{P}{\pi be}\left[\frac{3lx^3}{R^5}+\frac{(1-2\nu)}{4}\left\{4E\cos^2\alpha\cos^2\beta\frac{x}{R^3}+\right.\right.$$

$$+A^2B^2(C\cos\beta+D\cos\alpha)\left(\frac{xy^2(3R+z)}{R^3(R+z)^3}-\frac{x}{R(R+z)^2}\right)-$$

$$\left.\left.-C^2D^2(A\cos\beta+B\cos\alpha)\left(\frac{xy^2(3R-z)}{R^3(R-z)^3}-\frac{x}{R(R-z)^2}\right)\right\}\right],$$

$$\sigma_y = \frac{P}{\pi be}\Big[\frac{3lxy^2}{R^5} + \frac{(1-2\nu)}{4}\Big\{4E(2-E)\cos\alpha\cos\beta\frac{x}{R^3} + \\ + A^2B^2(C\cos\beta + D\cos\alpha)\Big(\frac{x^3(3R+z)}{R^3(R+z)^3} - \frac{3x}{R(R+z)^2}\Big) - \\ - C^2D^2(A\cos\beta + B\cos\alpha)\Big(\frac{x^3(3R-z)}{R^3(R-z)^3} - \frac{3x}{R(R-z)^2}\Big)\Big\}\Big],$$

$$\sigma_z = \frac{P}{\pi be}\Big[\frac{3lxz^2}{R^5} - (1-2\nu)E\cos^2\alpha\cos^2\beta\frac{x}{R^3}\Big],$$

$$\sigma_{yz} = \frac{P}{\pi be}\Big[\frac{3lxyz}{R^5} + \tfrac{1}{2}(1-2\nu)E\cos\alpha\cos\beta\Big\{CD\frac{xy(2R-z)}{R^3(R-z)^2} - AB\frac{xy(2R+z)}{R^3(R+z)^2}\Big\}\Big],$$

$$\sigma_{xz} = \frac{P}{\pi be}\Big[\frac{3lx^2z}{R^5} + \tfrac{1}{2}(1-2\nu)E\cos\alpha\cos\beta\Big\{AB\Big(\frac{1}{R(R+z)} - \frac{x^2(2R+z)}{R^3(R+z)^2}\Big) - \\ - CD\Big(\frac{1}{R(R-z)} - \frac{x^2(2R-z)}{R^3(R-z)^2}\Big) - \frac{2z}{R^3}\Big\}\Big],$$

$$= \frac{P}{\pi be}\Big[\frac{3lx^2y}{R^5} + \tfrac{1}{4}(1-2\nu)\Big\{A^2B^2(A\cos\beta + B\cos\alpha)\times \\ \times\Big(\frac{y}{R(R+z)^2} - \frac{x^2y(3R+z)}{R^3(R+z)^3}\Big) - C^2D^2(C\cos\beta + D\cos\alpha)\times \\ \times\Big(\frac{y}{R(R-z)^2} - \frac{x^2y(3R-z)}{R^3(R-z)^3}\Big) - 4E\cos\alpha\cos\beta\frac{y}{R^3}\Big\}\Big],$$

$$\sigma = \frac{2Pl(1+\nu)}{\pi be}\frac{x}{R^3}.$$

$$2\mu u = \frac{P}{\pi be}\Big[-\frac{lx^2}{R^3} + \{2(1-2\nu)E\cos\alpha\cos\beta - l\}\frac{1}{R} - \\ - \tfrac{1}{4}(1-2\nu)A^2B^2(C\cos\beta + D\cos\alpha)\Big(\frac{1}{(R+z)} - \frac{x^2}{R(R+z)^2}\Big) + \\ + \tfrac{1}{4}(1-2\nu)C^2D^2(A\cos\beta + B\cos\alpha)\Big(\frac{1}{(R-z)} - \frac{x^2}{R(R-z)^2}\Big)\Big],$$

$$2\mu v = \frac{P}{\pi be}\Big[-\frac{lxy}{R^3} + \tfrac{1}{4}(1-2\nu)\Big\{A^2B^2(C\cos\beta + D\cos\alpha)\frac{xy}{R(R+z)^2} - \\ - C^2D^2(A\cos\beta + B\cos\alpha)\frac{xy}{R(R-z)^2}\Big\}\Big],$$

$$2\mu w = -\frac{P}{\pi be}\Big[\frac{lxz}{R^3} + \tfrac{1}{4}(1-2\nu)AB\{E(C\cos\beta + D\cos\alpha) + b^2\}\frac{x}{(R+z)} + \\ + \tfrac{1}{4}(1-2\nu)CD\{E(A\cos\beta + B\cos\alpha) - b^2\}\frac{x}{(R-z)}\Big],$$

with a, b, l, s, e, A, B, C, D, E given by (68).

We may again obtain the stresses and displacements for the solid cone by putting $\beta = 0$. The results have been previously presented by Michell (9) who used the same approach as in the cone loaded by a force along the axis.

Further, by putting $\alpha = \frac{1}{2}\pi$ in the solid cone solution we can obtain the solution to Cerruti's problem of a semi-infinite body loaded by a tangential force at a point of its bounding plane. Westergaard illustrated his twinned gradient method by this problem.

Acknowledgement

The author wishes to express his gratitude to Professor R. Hill for the many helpful suggestions made during the preparation of this paper.

REFERENCES

1. J. H. Michell, *Proc. Lond. Math. Soc.* **31** (1899) 100.
2. E. G. Coker and L. N. G. Filon, *A Treatise on Photo-elasticity* (Cambridge, 1931).
3. H. M. Westergaard, *Theory of Elasticity and Plasticity* (Harvard, 1952).
4. J. Clerk Maxwell, *Scientific Papers*, vol. ii (Cambridge, 1890).
5. H. L. Langhaar and M. Stippes, *J. Franklin Inst.* **258** (1954) 371.
6. S. Timoshenko and J. N. Goodier, *Theory of Elasticity* (McGraw-Hill, 1951).
7. I. S. Sokolnikoff, *Mathematical Theory of Elasticity* (McGraw-Hill, 1956).
8. L. Rongved, *J. Appl. Mech.* **22** (1955) 545.
9. J. H. Michell, *Proc. Lond. Math. Soc.* **32** (1900) 23.
10. A. E. H. Love, *Mathematical Theory of Elasticity* (Cambridge, 1920).

THE DYNAMICS OF A BOWL

By M. N. BREARLEY (*University of Adelaide, Australia*)
and B. A. BOLT (*University of Sydney, Australia*)

[Received 4 July 1957]

SUMMARY

A mathematical model is set up which describes the dynamical behaviour of a bowl which rolls on a deformable plane surface. Approximate solutions of the equations of motion are obtained, adequate for prediction of a bowl's behaviour under normal playing conditions. These give the equation of the path and show that the angle of deflexion from a straight line is independent of the velocity of projection provided the bowling green conditions remain unchanged.

The intrinsic equation of the bowl path is found to be of the form $s \propto 1-e^{-p\psi}$, where the parameter p and the constant of proportionality depend on the type of bowl and the green conditions.

The results are compared with observations on bowling greens and test-tables.

1. Introduction

WHILE it is well known that the curved trajectory of a bowl results from the superposition on its forward motion of a precession caused by the bias of the bowl, so far no complete dynamical investigation appears to have been given (Walker (**1**)). Since observation shows that there is no slipping between bowl and rolling-surface the assumption of retardation by a frictional force proportional to the normal reaction is precluded. The analysis here presented assumes that the effect of the rolling-surface in retarding the forward motion can be represented by a couple **K**, of constant magnitude K, acting on the bowl, the axis of **K** being parallel to the ground and normal to the direction of motion. Comparison with observation has shown that the resulting mathematical model is adequate for a wide range of initial and rolling-surface conditions. In particular there is close agreement between theoretical and observed behaviour in the game of bowls. Some details of the comparison are given in section 10.

2. Frames of reference

Fig. 1 shows the axial frame $Oxyz$, fixed on the horizontal rolling-surface. O is the initial point of contact of the bowl with the surface, Ox is the initial direction of motion and Oz is vertically upwards. The distance OP travelled along the path in time t is s, the range of the bowl is R, and the total angle of deflexion Δ. The coordinates of the centre of mass G of the bowl at time t are (x, y, z).

A vertical section of the bowl is shown in Fig. 2. The moving axes $G\xi\eta\zeta$,

We may again obtain the stresses and displacements for the solid cone by putting $\beta = 0$. The results have been previously presented by Michell (**9**) who used the same approach as in the cone loaded by a force along the axis.

Further, by putting $\alpha = \frac{1}{2}\pi$ in the solid cone solution we can obtain the solution to Cerruti's problem of a semi-infinite body loaded by a tangential force at a point of its bounding plane. Westergaard illustrated his twinned gradient method by this problem.

Acknowledgement

The author wishes to express his gratitude to Professor R. Hill for the many helpful suggestions made during the preparation of this paper.

REFERENCES

1. J. H. Michell, *Proc. Lond. Math. Soc.* **31** (1899) 100.
2. E. G. Coker and L. N. G. Filon, *A Treatise on Photo-elasticity* (Cambridge, 1931).
3. H. M. Westergaard, *Theory of Elasticity and Plasticity* (Harvard, 1952).
4. J. Clerk Maxwell, *Scientific Papers*, vol. ii (Cambridge, 1890).
5. H. L. Langhaar and M. Stippes, *J. Franklin Inst.* **258** (1954) 371.
6. S. Timoshenko and J. N. Goodier, *Theory of Elasticity* (McGraw-Hill, 1951).
7. I. S. Sokolnikoff, *Mathematical Theory of Elasticity* (McGraw-Hill, 1956).
8. L. Rongved, *J. Appl. Mech.* **22** (1955) 545.
9. J. H. Michell, *Proc. Lond. Math. Soc.* **32** (1900) 23.
10. A. E. H. Love, *Mathematical Theory of Elasticity* (Cambridge, 1920).

THE DYNAMICS OF A BOWL

By M. N. BREARLEY (*University of Adelaide, Australia*)
and B. A. BOLT (*University of Sydney, Australia*)

[Received 4 July 1957]

SUMMARY

A mathematical model is set up which describes the dynamical behaviour of a bowl which rolls on a deformable plane surface. Approximate solutions of the equations of motion are obtained, adequate for prediction of a bowl's behaviour under normal playing conditions. These give the equation of the path and show that the angle of deflexion from a straight line is independent of the velocity of projection provided the bowling green conditions remain unchanged.

The intrinsic equation of the bowl path is found to be of the form $s \propto 1-e^{-p\psi}$, where the parameter p and the constant of proportionality depend on the type of bowl and the green conditions.

The results are compared with observations on bowling greens and test-tables.

1. Introduction

WHILE it is well known that the curved trajectory of a bowl results from the superposition on its forward motion of a precession caused by the bias of the bowl, so far no complete dynamical investigation appears to have been given (Walker (**1**)). Since observation shows that there is no slipping between bowl and rolling-surface the assumption of retardation by a frictional force proportional to the normal reaction is precluded. The analysis here presented assumes that the effect of the rolling-surface in retarding the forward motion can be represented by a couple **K**, of constant magnitude K, acting on the bowl, the axis of **K** being parallel to the ground and normal to the direction of motion. Comparison with observation has shown that the resulting mathematical model is adequate for a wide range of initial and rolling-surface conditions. In particular there is close agreement between theoretical and observed behaviour in the game of bowls. Some details of the comparison are given in section 10.

2. Frames of reference

Fig. 1 shows the axial frame $Oxyz$, fixed on the horizontal rolling-surface. O is the initial point of contact of the bowl with the surface, Ox is the initial direction of motion and Oz is vertically upwards. The distance OP travelled along the path in time t is s, the range of the bowl is R, and the total angle of deflexion Δ. The coordinates of the centre of mass G of the bowl at time t are (x, y, z).

A vertical section of the bowl is shown in Fig. 2. The moving axes $G\xi\eta\zeta$,

have $G\xi$ in the direction of motion, $G\eta$ along the axis of symmetry, $G\zeta$ in the vertical plane containing $G\eta$. A, B, A are the corresponding principal moments of inertia. The angular orientation of the bowl at time t is specified by the Eulerian angles θ, ψ, ϕ where θ is the inclination of $G\zeta$ to the vertical, ψ is the angle between the plane $G\eta\zeta$ and its initial position, ϕ is the angle

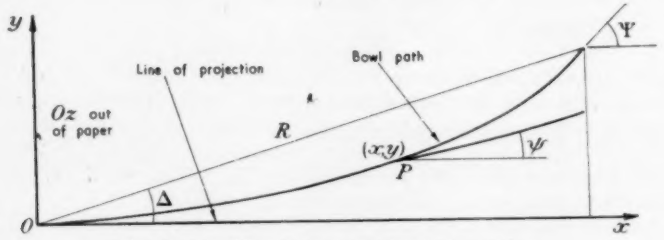

FIG. 1. Bowl trajectory and fixed frame $Oxyz$

between the plane $G\xi\eta$ and a plane fixed in the bowl containing $G\eta$. These angles are depicted on the unit sphere in the auxiliary diagram in Fig. 2. By analogy with a spinning top (Deimel (**2**)), the angular velocity $d\psi/dt$ is called the precession. From measurements of the curvature, the curve DPE

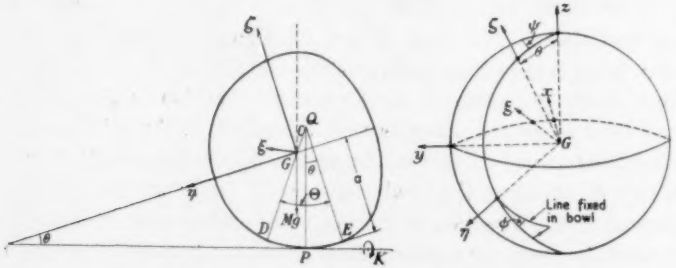

FIG. 2. Bowl section and moving frame $G\xi\eta\zeta$, and Eulerian angular coordinates θ, ψ, ϕ

is very closely the arc of a circle. Let the centre be Q; let $GQ = c$, and $\angle DQE = \Theta$.

Fig. 2 shows a point contact P between the bowl and the rolling-surface, giving an overturning moment equal to $Mgc\sin(\Theta-\theta)$. Since the bowl forms a small depression in a deformable rolling-surface this moment will be effectively reduced throughout the motion. The reduction may be adequately represented by ascribing to c a value less than its actual value. In the present paper this is the only way in which effects of a deformable rolling-surface will be considered.

The six coordinates x, y, z, θ, ψ, ϕ are connected by three constraint relations arising from the conditions of no slipping at P. It is easily verified that one of these relations is integrable, enabling z to be expressed in terms of θ. The other two constraint relations are non-integrable, so that the dynamical system is non-holonomic and requires the remaining five co-ordinates to specify its configuration.

For a typical 5-inch bowl, measured data are

$$M = 3{\cdot}30 \text{ lb}, a = 0{\cdot}208 \text{ ft}, A = 0{\cdot}0542 \text{ lb ft}^2, B = 0{\cdot}0586 \text{ lb ft}^2, \Theta \approx 15°,$$

where M is the mass and a the maximum radius.

3. Dynamical conditions

In the following analysis dots indicate time derivatives. If u is the velocity of the bowl when P is at O, we take as initial conditions

$$t = 0, \qquad s = x = y = 0, \qquad \theta = \psi = \phi = 0,$$
$$\dot{s} = a\dot{\phi} = \dot{x} = u, \qquad \dot{y} = 0, \qquad \dot{\theta} = \dot{\psi} = 0.$$

At the end of the trajectory all variables are denoted by the corresponding capital letters. The end conditions are

$$t = T, \qquad s = S, \qquad x = X, \qquad y = Y, \qquad \theta = \Theta, \qquad \psi = \Psi,$$
$$\dot{s} = \dot{x} = \dot{y} = 0, \qquad \dot{\theta} = \dot{\psi} = \dot{\phi} = 0.$$

Observations of the motion of bowls provide important information on the relative magnitudes of the angular coordinates and their derivatives. This information may be summarized as follows:

θ remains very small until close to the end of the motion,
Ψ may exceed $\frac{1}{2}\pi$,
θ/ψ is small throughout the motion,
$\dot{\theta}, \dot{\psi} \ll \dot{\phi}$ except close to the end.

Thus, at appropriate stages of the analysis, terms involving products and powers of $\dot{\theta}$ and $\dot{\psi}$ will be neglected and approximations with respect to θ made. A solution which shows the general character of the motion can, of course, be achieved by treating θ as a first order small quantity at the outset. This solution, however, has serious errors in the end conditions.

4. Kinematical relations

In the following, the components and rates of change denoted by a dot are taken relative to the moving frame $G\xi\eta\zeta$. Thus from Fig. 2, the angular velocity $\boldsymbol{\omega}$ of the frame $G\xi\eta\zeta$ has components given by

$$\boldsymbol{\omega} = \begin{bmatrix} -\dot{\theta} \\ -\dot{\psi}\sin\theta \\ \dot{\psi}\cos\theta \end{bmatrix}, \tag{4.1}$$

Also, the angular velocity $\boldsymbol{\Omega}$ of the bowl is

$$\boldsymbol{\Omega} = \begin{bmatrix} -\dot{\theta} \\ \dot{\phi} - \dot{\psi}\sin\theta \\ \dot{\psi}\cos\theta \end{bmatrix}. \tag{4.2}$$

Let $c_1 = c\cos\Theta$, $c_2 = c\sin\Theta$, so that from Fig. 2, writing $\mathbf{r} = \mathbf{GP}$, we have

$$\mathbf{r} = \begin{bmatrix} 0 \\ (a+c_1)\sin\theta - c_2 \\ -(a+c_1)\cos\theta + c_1 \end{bmatrix}. \tag{4.3}$$

For brevity we introduce

$$f_1(\theta) = (a+c_1)\cos\theta - c_1, \tag{4.4a}$$

$$f_2(\theta) = (a+c_1)\sin\theta - c_2, \tag{4.4b}$$

$$f_3(\theta) = a + c_1 - c\cos(\Theta-\theta) = f_1(\theta)\cos\theta + f_2(\theta)\sin\theta, \tag{4.4c}$$

$$f_4(\theta) = a + c_1 - 2c\cos(\Theta-\theta) = f_3(\theta) - c\cos(\Theta-\theta). \tag{4.4d}$$

Thus, we have

$$\dot{f}_1(\theta) = -(a+c_1)\dot{\theta}\sin\theta, \tag{4.5a}$$

$$\dot{f}_2(\theta) = (a+c_1)\dot{\theta}\cos\theta, \tag{4.5b}$$

$$\dot{f}_3(\theta) = -c\dot{\theta}\sin(\Theta-\theta). \tag{4.5c}$$

By (4.4a) and (4.4b) we can express (4.3) as

$$\mathbf{r} = \begin{bmatrix} 0 \\ f_2(\theta) \\ -f_1(\theta) \end{bmatrix}. \tag{4.6}$$

For use in the no slipping conditions we shall require the components, in $G\xi\eta\zeta$, of the velocity of P relative to G, i.e. $\boldsymbol{\Omega}\wedge\mathbf{r}$. From (4.2) and (4.6), on simplification we have

$$\boldsymbol{\Omega}\wedge\mathbf{r} = \begin{bmatrix} -f_1(\theta)\dot{\phi} + c\dot{\psi}\sin(\Theta-\theta) \\ -f_1(\theta)\dot{\theta} \\ -f_2(\theta)\dot{\theta} \end{bmatrix}.$$

It follows that

$$\frac{d}{dt}(\boldsymbol{\Omega}\wedge\mathbf{r}) = \begin{bmatrix} -f_1(\theta)\ddot{\phi} + (a+c_1)\dot{\phi}\dot{\theta}\sin\theta + c\ddot{\psi}\sin(\Theta-\theta) - c\dot{\psi}\dot{\theta}\cos(\Theta-\theta) \\ -f_1(\theta)\ddot{\theta} + (a+c_1)\dot{\theta}^2\sin\theta \\ -f_2(\theta)\ddot{\theta} - (a+c_1)\dot{\theta}^2\cos\theta \end{bmatrix}. \tag{4.7}$$

Also, from (4.1) and (4.6) we have

$$\boldsymbol{\omega}.\mathbf{r} = -f_3(\theta)\dot{\psi}. \tag{4.8}$$

5. Equations of motion

One of us (M. N. B.) has derived the equations of motion using the form of Lagrange's equations appropriate to the non-holonomic case. For brevity here we obtain the angular equations of motion directly by the usual moving axes method.

Let the operation d'/dt denote a rate of change relative to the fixed frame $G\xi'\eta'\zeta'$ which is instantaneously coincident with the moving frame $G\xi\eta\zeta$. Let

$\mathbf{h}$ = angular momentum of the bowl about G,
$\mathbf{v}$ = velocity of centre of mass G,
$\mathbf{F}$ = force on the bowl at P,
$\mathbf{K}$ = retarding couple on the bowl as in section 1.

It is easily seen from (4.2) and Fig. 2 that

$$\mathbf{h} = \begin{bmatrix} -A\dot{\theta} \\ B(\dot{\phi}-\dot{\psi}\sin\theta) \\ A\dot{\psi}\cos\theta \end{bmatrix}, \qquad \mathbf{K} = \begin{bmatrix} 0 \\ -K\cos\theta \\ -K\sin\theta \end{bmatrix},$$

and that the acceleration of gravity $\mathbf{g}$ is

$$\mathbf{g} = \begin{bmatrix} 0 \\ g\sin\theta \\ -g\cos\theta \end{bmatrix}. \tag{5.1}$$

The condition of no slipping at P is

$$\mathbf{v}+\boldsymbol{\Omega}\wedge\mathbf{r} = 0. \tag{5.2}$$

The linear equation of motion of the bowl, of mass M, is

$$M\frac{d'\mathbf{v}}{dt} = \mathbf{F}+M\mathbf{g}, \tag{5.3}$$

where

$$\frac{d'\mathbf{v}}{dt} = \frac{d\mathbf{v}}{dt}+\boldsymbol{\omega}\wedge\mathbf{v}.$$

Also the angular equation of motion of the bowl about its centre of mass is

$$\frac{d'\mathbf{h}}{dt} = \mathbf{r}\wedge\mathbf{F}+\mathbf{K}, \tag{5.4}$$

where

$$\frac{d'\mathbf{h}}{dt} = \frac{d\mathbf{h}}{dt}+\boldsymbol{\omega}\wedge\mathbf{h}.$$

Eliminating $\mathbf{v}$ from (5.3) by (5.2), we have

$$M\left[-\frac{d}{dt}(\boldsymbol{\Omega}\wedge\mathbf{r})-\boldsymbol{\omega}\wedge(\boldsymbol{\Omega}\wedge\mathbf{r})\right] = \mathbf{F}+M\mathbf{g}.$$

Hence it follows that

$$\mathbf{r}\wedge\mathbf{F} = -M\mathbf{r}\wedge\left[\frac{d}{dt}(\boldsymbol{\Omega}\wedge\mathbf{r})+\boldsymbol{\omega}\wedge(\boldsymbol{\Omega}\wedge\mathbf{r})+\mathbf{g}\right]$$

$$= -M\mathbf{r}\wedge\left[\frac{d}{dt}(\boldsymbol{\Omega}\wedge\mathbf{r})+(\boldsymbol{\omega}.\mathbf{r})\boldsymbol{\Omega}+\mathbf{g}\right]. \tag{5.5}$$

Substituting (5.5) in (5.4), we have

$$\frac{d\mathbf{h}}{dt}+\boldsymbol{\omega}\wedge\mathbf{h}+M\mathbf{r}\wedge\left[\frac{d}{dt}(\boldsymbol{\Omega}\wedge\mathbf{r})+(\boldsymbol{\omega}.\mathbf{r})\boldsymbol{\Omega}+\mathbf{g}\right]-\mathbf{K} = 0. \tag{5.6}$$

Now, using the component forms (4.1), (4.2), (4.6), (4.7), (4.8), (5.1), and performing the remaining differentiation and vector operations, the three component equations are

$$\{B\cos\theta+Mf_1(\theta)f_3(\theta)\}\dot{\phi}\dot{\psi}-Mgc\sin(\Theta-\theta)-$$
$$-\{(B-A)\sin\theta\cos\theta+Mcf_3(\theta)\sin(\Theta-\theta)\}\dot{\psi}^2+$$
$$+\{A+Mc^2+M(a+c_1)f_4(\theta)\}\ddot{\theta}-Mc(a+c_1)\dot{\theta}^2\sin(\Theta-\theta) = 0, \tag{5.7}$$

$$\{B+M[f_1(\theta)]^2\}\ddot{\phi}-M(a+c_1)f_1(\theta)\dot{\phi}\dot{\theta}\sin\theta-$$
$$-\{B\sin\theta+Mcf_1(\theta)\sin(\Theta-\theta)\}\ddot{\psi}-$$
$$-\{B\cos\theta+Mf_1(\theta)f_4(\theta)\}\dot{\psi}\dot{\theta}+K\cos\theta = 0, \tag{5.8}$$

$$Mf_1(\theta)f_2(\theta)\ddot{\phi}-\{B+M(a+c_1)f_2(\theta)\sin\theta\}\dot{\phi}\dot{\theta}+$$
$$+\{A\cos\theta-Mcf_2(\theta)\sin(\Theta-\theta)\}\ddot{\psi}-$$
$$-\{(2A-B)\sin\theta+Mf_2(\theta)f_4(\theta)\}\dot{\psi}\dot{\theta}+K\sin\theta = 0. \tag{5.9}$$

For convenience we obtain the angular equation of motion about the vertical through P by subtraction of $\sin\theta$ times (5.8) from $\cos\theta$ times (5.9). This yields

$$-\{B\sin\theta+Mcf_1(\theta)\sin(\Theta-\theta)\}\ddot{\phi}-$$
$$-\{B\cos\theta-Mc(a+c_1)\sin(\Theta-\theta)\sin\theta\}\dot{\phi}\dot{\theta}+$$
$$+\{A+(B-A)\sin^2\theta+Mc^2\sin^2(\Theta-\theta)\}\ddot{\psi}+$$
$$+\{2(B-A)\sin\theta\cos\theta+Mcf_4(\theta)\sin(\Theta-\theta)\}\dot{\psi}\dot{\theta} = 0. \tag{5.10}$$

In the next sections approximate first integrals which are sufficiently accurate to give a satisfactory solution of the problem are obtained from (5.7), (5.8), and (5.10).

6. The principle of angular momentum about a vertical axis

For a typical bowl both c and $B-A$ are very small. Since $\sin\theta$ and $\sin(\Theta-\theta)$ are also small, an approximate integral of (5.10) is

$$-B\dot{\phi}\sin\theta+A\dot{\psi} = \text{constant},$$

i.e. the angular momentum of the bowl about the vertical through P is a

constant under the adopted assumptions. (The 'rolling-surface moment' about this axis is of unknown form, but is certainly very small, and has been neglected as indicated in section 2.) Using the initial conditions $\theta = 0$, $\dot{\psi} = 0$ the equation becomes

$$A\dot{\psi} = B\dot{\phi}\sin\theta. \tag{6.1}$$

7. A momentum-impulse equation

The derivation of an approximate integral of (5.8) is facilitated by rewriting it in a different form using (6.1). Since $A/B \approx 1$, we take here

$$\dot{\psi} = \dot{\phi}\sin\theta$$

so that $$M(a+c_1)f_1(\theta)\dot{\psi}\dot{\theta} = M(a+c_1)f_1(\theta)\dot{\phi}\dot{\theta}\sin\theta.$$

Using this, (5.8) may be written as

$$\{B+M[f_1(\theta)]^2\}\ddot{\phi} - 2M(a+c_1)f_1(\theta)\dot{\phi}\dot{\theta}\sin\theta - \\ -\{B\sin\theta + Mcf_1(\theta)\sin(\Theta-\theta)\}\ddot{\psi} - \\ -\{B\cos\theta - 2Mcf_1(\theta)\cos(\Theta-\theta)\}\dot{\psi}\dot{\theta} + K\cos\theta = 0. \tag{7.1}$$

On neglecting terms in c and integrating we have

$$\{B+M[f_1(\theta)]^2\}\dot{\phi} - B\dot{\psi}\sin\theta + K\int_0^t \cos\theta\, dt = \text{constant}. \tag{7.2}$$

It is satisfactory to simplify this further by writing $\cos\theta = 1$. Thus $f_1(\theta) = a$, and using the initial conditions $\dot{\phi} = u/a$, $\dot{\psi} = 0$, (7.2) becomes

$$(B+Ma^2)\dot{\phi} - B\dot{\psi}\sin\theta + Kt = (B+Ma^2)u/a. \tag{7.3}$$

This is an approximate form of the momentum-impulse equation for the axis through P parallel to $G\eta$.

8. The principle of energy

An energy integral may be obtained from (5.7), (5.8), (5.10) in the usual way. We multiply these equations by $\dot{\theta}$, $\dot{\phi}$, $\dot{\psi}$ respectively, add and obtain on integration

$$\tfrac{1}{2}\{B+M[f_1(\theta)]^2\}\dot{\phi}^2 - \{B\sin\theta + Mcf_1(\theta)\sin(\Theta-\theta)\}\dot{\phi}\dot{\psi} + \\ + K\int_0^t \dot{\phi}\cos\theta\, dt + \tfrac{1}{2}\{A+(B-A)\sin^2\theta + Mc^2\sin^2(\Theta-\theta)\}\dot{\psi}^2 + \\ + \tfrac{1}{2}\{A+Mc^2+M(a+c_1)f_4(\theta)\}\dot{\theta}^2 - Mgc\cos(\Theta-\theta) = \text{constant}. \tag{8.1}$$

The equation (8.1) is the principle of energy, and includes the work done in time t against the retarding couple K. An excellent approximation is

obtained by neglecting the very small terms in $\dot{\psi}^2$ and $\dot{\theta}^2$. Since by (6.1) the term in $\dot{\phi}\dot{\psi}$ is also negligible to the same order, (8.1) becomes

$$\tfrac{1}{2}\{B+M[f_1(\theta)]^2\}\dot{\phi}^2+K\int_0^t \dot{\phi}\cos\theta\,dt-Mgc\cos(\Theta-\theta)=\text{constant}. \quad (8.2)$$

This approximation neglects the kinetic energy of tilting and precession. As in section 7 we put $\cos\theta=1$ in the first two terms of (8.2), and using the initial conditions $\phi=\theta=0$, $\dot{\phi}=u/a$, we have

$$\tfrac{1}{2}(B+Ma^2)\dot{\phi}^2+K\phi-Mgc\cos(\Theta-\theta)=\tfrac{1}{2}(B+Ma^2)u^2/a^2-Mgc_1. \quad (8.3)$$

9. Solution of the differential equations

On writing $B'=B+Ma^2$ the first integrals (6.1), (7.3), (8.3) are expressible as

$$\dot{\psi}=\frac{B}{A}\dot{\phi}\sin\theta, \quad (6.1\,a)$$

$$\dot{\phi}=\frac{u}{a}-\frac{K}{B'}t+\frac{B}{B'}\psi\sin\theta, \quad (7.3\,a)$$

$$\tfrac{1}{2}\dot{\phi}^2=\frac{u^2}{2a^2}-\frac{K}{B'}\phi+\frac{Mg}{B'}[c\cos(\Theta-\theta)-c_1]. \quad (8.3\,a)$$

On transposing $(B/B')\dot{\psi}\sin\theta$ in (7.3 a), squaring and neglecting terms in $\dot{\psi}^2$ (by virtue of (6.1 a)) we have

$$\dot{\phi}^2=\frac{u^2}{a^2}-\frac{2Ku}{aB'}t+\frac{K^2}{B'^2}t^2, \quad (9.1)$$

while integrating (7.3 a) over the interval $(0,t)$ gives

$$\phi=\frac{u}{a}t-\frac{K}{2B'}t^2+\frac{B}{B'}\int_0^t \psi\sin\theta\,dt. \quad (9.2)$$

On substitution for $\dot{\phi}^2$ and ϕ from (9.1), (9.2) in (8.3 a) it reduces to

$$\int_0^t \dot{\psi}\sin\theta\,dt=\frac{MgB'}{KB}[c\cos(\Theta-\theta)-c_1].$$

Differentiation with respect to t gives

$$\frac{d\psi}{d\theta}=\frac{1}{p}\frac{\sin(\Theta-\theta)}{\Theta\sin\theta}, \quad (9.3)$$

where

$$p=\frac{KB}{B'Mg\Theta c}. \quad (9.4)$$

Integrating (9.3), after writing $\sin(\Theta-\theta)=\Theta-\theta$, $\sin\theta=\theta$, we have

$$\psi=\frac{1}{p}\left(\log\theta-\frac{\theta}{\Theta}\right)+\text{constant}. \quad (9.5)$$

Since $\theta/\Theta \ll |\log\theta|$, except close to the end of the motion, and $\theta/p\Theta\psi$ is found to be small, it is satisfactory to write (9.5) as

$$\psi = \frac{1}{p}\log\theta + \text{constant},$$

whence, using the end conditions $\psi = \Psi$, $\theta = \Theta$, we have

$$\theta = \Theta e^{p(\psi-\Psi)}. \tag{9.6}$$

This equation does not satisfy exactly the initial conditions $\theta = \psi = 0$ but $\theta/\Theta = e^{-p\Psi}$ would be expected to be very small. This is verified by observations of p and Ψ given in section 10.

We next consider the first integral (6.1 a). Using the approximation $c = 0$, $\cos\theta = 1$ we have

$$\dot{s} = a\dot{\phi}. \tag{9.7}$$

Using (9.7) and putting $\sin\theta = \theta$, (6.1 a) reduces to

$$\frac{ds}{d\psi} = \frac{aA}{B}\frac{1}{\theta}. \tag{9.8}$$

Thus, approximately, *the radius of curvature of the trajectory varies inversely as the angle of tilt of the bowl.*

Equation (9.8) becomes, on substitution for θ from (9.6),

$$\frac{ds}{d\psi} = \frac{aA}{B\Theta}e^{p(\Psi-\psi)}. \tag{9.9}$$

The solution of (9.9), using the initial conditions $s = 0$, $\psi = 0$, is

$$s = \frac{1}{q}e^{p\Psi}(1-e^{-p\psi}), \tag{9.10}$$

where

$$q = \frac{pB\Theta}{aA} = \frac{KB^2}{aAB'Mgc}. \tag{9.11}$$

Equation (9.10) is the intrinsic equation of the bowl path. Expressions for the coordinates x and y of the centre of mass suitable for computation of the bowl trajectory can now be obtained. For convenience we introduce λ defined by

$$\lambda = e^{-p\psi}, \tag{9.12}$$

so that the range of λ corresponding to $0 \leqslant s \leqslant S$ is, from (9.10),

$$1 \geqslant \lambda \geqslant 1/(1+qS).$$

From Fig. 1, $\dot{x} = \dot{s}\cos\psi$, $\dot{y} = \dot{s}\sin\psi$, so that

$$x+iy = \int_0^t \dot{s}e^{i\psi}\,dt = \int_0^\psi e^{i\psi}\frac{ds}{d\psi}\,d\psi = \frac{aAe^{p\Psi}}{B\Theta}\int_0^\psi e^{(i-p)\psi}\,d\psi, \quad \text{by (9.9)},$$

$$= \frac{p(p+i)e^{p\Psi}}{q(p^2+1)}\{1-\lambda(\cos\psi+i\sin\psi)\},$$

on substituting from (9.11), (9.12). Equating real and imaginary parts we have

$$x = \frac{p}{p^2+1}\frac{e^{p\Psi}}{q}\{p-\lambda(p\cos\psi-\sin\psi)\}, \tag{9.13}$$

$$y = \frac{p}{p^2+1}\frac{e^{p\Psi}}{q}\{1-\lambda(\cos\psi+p\sin\psi)\}. \tag{9.14}$$

For computation it is convenient to introduce *the range* $R = \sqrt{(X^2+Y^2)}$ into (9.13), (9.14). Now from (9.13), (9.14), inserting the end conditions $x = X$, $y = Y$, $\lambda = e^{-p\Psi}$, we find

$$R = \frac{p}{\sqrt{(p^2+1)}}\frac{e^{p\Psi}}{q},$$

omitting second-order terms. Thus (9.13), (9.14) may be written

$$x = \frac{R}{\sqrt{(p^2+1)}}\{p-\lambda(p\cos\psi-\sin\psi)\}, \tag{9.13a}$$

$$y = \frac{R}{\sqrt{(p^2+1)}}\{1-\lambda(\cos\psi+p\sin\psi)\}, \tag{9.14a}$$

where the angle ψ is, from (9.12), given by

$$\psi = \frac{1}{p}\log\frac{1}{\lambda}, \tag{9.15}$$

for $$1 \geqslant \lambda \geqslant \left[\frac{q}{p}\sqrt{(p^2+1)}R\right]^{-1}.$$

Hence for particular values of p and R values of coordinates (x, y) corresponding to a suitable set of values of λ may be calculated. In particular, since λ is very small close to the end of the trajectory, we have with sufficient accuracy

$$X = \frac{p}{\sqrt{(p^2+1)}}R, \qquad Y = \frac{1}{\sqrt{(p^2+1)}}R, \tag{9.16}$$

$$\Psi = \frac{1}{p}\log\left[\frac{q}{p}\sqrt{(p^2+1)}R\right]. \tag{9.17}$$

10. Discussion

The formulae giving x, y, and ψ for a particular bowl depend upon the range R and, through the parameters p and q, the moment K. Since we would expect K to vary with surface conditions it must be estimated for any given surface as follows. From (7.3a) and (9.7), neglecting the small term containing $\dot{\psi}\sin\theta$ we have

$$\dot{s} = u - \frac{Ka}{B'}t. \tag{10.1}$$

Since K has been taken as constant the acceleration of G is thus approximately $-Ka/B'$. Thus

$$S = \frac{Ka}{2B'}T^2 \quad \text{and} \quad K = \frac{2B'}{a}\frac{S}{T^2}. \tag{10.2}$$

In practice it is sufficiently accurate to replace S by R in (10.2) since experiments on various types of surface give $0{\cdot}9 < R/S < 1$. Table 1 shows values of R/T^2 obtained with the same bowl on three bowling green surfaces described as 'fast', 'medium', and 'slow' respectively.

TABLE 1

Observed ranges (ft) and times (sec)

Trial number	*Green 1 (fast)*			*Green 2 (medium)*			*Green 3 (slow)*		
	R	T	R/T^2	R	T	R/T^2	R	T	R/T^2
1	9·2	4·5	0·45	11·5	4·9	0·48	13·1	4·6	0·62
2	17·4	6·3	0·44	16·3	5·7	0·50	21·9	5·7	0·67
3	30·7	8·6	0·42	26·3	7·2	0·51	29·6	6·7	0·66
4	47·7	10·2	0·46	35·1	8·2	0·52	37·6	7·6	0·65
5	57·7	11·7	0·41	43·0	8·8	0·56	46·6	9·1	0·56
6	64·4	12·5	0·41	54·3	10·3	0·51	55·4	9·9	0·57
7	78·2	13·6	0·42	61·9	10·9	0·52	65·0	10·5	0·59
8	89·4	14·7	0·41	72·2	11·9	0·51	74·8	11·0	0·62
9	97·3	14·9	0·44	83·4	12·3	0·55	81·0	11·1	0·66
10				91·2	12·7	0·56	90·5	12·1	0·62
11				100·6	13·6	0·54			

The values of R/T^2, by (10.2), indicate that K for a particular green and bowl is essentially independent of R and hence of the initial speed of the bowl, at least for the ranges investigated. This provides experimental support for the hypothesis introduced in section 1 *that K may be taken constant for the same bowl and bowling surface*. From (10.2) and the mean values of R/T^2 given in Table 1, the values of K for each green are 0·84, 1·01, and 1·20 ft pdls respectively.

Insertion of the end conditions $\dot{s} = 0$, $t = T$ in (10.1) shows the total time of travel of the bowl to be

$$T = \frac{B'u}{Ka}.$$

On substituting this in (10.2) and writing S as R, the range achieved for a speed u of projection is found to be

$$R = \frac{B'}{2Ka}u^2.$$

For given u, the range is therefore directly proportional to the speed of the green as measured by the factor $1/K$.

To plot trajectories for a particular bowl and bowling surface an appropriate value of p must be found. This may be determined as follows. The angle of deflexion Δ, shown in Fig. 1, is given by $\tan\Delta = Y/X$, in which substitution from (9.16) gives

$$\tan\Delta = p^{-1}. \tag{10.3}$$

Thus p may be found by measurement of Δ in a trial trajectory.

If the value of p so found is used in (9.4), this equation then gives the value of c appropriate to the bowl and surface concerned. We note that for a 5-inch bowl numerous dynamical experiments on various bowling greens show that if the values $\Theta = 15°$, $c = 0{\cdot}0016$ ft are used in (9.4) to obtain p as a function of K, satisfactory agreement between calculated and observed paths is obtained. In agreement with section 2, this value of c for a deformable surface is considerably smaller than that obtained from statical experiments on a polished steel surface, namely

$$c = 0{\cdot}01 \pm 0{\cdot}002 \text{ ft}.$$

The equation (10.3) shows *that for the same bowl and rolling-surface the angle of deflexion is the same for all ranges R.*

This theoretical prediction was tested by measuring values of (X, Y) for each range on the three greens used in Table 1. When plotted the values showed no systematic trend from a linear relation. The least-square solutions with their standard errors were:

$$\text{Green 1.} \quad Y = (0{\cdot}182 \pm 0{\cdot}003)X - (0{\cdot}57 \pm 0{\cdot}21)$$

$$\text{Green 2.} \quad Y = (0{\cdot}156 \pm 0{\cdot}004)X + (0{\cdot}60 \pm 0{\cdot}20)$$

$$\text{Green 3.} \quad Y = (0{\cdot}141 \pm 0{\cdot}003)X - (1{\cdot}51 \pm 0{\cdot}33)$$

The result provides a very satisfactory check on (10.3) and hence on the approximations of sections 6–8. The corresponding values of Δ are $10{\cdot}3° \pm 0{\cdot}1$, $8{\cdot}9° \pm 0{\cdot}2$, $8{\cdot}0° \pm 0{\cdot}1$. The decrease in the angle of deflexion with the decrease of speed of the green, by (10.3), entails an increase in p. This is in agreement with (9.4).

Finally, we give in Fig. 3 a comparison between the calculated and observed trajectories for two indoor test-tables.

The test-tables, one at Sydney and the other at Adelaide, are canvas, over sponge rubber, over slate. They are used to check the bias of bowls used in competition against the bias of a standard bowl. Fig. 3 shows excellent agreement between theoretical and observed trajectories in both

cases. In particular, measurements of Ψ at the end of each trajectory are of the right order, as shown in the following table.

	R (*ft*)	Δ (*degrees*)	K (*ft pdls*)	p	c (*ft*)	Ψ *calc.* (*degrees*)	Ψ *obs.* (*degrees*)
Sydney table	25·2	22·5	0·397	2·41	0·0018	106	100
Adelaide table	31·5	22·6	0·392	2·40	0·0017	113	119

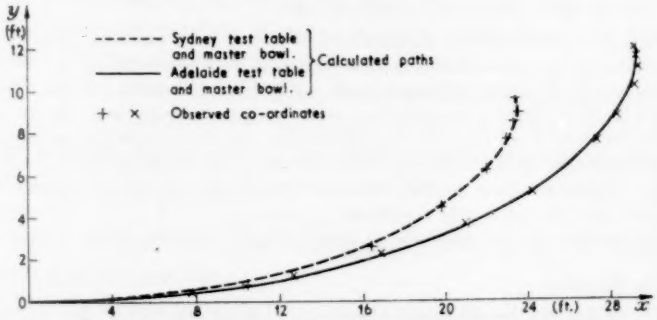

FIG. 3. Comparison of calculated and observed paths

These results show that the treatment presented is adequate to deal with the dynamics of a bowl under normal conditions.

Acknowledgements

The authors wish to thank Mr. L. J. Luke, President of the Adelaide Bowling Club, for the provision of facilities for green experiments. They are specially grateful to Mr. A. F. A. Harper, Principal Research Officer of the Division of Physics, National Standards Laboratory, C.S.I.R.O., Sydney, for important collaboration in the experimental side of the work.

REFERENCES

1. G. T. WALKER, 'Spiel und Sport', *Encyk. der Math. Wiss.* **4** (1900) **129**.
2. R. F. DEIMEL, *Mechanics of the Gyroscope* (Dover, 1952), p. 76.

TECHNIQUES OF MULTIPLICATION AND DIVISION FOR AUTOMATIC BINARY COMPUTERS

By K. D. TOCHER (*Imperial College*)

[Received 27 June 1957]

SUMMARY

Methods are developed for representing numbers in a modified ternary scale, which enables the operation of multiplication to be fabricated in an automatic binary computer with the minimum number of additions or subtractions. Two cases arise according to whether a parallel or serial machine is being used. In the former case, the number of additions (or subtractions) can be reduced to an average of a third the number of digits in the multiplier with a maximum of a half the number of digits. In the serial case a multiplication by a $2p$-digit multiplier can be achieved as a single operation with only p adders.

The application of this technique to division is also considered.

1. Introduction

In both serial and parallel automatic computing machines, the operations taking the longest time are usually multiplication and division and these occur sufficiently often in programmes to make the reduction of multiplication and division time a worthwhile project.

In fact many schools of programming at present estimate the time of any given problem by counting the number of multiplications and multiplying by some fixed multiple of the multiplication time.

Many machines now available or under construction already have additional mechanisms to speed multiplication.

This paper gives a survey of some possible schemes for fast multiplication and gives the necessary mathematical analysis to effect further improvements over those already incorporated or envisaged for the present generation of automatic computers.

This analysis hinges on the representation of a binary number as the sums and differences of a set of binary powers.

From this analysis it is possible to derive optimum schemes of division.

2. Multipliers in serial machines

The simple multipliers in serial machines are based on the binary analogue of the continued addition method used in desk calculators.

This consists, for each digit in turn, of either (i) adding the multiplicand to the partial product and then shifting the latter or (ii) just shifting the partial product, obeying (i) or (ii) according to the value of a digit of the multiplier.

The inspection of each digit of the multiplier is usually achieved by holding this in a circulating register $n+1$ digits in length (n-digit numbers). In each cycle the binary pattern is shifted back one place and by inspection of a fixed digital position at a fixed time in each cycle the digits are inspected in turn, the least significant digit first.

Similarly, the partial product can be shifted back one place per cycle. An adder is provided in its circulation path to allow the multiplicand to be added. The least significant digit in each cycle is deliberately lost unless a double precision product is required when these digits can be stored in the used positions of the multiplicand register.

Thus about n cycle times are required for a multiplication independent of the digital pattern of the multiplier. This is a twofold improvement over the original design of multiplier which used registers of length $2n+1$ to hold the partial product and the multiplier and each cycle of the multiplication took two machine cycles.

To reduce the multiplication time below n cycle times two alternative arrangements are possible:

(a) arrange that the shift without addition which is required if the multiplier digit is zero can be effected without a complete circulation cycle;

(b) add the increments to the partial product arising from several digits of the multiplier in each machine cycle.

The alternative (a) involves the provision of adjustable delays which can be inserted in the two circulation loops to shift these numbers over a number of places determined by the length of a chain of zeros in the multiplier. Mechanisms must be provided to sense the length of the next most significant chain of zeros before each addition cycle so that the delays can be set to the required value during that cycle.

The alternative (b) involves a multi-input adder in the circulation loop of the product register, each input feed having a gated and suitably delayed copy of the multiplicand. The contents of the multiplier must be used to control the gates on these inputs.

In practice the multi-input of say n inputs is constructed from a chain of n ordinary adders with the output of each feeding as one input to the next. Thus to deal with p digits of the multiplier in each cycle p adders are required.

A second method of applying alternative (b) is to use a set of adders to produce a unit giving on 2^p different outputs all possible 2^p multiples of p digits. For each successive pattern of p digits in the multiplier, the appropriate output is gated to the input of the ordinary adder in the circulation path. This is an uneconomic method for large p since the unit

will require $2^{p-1}-1$ ordinary adders (one to produce each of the odd multiples) giving a total of 2^{p-1} adders compared with p adders in the first scheme.

In alternative (a) the multiplication time is directly proportional to the number of ones in the multiples and so assuming that all n-digit numbers are equally likely, the average number of cycles is $\frac{1}{2}n$ and the multiplication is, on average, halved in comparison to the original simple multiplier.

Any further decreases in multiplication time by this method must depend on finding a representation of the multiplier which contains fewer ones than the normal binary representation. Since a binary adder-subtractor switchable from one function to the other at will is a well known device which is not much more complicated than a simple adder, it is natural to consider representations of the form

$$\sum_{r=0}^{n} (-)^{s_r} d_r 2^r \quad (s_r, d_r = 0, 1)$$

for the multiplier which will correspond in the multiplication process to adding or subtracting the multiplicand (according to the value of s_r) when $d_r = 1$.

For this form of multiplication unit the problem arises of choosing the form so that the number of non zero d's is minimized.

The multi-input adder type of serial multiplier can be generalized by replacing the adders by adder-subtractors and using a similar form for the multiplier to control both the gates and the function of the separate adder-subtractors.

If p adder-subtractors are provided the problem arises of determining the range of multipliers that can be encoded with not more than p non-zero digits.

To produce a workable scheme of this kind each delayed version of the multiplicand must be fed to a fixed input of the adder and since, if the scheme is to have any value, the range of multipliers will have more than p digits, some or all of the inputs will be fed with more than one version of the multiplicand. We require that these multiple inputs to each adder input can be mixed in a simple gate and so the problem arises of allocating the digital positions of the multiplier among the p inputs in sets so that every multiplier in the possible range can be represented with at most one non-zero digit in each set.

3. Multipliers in parallel machines

The original von Neumann parallel arithmetic unit works on the familiar principle of the Brunsviga machine with the exception that multiplication proceeds the least significant digit first and the least significant digits of the

product, if required, are stored in the multiplier register (**1**). This arrangement ensures that only a single length adder is required.

In some machines the process of adding and shifting takes place in a single phase. If the addition is not required the phase will be considerably shorter in time since no carry propagation time is needed.

Other machines separate the two processes of adding and shifting and once again the cycle time for zero multiplier digits is shorter than for non-zero ones.

In either case if the shift time can be neglected compared with the addition time the multiplication time is roughly proportional to the number of non-zero digits in the multiplier.

Subtraction is often performed by complementing the contents of the multiplicand register and if this also takes a time negligible to the addition time, the possibility arises of using the form discussed in the preceding section for the multiplier which will further reduce the multiplication time.

The possibility of achieving further decreases in multiplication time by using multiple input parallel adders need not be considered, since the cost of such units rules them out of serious consideration.

The remainder of this paper is concerned with the mathematical analysis of the representations of binary numbers in the various forms and an investigation of the recursive type of representations suitable for mechanization in multipliers.

The analysis is then applied to the mechanization of the division process.

4. The representation of binary numbers

It is clear that the discussion can be restricted to integer multipliers since the products formed using other multipliers can be derived from that of a corresponding integer by a simple shift.

Suppose a given integer N is represented as

$$N = \sum_{r=0}^{\infty} b_r 2^r \quad (b_r = 0, 1; r = 0, 1, \ldots). \tag{1}$$

For n-digit numbers $b_r = 0$ $(r \geqslant n)$, but in the following analysis which gives recursive relations the finite nature of N is irrelevant.

We require to find the condition on s_r and d_r such that

$$N = \sum_{r=0}^{\infty} b_r 2^r = \sum_{r=0}^{\infty} (-)^{s_r} d_r 2^r \quad (b_r, s_r, d_r = 0, 1; r = 0, 1, \ldots). \tag{2}$$

From (2) we have

$$\sum_{r=1}^{\infty} \{(-)^{s_r} d_r - b_r\} 2^r = b_0 - (-)^{s_0} d_0 = e_0 \quad \text{(say)} \tag{3}$$

where e_0 can take the values $-1, 0, 1, 2$. But

$$e_0 \equiv 0 \pmod 2,$$

i.e.

$$b_0 \equiv d_0 \pmod 2,$$

and since b_0, d_0 are binary elements,

$$b_0 = d_0. \tag{4}$$

Now define $g(e) = 0 \quad (e \neq 2, \text{ i.e. } e = 0, \pm 1)$

and $g(a) = 1 \quad (\text{otherwise})$ $\Big\}$. (5)

Then (3) becomes $$\sum_{r=1}^{\infty} \{(-)^{s_r} d_r - b_r\} 2^{r-1} = g(e_0). \tag{6}$$

Hence $$\sum_{r=2}^{\infty} \{(-)^{s_r} d_r - b_r\} 2^{r-1} = g(e_0) + b_1 - (-)^{s_1} d_1 = e_1 \quad \text{say.} \tag{7}$$

As before,

$$e_1 \equiv 0 \pmod 2$$

$$d_1 \equiv \{b_1 + g(e_0)\} \pmod 2. \tag{8}$$

This shows that e_1 can only take values 0, 2, and applying the above process successively we obtain

$$\sum_{r=t+1}^{\infty} \{(-)^{s_r} d_r - b_r\} 2^{r-t} = f_t + b_t - (-)^{s_t} d_t = e_t, \quad \text{say,} \tag{9}$$

where $$f_t = g(e_{t-1}),$$

whence $$d_t \equiv \{b_t + f_t\} \pmod 2. \tag{10}$$

Since $e_t = 0, 2$ are the only possible cases it is easy to verify that

$$f_{t+1} = f_t b_t + s_t d_t. \tag{11}$$

Equation (10) may be written in the forms

$$f_t = (b_t + d_t) \pmod 2 = b_t + d_t - 2b_t d_t = (b_t - d_t)^2, \tag{12}$$

$$d_t = f_t + b_t - 2f_t b_t = (b_t - f_t)^2 \tag{13}$$

since $x^2 = x$ for a binary element. We can eliminate f_t from these equations. Substituting (12) in (11)

$$\begin{aligned} f_{t+1} &= (b_t + d_t - 2b_t d_t) b_t + s_t d_t \\ &= b_t - b_t d_t + s_t d_t. \end{aligned}$$

Replacing t by $t+1$ in (13) and substituting for f_{t+1},

$$\begin{aligned} d_{t+1} &= (b_t - b_t d_t + s_t d_t)(1 - 2b_{t+1}) + b_{t+1} \\ &= b_t + b_{t+1} - 2b_t b_{t+1} - (b_t - s_t)(1 - 2b_{t+1}) d_t \\ &= (b_t - b_{t+1})^2 - (b_t - s_t)(1 - 2b_{t+1}) d_t. \end{aligned} \tag{14}$$

Thus for any arbitrary sequence of s_r, we may represent any integer N given by (1) in the form (2) by a sequence d_r satisfying $d_0 = b_0$ and the recurrence relation (14).

5. The minimal digit representation

We require to choose the sequence s_r so that $\sum d_r$ is minimized for any integer N, where

$$\sum_{r=0}^{\infty} d_r = d_0 + \sum_{r=0}^{\infty} d_{r+1} = b_0 + \sum_{r=0}^{\infty} (b_r - b_{r+1})^2 - \sum_{r=0}^{\infty} (b_r - s_r)(1-2b_{r+1})d_r.$$

For a fixed n-digit N, $b_r = 0$ $(r \geqslant n)$ and the first two terms are a finite fixed sum. Hence $\sum d_r$ is minimized if $\sum_{r=0}^{\infty} (b_r - s_r)(1-2b_{r+1})d_r$ is maximized.

This in turn is maximized if $c_r = (b_r - s_r)(1-2b_{r+1})$ is maximized for each non-zero d_r. $c_r = 1$ if and only if

$$\text{(i)} \quad b_r = 1, \quad s_r = 0, \quad b_{r+1} = 0$$

or

$$\text{(ii)} \quad b_r = 0, \quad s_r = 1, \quad b_{r+1} = 1,$$

i.e.

$$b_r \neq b_{r+1} = s_r.$$

If $b_r = b_{r+1}$,

$$c_r = (b_{r+1} - s_r)(1-2b_{r+1}) = -(b_{r+1} - s_r)^2.$$

In this case c_r is maximized at value 0 if $s_r = b_{r+1}$.

Thus the sequence $s_r = b_{r+1}$ gives the minimum value of $\sum d_r$ since this maximizes c_r for all r and hence for all r with $d_r \neq 0$.

For these values of s_r, (14) leads to

$$\begin{aligned} d_{r+1} &= (b_{r+1} - b_r)^2 + (b_{r+1} - b_r)(1-2b_{r+1})d_r \\ &= (b_{r+1} - b_r)^2(1-d_r) \qquad (15) \end{aligned}$$

$$s_r = b_{r+1}. \qquad (16)$$

Thus, the minimal digit representation D is given by the rule that a non-zero digit occurs in D if and only if the corresponding digit in the binary representation differs from its lower neighbour and the preceding digit of D is zero. The digit is positive or negative according to the value 0 or 1 of the higher neighbouring digit in the binary representation.

A direct proof that this rule gives a minimal digit representation can also be given.†

Denote the sequence of d's given by the rule $s_r = b_{r+1}$ by $\{\hat{d}_r\}$ and the sequence by any other rule $\{d_r\}$.

Let

$$T_n = \sum_{0}^{n} (d_r - \hat{d}_r).$$

Then

$$T_0 = 0.$$

It is required to prove that $T_n \geqslant 0$ for all n such that $b_{n+1} = b_n$ and for all sequences $\{s_r\}$, $\{b_r\}$.

† This alternative proof was added to the original paper at the suggestion of a referee, who was not convinced by the earlier argument.

Consider the following transition table:

d_r	$\hat{d}_r$	$d^{(0)}_{r+1}\,(s_r = b_{r+1})$	$d^{(1)}_{r+1}\,(s_r \neq b_{r+1})$	$\hat{d}_{r+1}$	$\min(d^{0}_{r+1}, d^{(1)}_{r+1}) - \hat{d}_{r+1}$
0	0	$(b_{r+1}-b_r)^2$	$(b_{r+1}-b_r)^2$	$(b_{r+1}-b_r)^2$	0
0	1	$(b_{r+1}-b_r)^2$	$(b_{r+1}-b_r)^2$	0	$(b_{r+1}-b_r)^2$
1	0	0	1	$(b_{r+1}-b_r)^2$	$-(b_{r+1}-b_r)^2$
1	1	0	1	0	0

Thus $T_{n+1} \geqslant T_n$ unless $d_n = 1$, $\hat{d}_{n+1} = 0$ and $b_{n+1} \neq b_n$. Suppose $n_1, n_2, \ldots$ are the ascending sequence of n's for which $d_n = 1$, $\hat{d}_{n+1} = 0$ and $b_{n+1} \neq b_n$.

Then $$T_{n_s+1} = T_{n_s} - 1.$$

Now $$T_{n_s} = T_{n_s-1} + 1,$$

thus $$T_{n_s+1} = T_{n_s-1}.$$

Hence $$T_n \geqslant T_0 = 0 \qquad (n = 0, 1, \ldots, n_1 - 1),$$

$$T_n \geqslant T_{n_1+1} = T_{n_1-1} \geqslant 0 \quad (n = n_1+1, \ldots, n_2-1),$$

$$T_n \geqslant T_{n_s+1} = T_{n_s-1} \geqslant 0 \quad (n = n_s+1, \ldots, n_{s+1}-1).$$

If n is not in the set $n_1, n_2, \ldots$,

$$T_n \geqslant 0.$$

If $b_{n+1} = b_n$, n is not in the set $n_1, n_2, \ldots$.
Therefore, if $b_{n+1} = b_n$, $T_n \geqslant 0$.

This rule is particularly easy to mechanize since it only involves scanning three digits of the multiplier and storing the preceding d digit.

Since no two successive d digits can both be non-zero, in a parallel unit each actual addition can be followed by a double shift and the d-digit store eliminated. Similarly, in the analogous serial unit the variable shift can be adjusted to give the same result.

6. The number of digits in minimal digit representations

For any given N, $\sum d_r$ can be calculated from

$$\begin{aligned}
\sum d_r = b_0 + \sum d_{r+1} &= b_0 + \sum (b_{r+1}-b_r)^2(1-d_r) \\
&= b_0 + \sum (b_{r+1}-b_r)^2 - \sum (b_{r+1}-b_r)^2 d_r \\
&= b_0 + \sum (b_{r+1}-b_r)^2 - \sum (b_{r+1}-b_r)^2(b_r+b_{r-1})^2 + \\
&\qquad + \sum (b_{r+1}-b_r)^2(b_r-b_{r-1})^2 d_{r-1} \\
&= b_0 + \sum (\ )^2 - \sum (\ )^2(\ )^2 + \sum (\ )^2(\ )^2(\ )^2 - \\
&\qquad - \sum (\ )^2(\ )^2(\ )^2(\ )^2 + \ldots .
\end{aligned}$$

Now $\sum (b_{r+1}-b_r)^2$ is the number of changes of value in the sequence $b_0, b_1, \ldots$. $\sum (b_{r+1}-b_r)^2(b_r-b_{r-1})^2$ is the number of chains of alternating terms of length 3, $\sum (b_{r+1}-b_r)^2 \ldots (b_{s+3}-b_{s+2})^2$ the number of chains of length $r-s$.

Hence the number of non-zero digits in the minimal digit representation of N is the number of chains of alternating terms of even length less the number of chains of alternating terms of odd length.

For example if $N = 1466 = 10\,110\,111\,010$ we have

Chain length . .	2	3	4	5
Number of chains .	8	5	2	0

The number of digits required is $8-5+2-0 = 5$. The coding proceeds as follows:

r	0	1	2	3	4	5	6	7	8	9	10	11	12	13
b	0	1	0	1	1	1	0	1	1	0	1	0	0	0
$(\Delta b)^2$	0	1	1	1	0	0	1	1	0	1	1	1	0	0
d	0	1	0	1	0	0	1	0	0	1	0	1	0	0
s	1	0	1	1	1	0	1	1	0	1	0	0	0	0

$$N = 2^{11}-2^9-2^6-2^3+2$$

$$= 2048-512-64-8+2 = 1466.$$

The chain rule is rather cumbersome to operate and a count in the recoded form is in practice a quicker method.

For any assessment of the efficiency of the method, however, it is the average number of digits occurring which is required. If it is assumed that all n-digit numbers are equally likely the result may be obtained from the total number of non-zero digits in the representations of all the integers in the range $[0, 2^n-1]$.

Let $S_n(b, d, d')$ denote the set of sequences of b's for which

(i) $b_r = 0\ (r > n)$, (ii) $b_n = b$, (iii) $d_n = d$, (iv) $d_{n+1} = d'$

and let $S_n(X)$ denote the number of sequences in $S_n(X)$, where X denotes any ordered triple (b, d, d').

From the relation $d_{n+1} = (b_{n+1}-b_n)^2(1-d_n)$,

$$S_n(0, 0, 1) = S_n(0, 1, 1) = S_n(1, 0, 0) = S_n(1, 1, 1) = 0.$$

Consider the relation between $S_n(X)$ and $S_{n+1}(X)$. We have the following transition table:

Case	b_n	d_n	d_{n+1}	$b_{n+1} = 0$		$b_{n+1} = 1$	
				d_{n+1}	d_{n+2}	d_{n+1}	d_{n+2}
A	0	0	0	0	0	1	0
B	0	1	0	0	0	0	1
C	1	0	1	1	0	0	1
D	1	1	0	0	0	0	1

Thus we have

$$\left.\begin{aligned} S_{n+1}(A) &= S_n(A)+S_n(B)+S_n(D) \\ S_{n+1}(B) &= S_n(C) \\ S_{n+1}(C) &= S_n(B)+S_n(C)+S_n(D) \\ S_{n+1}(D) &= S_n(A) \end{aligned}\right\}. \tag{17}$$

This is a system of linear difference equations whose characteristic equation is easily calculated as

$$E(E-1)(E+1)(E-2) = 0.$$

Thus $S_n(X) = A_x 2^n + B_x + C_x(-)^n$, where A_x, B_x, C_x are constants. In the sequel it transpires that we only require $S_n(C)$,

$$\begin{aligned} S_0(C) = S_0(1,0,1) &= 0, \\ S_1(C) &= 1, \\ S_2(C) &= 2. \end{aligned}$$

Substituting these boundary conditions gives

$$S_n(1,0,1) = \tfrac{2}{3}2^n - \tfrac{1}{2} - \tfrac{1}{6}(-)^n. \tag{18}$$

If $d_n(X)$ denotes the total number of non-zero d's in the minimal digit representation of the sequences of $S_n(X)$, reference to the table shows that

$$\left.\begin{aligned} d_{n+1}(A) &= d_n(A)+d_n(B)+d_n(D) \\ d_{n+1}(B) &= d_n(C) \\ d_{n+1}(C) &= d_n(B)+d_n(C)+d_n(D)+S_n(B)+S_n(D) \\ d_{n+1}(D) &= d_n(A)+S_n(A) \end{aligned}\right\}. \tag{19}$$

If $d_n = \sum_X d_n(X)$ is the total number of non-zero d's in $\sum S_n(\alpha)$,

$$d_{n+1} = 2d_n + S_n(A)+S_n(B)+S_n(D).$$

Clearly $$S_n(A)+S_n(B)+S_n(C)+S_n(D) = 2^{n+1},$$

whence $$(E-2)d_n = 2^{n+1} - S_n(C) = \tfrac{2}{3}2^{n+1} + \tfrac{1}{2} + \tfrac{1}{6}(-)^n.$$

The general solution of this difference equation is

$$d_n = A2^n + \tfrac{1}{3}n2^{n+1} - \tfrac{1}{2} - \tfrac{1}{18}(-)^n. \tag{20}$$

The boundary condition is $d_0 = 1$ whence

$$d_n = \tfrac{1}{18}[(3n+7)2^{n+2} - 9 + (-)^{n+1}]. \tag{21}$$

This gives the number of non-zero d's in the set of $n+1$ digit numbers and must be compared with $(n+1)2^n$ for the binary set. For large n, $d_n/(n+1)2^n \sim \frac{2}{3}$ showing a 33 per cent. saving of digits and corresponding decrease in multiplication time.

7. The minimum number of digits required to represent a range of integers

We now consider the multi-input form of serial multiplier. Given n inputs we require to find N so that all integers in the range $0 \leqslant x \leqslant N$ can be represented so that $\sum d \leqslant n$. This is equivalent to determining the *least* $N+1$ for which $\sum d > n$ for all representations.

Consider the generating function

$$G(x,y) = \prod_{i=0}^{\infty} (x^{2^i}y+1+x^{-2^i}y) = \sum_{r=-\infty}^{\infty} \sum_{s=0}^{\infty} a_{rs}\, x^r\, y^s. \tag{22}$$

Then a_{rs} represents the number of ways of representing r with s non-zero elements. Write

$$\sum_{s=0}^{\infty} a_{rs}\, y^s = a_r(y) = y^{n_r} \sum_{t=0}^{\infty} b_{rt} y^t \quad (b_{r0} \neq 0), \tag{23}$$

so that n_r is the lowest power of y in $a_r(y)$, i.e. the minimal digit representation of r has n_r non-zero digits. Now

$$G(x,y) = (xy+1+x^{-1}y)G(x^2,y);$$

hence
$$\sum_{r=-\infty}^{\infty} a_r(y)x^r = (xy+x^{-1}y) \sum_{r=-\infty}^{\infty} a_r(y)x^{2r} + \sum_{r=-\infty}^{\infty} a_r(y)x^{2r}$$

$$= \sum_{r=-\infty}^{\infty} y\{a_r(y)+a_{r+1}(y)\}x^{2r+1} + \sum_{r=-\infty}^{\infty} a_r(y)x^{2r}. \tag{24}$$

Comparing coefficients of x^n

$$a_{2r}(y) = a_r(y), \tag{25}$$

$$a_{2r+1}(y) = y\{a_r(y)+a_{r+1}(y)\}, \tag{26}$$

and comparing leading powers of these polynomials, we find

$$n_{2r} = n_r, \tag{27}$$

$$n_{2r+1} = \min(n_r, n_{r+1})+1. \tag{28}$$

(25) expresses analytically that doubling a number in the binary scale does not alter the number of representations with a fixed number of non-zero digits.

The first appearance of the value n occurs in the sequence n_1, n_2, n_3 at an odd position, say $2s_n+1$. Then $n+1$ cannot appear in the sequence until position $2r+1$, where r is least solution of $n_r = n_{r+1} = n$ (from (28)). One of r, $r+1$ is even and the least even value of r is $4s_n+2$. Consider the value of n_r for $r = 4s_n+1$:

$$n_{4s_n+1} = \min(n_{2s_n}, n_{2s_n+1})+1,$$

or using (27),
$$n_{4s_n+1} = \min(n_{s_n}, n)+1. \tag{29}$$

From (28)
$$s_{2s_n+1} = n = \min(n_{s_n} n_{s_n+1})+1.$$

But $n_{s_n} < n$, $n_{s_n+1} < n$ by definition of s_n. Hence

$$n_{s_n} = n_{s_n+1} = n-1.$$

Hence the least solution of $n_r = n_{r+1} = n$ is $r = 4s_{n+1}$ and first appearance of $n+1$ is at $8s_{n+3}$.

Putting $2s_{n+1} = t_n$ we have the recurrence relation

$$t_{n+1} = 4t_{n-1} \tag{30}$$

with boundary condition $t_1 = 1$. Hence

$$t_n = \tfrac{2}{3}4^{n-1} + \tfrac{1}{3}.$$

Thus the largest range of integers which can all be represented with not more than n non-zero digits is $0 \leqslant x \leqslant \frac{2}{3}(4^n - 1)$.

Thus all $(2n-1)$-digit integers can be so represented and those $2n$-digit numbers less than 10 10 10...10 can also be so represented.

The above proof has not used a knowledge of the form of the minimal digital representation. If the fact that no two successive digits can be both non-zero is used a simple heuristic proof follows by observing that a number of $2n$ places will contain at most $n+1$ non-zero digits (we must allow the possibility of $d_{2n} = 1$) in its minimal digital representation. If $d_{2n} = 0$, the maximum value that can be represented will be a number $s_r = 0,\ d_{2r} = 0,\ d_{2r+1} = 1\ (r = 0, 1, \ldots, n-1)$. This gives the result required.

8. The allocation of digital positions to inputs in a multi-input adder-type multiplier

As explained in section 2 for a practical utilization of the result of section 7 each of the $2n$ digital positions of the possible multipliers must be assigned to fixed inputs of the adder. It is now necessary to determine the restrictions on the division of the digital positions among the inputs necessary to allow each number to be represented.

Suppose, if possible, that digits $d_r, d_s, d_t\ (r > s > t)$ are associated with a common input. Then for all numbers in the range $[0, \frac{2}{3}(4^m - 1)]\ (m = 2n-1)$ only one of d_r, d_s, d_t can be non-zero. Consider the representations of the number $2^r - 2^t$. We have

$$\begin{aligned} b_u &= 0 \quad (u < t) \\ &= 1 \quad (t \leqslant u < r) \\ &= 0 \quad (u \geqslant r). \end{aligned}$$

For an arbitrary sequence s_u we have equation (14) which can be summarized in the following table.

b_{r+1}	b_r	d_{r+1}
0	0	$s_r\, d_r$
0	1	$1-(1-s_r)d_r$
1	0	$1-s_r\, d_r$
1	1	$(1-s_r)d_r$

Hence for any representation of 2^r-2^t we have

$$\begin{aligned} d_{v+1} &= s_v d_v && (v < t-1) && \text{(a)} \\ &= 1-s_{t-1}d_{t-1} && (v = t-1) && \text{(b)} \\ &= (1-s_v)d_v && (t \leqslant v < r-1) && \text{(c)} \\ &= 1-(1-s_{r-1})d_{r-1} && (v = r-1) && \text{(d)} \\ &= s_v d_v && (v \geqslant r) && \text{(e)} \end{aligned} \qquad (31)$$

Now if $t \neq 0$, $d_0 = 0$, hence $d_v = 0$ $(v < t)$ from (31 a), $d_t = 1$ from (31 b). If $t = 0$, $d_0 = d_t = 1$, and hence $d_r = 0$ by the input rule from (31 d) $(1-s_{r-1})d_{r-1} = 1$, i.e. $d_{r-1} = 1$. Hence, for (31 c), $d_v = 1$ $(t < u \leqslant r-1)$ and in particular $d_s = 1$, contrary to input rule.

Hence at most two digits can be associated with each input and since there are only $2n$ digits to associate with n inputs each input is associated with exactly two digits.

Suppose digits r and t $(r > t)$ are associated with one input and p and q $(p > q)$ with another input. We can assume without loss of generality that $r > p$. Three possibilities arise:

(i) $r > p > q > t$,

(ii) $r > p > t > q$,

(iii) $r > t > p > q$.

In case (i) consider the representations of 2^r-2^t given by (31) $d_t = 1$; $d_r = 0$; $d_v = 1$; $t \leqslant u \leqslant r-1$ and in particular $d_p = d_q = 1$ contrary to input rule.

In case (ii) consider the representations of the $2^r-2^p+2^t-2^q$,

$$\begin{aligned} b_u = 0 \quad (u < q) \qquad & d_{u+1} = s_u d_u && (u < q-1) && \text{(a)} \\ = 1 \quad (q \leqslant u < t) \qquad & = 1-s_{q-1}d_{q-1} && (u = q-1) && \text{(b)} \\ = 0 \quad (t \leqslant u < p) \qquad & = (1-s_u)d_u && (q \leqslant u < t-1) && \text{(c)} \\ = 1 \quad (p \leqslant u < r) \qquad & = 1-(1-s_{t-1})d_{t-1} && (u = t-1) && \text{(d)} \\ = 0 \quad (u \geqslant r) \qquad & = s_u d_u && (t \leqslant u < p-1) && \text{(e)} \\ & = 1-s_{p-1}d_{p-1} && (u = p-1) && \text{(f)} \\ & = (1-s_u)d_u && (p \leqslant u < r-1) && \text{(g)} \\ & = 1-(1-s_{r-1})d_{r-1} && (u = r-1) && \text{(h)} \\ & = s_u d_u && (u \geqslant r) && \text{(i)} \end{aligned} \qquad (32)$$

As before $d_q = 1$, so that by input rule $d_p = 0$. From (32 f) $d_{p-1} = 1$ and hence by (32 e) $d_0 = 1$ $(t \leqslant u < p)$, and in particular $d_t = 1$ so that by input rule $d_r = 0$ whence, by (32 h), $d_{r-1} = 1$ and thus by (32 g),

$d_u = 1$ $(p \leqslant u \leqslant r-1)$; in particular $d_p = 1$ which gives a contradiction.

Thus only case (iii) can occur. Given r, p can be chosen to have any value less than r and not equal to t. Hence $t = r-1$.

Put $r = m$, then the mate to m is $m-1$.

Put $r = m-2$, then the mate to $m-2$ is $m-3$.

Generally 2_p, 2_{p+1} are mates $p = 0, 1, 2, \ldots$ $(n = 1)$. The numbers 2^r-2^t, $2^r-2^p+2^t-2^q$ are (for any choice of r, t, p, q) all less than 2^m-1, and so if range of multipliers to be represented is restricted to m-digit numbers this pairing is still necessary.

9. The choice of s_r for multi-input adder type multipliers

We introduce the parity function

$$p_0 = 1, \qquad p_{r+1} = 1-p_r. \tag{33}$$

Then the input rule can be expressed as

$$p_r d_r d_{r+1} = 0. \tag{34}$$

From (14) we obtain

$$(1-2b_{r+1})p_r d_r d_{r+1} = p_r d_r\{(b_{r+1}-b_r)^2(1-2b_{r+1})+(s_r-b_r)\} = 0$$

since $(1-2x)^2 = 1$ for binary x.

This is easily reduced to

$$p_r d_r(b_{r+1}-s_r) = 0; \tag{35}$$

if $p_r = 0$, i.e. $r = 2t+1$, (35) gives no restriction. If $p_r = 1$, i.e. $r = 2t$, (35) gives by $d_{2t} = 1$,

$$s_{2t} = b_{2t+1}. \tag{36}$$

If $d_{2t} = 0$, s_{2t} can be arbitrary. Without loss of generality it can be taken as in (36). Hence

$$d_{2t+1} = (b_{2t+1}-b_{2t})^2(1-d_{2t}), \tag{37}$$

i.e. equations (25) and (26) hold for even r.

To obtain a unique formula we must add further restrictions. Suppose s_r is a recursive function, i.e. does not depend on the value of n. Then

$$d_{2r+2} = (b_{2r+2}-b_{2r+1})^2+(s_{2r+1}-b_{2r+1})(1-2b_{2r+2})d_{2r+1}. \tag{38}$$

If $d_{2r+1} = 0$, s_{2r+1} can be arbitrary. If $d_{2r+1} = 1$, $(b_{2r+1}-b_{2r})^2 = 1$, i.e. $b_{2r+1} \neq b_{2r}$. Two cases arise:

(i) $b_{2r+1} = 0$, $b_{2r} = 1$. If $r = n-1$, $d_{2r+2} = d_{2r}$ must be zero and hence for a recursive rule $d_{2r+2} = 0$ for all cases $b_{2r+2} = 0$, i.e. $s_{2r+1}(d_{2r}) = 0$ for all cases $b_{2r+2} = 0$. Hence in this case we must have $s_{2r+1} = 0$.

(ii) $b_{2r+1} = 1$, $b_{2r} = 0$. A similar argument shows that, if the full range of multipliers is to be used,

$$(1-s_{2r+1})(1-d_{2r}) = 1, \text{ for all cases } b_{2r+2} = 0.$$

Thus $s_{2r+1} = 0$ if $b_{2r+2} = 0$. If $b_{2r+2} = 1$, the recursive restriction gives no information and we therefore write

$$s_{2r+1} = b_{2r+2} g_{2r+1} \tag{39}$$

where g is arbitrary.

Substituting (37) and (39) in (38) we obtain

$$d_{2r+2} = b_{2r+2}(1-g_{2r+1}d_{2r+1})+b_{2r+1}(1-2b_{2r+2})[b_{2r}+(1-b_{2r})d_{2r}]. \tag{40}$$

This recursive scheme can be simplified by the choice of $g_{2r+1} = 0$ or $g_{2r+1} = 1-d_{2r+1}$ which reduces (40) to

$$d_{2r+2} = b_{2r+2}+b_{2r+1}(1-2b_{2r+2})\{b_{2r}+(1-b_{2r})d_{2r}\}. \tag{41}$$

(It is not possible to choose g_{2r+1} so that any of b_{2r+2}, b_{2r+1}, b_{2r}, d_{2r}, d_{2r+1} are eliminated from (40).) Equation (41) can be expressed in a simpler form by introducing an auxiliary variable c_{2r} defined by

$$c_{2r} = (1-2b_{2r})d_{2r}+b_{2r}. \tag{42}$$

Multiplying by $1-2b_{2r}$ and rearranging we obtain

$$d_{2r} = (1-2b_{2r})c_{2r}+b_{2r},$$

and hence

$$(1-b_{2r})d_{2r} = (1-b_{2r})c_{2r},$$

so that using (41), we find

$$\begin{aligned}(1-2b_{2r+2})c_{2r+2}+b_{2r+2} &= b_{2r+2}+b_{2r+1}(1-2b_{2r+2})\{b_{2r}+(1-b_{2r})d_{2r}\}\\ c_{2r+2} &= b_{2r+1}\{b_{2r}+(1-b_{2r})c_{2r}\} \qquad (43)\\ d_{2r+2} &= b_{2r+2}+(1-2b_{2r+2})c_{2r+2} = (b_{2r+2}-c_{2r+2})^2\\ &= (b_{2r+2}+c_{2r+2}) \pmod 2.\end{aligned}$$

(43) expresses the short cut method of multiplication in the scale of 4. The carry into the binary pair b_{2r+2}, b_{2r+3} takes place if and only if the preceding pair b_{2r+1}, b_{2r} is the form 11, or the form 10 with a carry into that pair. The resulting digit d_{2r+2} is the sum of b_{2r+2} and the carry c_{2r+2}.

The digit d_{2r+3} is given by (37) and is non-zero if and only if, after adding the carry into the pair b_{2r+3}, b_{2r+2} we have the form 1, 0.

In practical multipliers the range of multiples will be restricted to $[0, 2^m-1]$. In this case the recursive restriction will give no guide to the form of s_{2r+1} in the case $b_{2r+1} = 1$, $b_{2r} = 0$ since this pattern will not occur in the leading position. Thus we may take a more general form for s_{2r+1}:

$$s_{2r+1} = \{1-(1-b_{2r+1})b_{2r}\}g_{2r+1},$$

which ensures $s_{2r+1} = 0$ in the case $b_{2r+1} = 0$, $b_{2r} = 1$.

Since s_{2r+1} is arbitrary if $b_{2r+1} = b_{2r}$ we may take

$$s_{2r+1} = b_{2r+1} g_{2r+1}. \tag{44}$$

Hence, from (37) and (38),

$$d_{2r+2} = (b_{2r+2}-b_{2r+1})^2-b_{2r+1}(1-2b_{2r+2})(1-b_{2r})(1-g_{2r+1})(1-d_{2r})$$
$$= (b_{2r+2}-b_{2r+1})^2-b_{2r+1}(1-2b_{2r+2})(1-g_{2r+1})d_{2r+1}. \tag{45}$$

One simple case arises if we choose $g_{2r+1} = 1$. Equations (44) and (45) reduce to

$$d_{2r+2} = (b_{2r+2}-b_{2r+1})^2, \tag{46}$$

$$s_{2r+1} = b_{2r+1}. \tag{47}$$

Combining (36) and (37) with (46) and (47) we have the simple formulae

$$\left.\begin{aligned} d_{r+1} &= (b_{r+1}-b_r)^2(1-p_r d_r) \\ s_r &= p_r b_{r+1}+p_{r+1} b_r \end{aligned}\right\}. \tag{48}$$

Another useful case is given by $g_{2r+1} = b_{2r+2}$. Equation (45) then becomes

$$d_{2r+2} = (b_{2r+2}-b_{2r+1})^2(1-b_{2r+1}d_{2r+1}), \tag{49}$$

and (44) becomes $\qquad s_{2r+1} = b_{2r+1}b_{2r+2}$,

giving the combined equations

$$\left.\begin{aligned} d_{r+1} &= (b_{r+1}-b_r)^2\{1-(p_r+p_{r+1}b_r)d_r\} \\ s_r &= (p_r+p_{r+1}b_r)b_{r+1} \end{aligned}\right\}. \tag{50}$$

10. The representation of negative numbers

Signed numbers are represented by adding an extra digit in the leading position, zero for positive numbers and non-zero for negative numbers. Two representations of negative numbers are possible. If $-N$ is represented by $\sum b'_r 2^r$, then

(i) in 1's the complement system is

$$b'_r = 1-b_r, \tag{51}$$

(ii) in 2's the complement system is

$$\sum_0^n b'_r 2^r + \sum_0^n b_r 2^r = 2^{n+1}. \tag{52}$$

The minimal digit representation is easily extended to these systems. Suppose N has minimal digit representation $\sum (-)^{s_r} d_r 2^r$.

For the 1's complement system suppose the minimal digit representation is $\sum (-)^{s'_r} d'_r 2^r$. Also

$$(b'_{r+1}-b'_r)^2 = (b_{r+1}-b_r)^2,$$
$$d'_{r+1} = (b_{r+1}-b_r)^2(1-d'_r). \tag{53}$$

Let $\qquad d'_0 = 1-b'_0 = b_0 = d_0$.

By induction it follows that $d'_r = d_r$. Also

$$s'_r = b'_{r+1} = 1-b_{r+1} = 1-s_r.$$

Thus

$$\sum (-)^{s'_r} d'_r 2^r = \sum (-)^{1-s_r} d_r 2^r = -\sum (-)^{s_r} d_r 2^r = -N.$$

Equations (15) and (16) applied to all numbers in 1's complements will therefore give the correct minimal representation if the boundary condition

$$d_0 = (b_0 - b_{(s)})^2 \tag{54}$$

is used, where $b_{(s)}$ is the sign digit. Alternatively, define

$$b_r = b_{(s)} \quad (r < 0) \tag{55}$$

then no boundary condition is required.

Suppose $\sum b_r 2^r$ represents a negative number N in 2's complements; then its minimal digit representation is the same as that of $\sum b'_r 2^r$ in 1's complement where

$$\sum b'_r 2^r = \sum b_r 2^r - 2^0. \tag{56}$$

A similar analysis to that of section 4 shows that b'_r are defined recursively by

$$\left.\begin{aligned} b'_r &= (b_r - e_r)^2 \\ e_{r+1} &= e_r(1 - b_r) \\ e_0 &= 1 \end{aligned}\right\}. \tag{57}$$

Hence if $\sum (-)^s d_r 2^r$ is the minimal digit representation of N then

$$\left.\begin{aligned} d_{r+1} &= (b'_{r+1} - b'_r)^2(1 - d_r) \\ d_0 &= 1 - b'_0 = b_0 \\ s_r d_r &= b'_{r+1} d_r \end{aligned}\right\}. \tag{58}$$

We require the following easily derived relations

$$\left.\begin{aligned} e_r e_r - 1 &= e_r \quad \text{(a)} \\ e_r b_{r-1} &= 0 \quad \text{(b)} \\ e_r b'_{r-1} &= e_r \quad \text{(c)} \\ e_{r+1} d_r &= 0 \quad \text{(d)} \\ e_r b_r d_r &= e_r b_r \quad \text{(e)} \end{aligned}\right\}. \tag{59}$$

After some simplification we find that

$$(b'_{r+1} - b'_r)^2 = (b_{r+1} - b_r)^2 - e_r b_r(1 - 2b_{r+1}). \tag{60}$$

Hence, from (58) and (59e),

$$\begin{aligned} d_{r+1} &= (b_{r+1} - b_r)^2(1 - d_r) - e_r b_r(1 - 2b_{r+1})(1 - d_r) \\ &= (b_{r+1} - b_r)^2(1 - d_r). \end{aligned} \tag{61}$$

From (59d), $$(b'_{r+1} - b_{r+1})^2 d_r = 0.$$

From (58),

$$\begin{aligned} \{b'_{r+1}(1 - 2b_{r+1}) + b_{r+1}\} d_r &= \{s_r(1 - 2b_{r+1}) + b_{r+1}\} d_r \\ &= (b_{r+1} - s_r)^2 d_r = 0, \end{aligned}$$

whence $$s_r d_r = b_{r+1} d_r. \tag{62}$$

Equations (61) and (62) with the boundary condition $d_0 = b_0$ show that

all numbers in 2's complements are correctly represented in minimal digit form by the rules (15) and (16).

Thus in a parallel arithmetic unit, either complementing system can be used without complicating the control for negative multipliers.

In a serial machine using a multi-input adder either of the equations (48) or (50) can be mechanized.

Clearly both these schemes will continue to work for negative numbers in the 1's complement system with the boundary condition (54) or the equivalent situation in (55).

Unfortunately, this system is not very attractive for serial machines, and the behaviour of (48) and (50) applied to negative numbers in 2's complements must be investigated.

For equations (48) applied to the negative numbers $\sum b_r 2^r$ (in 2's complements) using (60), (59e), and (33) we find

$$\begin{aligned} d_{r+1} &= (b_{r+1}-b_r)^2(1-p_r d_r)-e_r b_r(1-2b_{r+1})(1-p_r d_r) \\ &= (b_{r+1}-b_r)^2(1-p_r d_r)-p_{r+1}e_r b_r(1-2b_{r+1}). \end{aligned}$$

The second term in this expression will not vanish in the cases when $p_{r+1}=1,\ b_r=1,\ b_s=0\ (s<r)$. Hence the scheme (48) is not very suitable for negative numbers in 2's complements.

Similarly, it can be shown that the scheme (50) is not suitable for negative numbers in 2's complements.

We may investigate the choice of g_r in equation (44) which will give a scheme independent of sign of number in 2's complements. Equations (37) and (45) can be combined to give

$$\left.\begin{aligned} d_{r+1} &= (b_{r+1}-b_r)^2(1-p_r d_r)-p_{r+1}b_r(1-2b_{r+1})(1-g_r)d_r \\ s_r &= p_r b_{r+1}+p_{r+1}b_r g_r \end{aligned}\right\}. \tag{63}$$

For a negative number in 2's complements (63) with (57) gives, after some simplification

$$\begin{aligned} d_{r+1} &= (b'_{r+1}-b'_r)^2(1\quad p_r d_r)-p_{r+1}b'_r(1-2b'_{r+1})(1-g'_r)d_r \\ &= (b_{r+1}-b_r)^2(1-p_r d_r)-p_{r+1}b_r(1-2b_{r+1})(1-g_r)d_r- \\ &\quad -p_{r+1}(1-2b_{r+1})[e_r\{b_r+(1-2b_r)(1-g'_r)\}+b_r(g_r-g'_r)]d_r \end{aligned} \tag{64}$$

and

$$\begin{aligned} s_r d_r &= (p_r b'_{r+1}+p_{r+1}b'_r g'_r)\,d_r \\ &= (p_r b_{r+1}+p_{r+1}b_r g_r)d_r+p_{r+1}(b'_r g'_r-b_r g_r)d_r \end{aligned} \tag{65}$$

where g'_r is the transform of g_r under $b_r \to b'_r$.

The scheme will be independent of sign if and only if

$$b'_r g'_r d_r = b_r g_r d_r \tag{66}$$

and

$$[e_r\{b_r+(1-2b_r)(1-g'_r)\}+b_r(g_r-g'_r)]d_r = 0. \tag{67}$$

The possible solutions of (66) are

(i)	$g_r = 0$	(ii)	$g_r = 1-b_r$	(iii)	$g_r = 1-d_r$	(iv)	$g_r = b_r$
	$g'_r = 0$		$g'_r = 1+b'_r$		$g'_r = 1-d_r$	(v)	$g'_r = b_r$.

Substituting these solutions in turn in (67) it will be seen that (67) will only be satisfied by (i) and (iii) but not by (ii) or (iv). The former reduce (63) to the common form

$$d_{r+1} = (b_{r+1}-b_r)^2(1-p_r d_r)-p_{r+1}b_r(1-2b_{r+1})d_r. \tag{68}$$

Since this is obtained by putting $s_{2r+1} = 0$, (68) is the combined version of (37) and (41) and represents the method of short cut in the scale of four.

Hence we have the result that this is the only scheme for use with multi-input type multipliers in a serial machine.

In practice it may be more convenient to use the schemes (48) or (50) and precede the multiplication in cases of a negative multiplier with one subtraction of the multiplicand from the product register.

11. The application of the mathematical analysis to division processes

The usual restoring technique of division involves for n-digit numbers n trial subtractions and on average of $\frac{1}{2}n$ corrections—a total of $\frac{3}{2}n$ 'addition' times.

To reduce the division time von Neumann suggested that the non-restoring technique should be used when every division requires n addition times. This can be generalized to a process in which for each digital position the divisor is added to or subtracted from the remainder or not according to some rules. In this case the quotient is represented in the form $\sum(-)^{s_r}d_r 2^r$ which has been studied in the earlier sections.

Two questions then arise. Can the digits b be recovered from the form $\sum(-)^{s_r}d_r 2^r$? What is the rule deciding whether to change the remainder which will produce the minimum digit representation of the quotient?

The first question is easily answered. Rearranging (14) we obtain

$$\begin{aligned} d_{t+1} &= b_{t+1}+b_t(1-2b_{t+1})(1-d_t)+s_t d_t(1-2b_{t+1}) \\ b_{t+1}+d_{t+1}(1-2b_{t+1}) &= b_t(1-d_t)+s_t d_t \\ b_{t+1}(1-2d_{t+1})+d_{t+1} &= b_t(1-d_t)+s_t d_t \\ b_{t+1} &= d_{t+1}+\{b_t(1-d_t)+s_t d_t\}(1-2d_{t+1}). \end{aligned} \tag{69}$$†

This defines the b's recursively from $b_0 = d_0$. In the special case of ordinary non-restoring division $d_r = 1$ for all r, when (69) reduces to

$$b_{t+1} = 1-s_t. \tag{70}$$

† In the derivation of (69) free use is made of the identity $(1-2x)^2 \equiv 1$.

This, with the forcing rule $b_0 = 1$ (for positive quotients) enables the digits of the quotient to be obtained in descending order as the division proceeds. This result was first obtained by von Neumann.

For the general form, the recursion from most to least significant digits is not possible. Rearranging (69) we have

$$b_t(1-d_t) = d_{t+1}+b_{t+1}(1-2d_{t+1})-s_t d_t. \tag{71}$$

If $d_t = 0$ this gives $\quad b_t = d_{t+1}+b_{t+1}(1-2d_{t+1})$

$$= (b_{t+1}-d_{t+1})^2 \tag{72}$$

but if $d_t = 1$, (71) gives no information about b_t. In the division process, however, the relative signs of remainder and divisor determine the value of s for the next non-zero d and with this added information a reverse recursion is possible.

Suppose, without loss of generality, positive dividend and divisor and record $s = 0$ for subtractions, $s = 1$ for additions. Let t_u denote the sign of the remainder at the end of a cycle to determine the digit d_u, $t = 0$ denoting positive remainder. Then

$$s_u = t_{u+1}. \tag{73}$$

The fact that the sign of the remainder does not change unless an addition or subtraction is performed can be expressed by the equation

$$(t_{u-1}-t_u)(1-d_u) = 0. \tag{74}$$

Consider the sequence

$$d_u = 1, \quad d_{u-1} = d_{u-2}, \quad \ldots, \quad d_{u+1} = 0, \quad d_u = 1,$$

and let $b_u = 1-x$. Then applying (49) for $t = u-1$ we obtain $b_{u-1} = x$. Similarly $b_{u-2} = b_{u-3},\ldots, b_{u+1} = x$. Now apply (49) with $t = u$; this gives $x = s_u = t_{u+1} = t_{u+2},\ldots, t_{u-1} = t_u$, i.e. $b_u = 1-t_u$. Similarly if

$$d_u = d_{u-1} = 1, \qquad b_u = 1-s_{u-1} = 1-t_u.$$

Thus the recursive rule for obtaining the b's is

$$b_r = (d_{r+1}-b_{r+1})^2(1-d_r)+(1-t_r)d_r, \tag{75}$$

which reduces to (70) if $d_r = 1$ for all r by using (73).

We now turn to the second question. In the notation of equation (2) put

$$R_u = \Big| \sum_0^u (-)^{s_r} d_r 2^r \Big|.$$

Then we have the result that the minimum digit representation is the only form which for all integers has the property:

$$R_{u+1} = R_u \quad \text{or} \quad R_{u+1} > 2R_u \quad \text{for all } u. \tag{76}$$

Clearly, if $R_{u+1} \neq R_u$, $\qquad R_{u+1} = 2^{u+1} \pm R_u$.

If the upper sign applies (76) clearly holds. If the lower sign applies,

$$R_{u+1}-2R_u = 2^{u+1}-3R_u$$
$$= 2^{u+1}-3d_u 2^u \pm 3R_{u-1}. \tag{77}$$

This must hold for all sequences b_r and, in particular, for $b_r = 0$ $(r < u)$. For all s_r this implies $d_r = 0$ $(r < u)$ and hence $R_{u-1} = 0$. In this case, $d_u = 0$. Thus, $d_u d_{u+1} = 0$ is a necessary condition for (76). It is also sufficient, for in this case

$$R_{2p} \leqslant \sum_{s=0}^{p} 4^s = \tfrac{1}{3}(4^{p+1}-1),$$

$$R_{2p+1} \leqslant 2\sum_{s=0}^{p} 4^s = \tfrac{2}{3}(4^{p+1}-1),$$

$$R_u = \tfrac{1}{3}\{2^{u+2}-1-u(\mathrm{mod}\,2)\},$$

$$R_{u+1}-2R_u \geqslant R_{u+1}-3R_{u-1} > 1+(u-1)(\mathrm{mod}\,2) > 0.$$

The condition $d_{u+1}d_u = 0$ gives from (14)

$$\{(b_{u+1}-b_u)^2-(b_u-s_u)(1-2b_{u+1})\}d_u = 0,$$

$$\{b_{u+1}+s_u(1-2b_{u+1})\} = (1-2b_{u+1})(s_u-b_{u+1})d_u = 0,$$

i.e. if $$d_u = 1, \qquad s_u = b_{u+1}.$$

Hence (76) implies d's given by (15) and (16), the minimal digital representation.

If the dividend is s_0, the divisor D, and the quotient is N given by (2) then

$$s_0 = ND$$

and the remainder at the $u'(n-u)'$ stage is

$$s_u = s_0-\Big(\sum_{u+1}^{n}(-)^{s_r}d_r 2^r\Big)D = \Big(\sum_{0}^{u}(-)^{s_r}d_r 2^r\Big)D,$$
$$|s_u| = R_u|D|. \tag{78}$$

Hence for minimal digit representation

$$|s_{u+1}| = |s_u| \quad \text{or} \quad |s_{u+1}| > 2|s_u|.$$

Thus the remainder changes if and only if

$$|s_u| > \tfrac{2}{3}|D|2^u. \tag{79}$$

Thus in a practical divisor, after an addition or subtraction, the remainder should be shifted forward until it first exceeds $\frac{2}{3}$ of the divisor. This is not a practical possibility for a parallel machine, but this rule is easily mechanized into a serial divisor which determines two or three digits of the divisor in each cycle.

To obtain two digits in each cycle an adder is provided which produces $3s_u$ in each cycle. This is fed to adder-subtractor units which produce the correctly signed versions of $3|s_u|-|D|$ and $3|s_u|-2|D|$. Two other adder-subtractors produce the correctly signed versions of $|s_u|-|D|$ and

$|s_u|-\frac{1}{2}|D|$ which are fed into delay lines. s_u is also fed into a delay line.

At the conclusion of the cycle the sign digits of the outputs are inspected and the appropriate gate opened to feed the correct value of s_{u-2} into the trebling adder during the next cycle. These same sign digits determine the value of d_u and d_{u-1} from which the values of b_u, b_{u-1} can be found using (75).

This mechanization depends on the fact that both possible subtractions will not take place in any cycle. If $d_{u-1} = 1$, it is known that $d_{u-2} = 0$ and the delay lines can be adjusted to pass s_{u-3} to the trebling adder.

To obtain three digits in each cycle additional adders must be incorporated to form the correctly signed versions of

$$3|s_u|-2\tfrac{1}{2}|D|, \quad 3|s_u|-1\tfrac{1}{2}|D|, \quad |s_u|-\tfrac{1}{4}|D|, \quad \text{and} \quad |s_u|-1\tfrac{1}{4}|D|$$

in addition to the others, so that the possibility of the digital pattern $d_u = 1$, $d_{u-1} = 0$, $d_{u-2} = 1$ can be dealt with.

For parallel machines, the most natural rule is to change the remainder if $|s_u| > \alpha$ independent of D. If α is chosen as 2^{u-1} this corresponds to shifting the remainder to standard form after each change.

An analysis of the resulting digital pattern is very complex and the author has been unable to solve the problem. It is conjectured that the average number of digits in the resulting representation of a uniformly distributed quotient is half the number of places, but this is based on a dubious hypothesis concerning the distribution of successive remainders.

Conclusions

The application of Boolean algebra to the problems of making fast multipliers and dividers in a binary computing machine results in several practical procedures which have hitherto not been explored.

Acknowledgements

The idea of systematically exploiting an adder subtractor mechanism in multiplication appears first, to the author's knowledge, in M. Lehman's doctorial thesis (3) where an empirical and heuristic analysis is made.

I should like to acknowledge the helpful discussions with M. Lehman on the practical implications of this paper.

REFERENCES

1. A. W. Burks, H. H. Goldstone, and J. von Neumann, *Preliminary Discussion of the Logical Design of an Electronic Computing Instrument*, Part. I. Institute of Advanced Studies (Princeton, 1947).
2. R. K. Richards, *Arithmetic Operations in Digital Computers* (Van Nostrand, 1955).
3. M. Lehmman, *Parallel Arithmetic Units and their Control*. Ph.D. Thesis, University of London, 1957.

$|s_u| - \frac{1}{2} D$ which are fed into delay lines. s_u is also fed into a delay line.

At the conclusion of the cycle the sign digits of the outputs are inspected and the appropriate gate opened to feed the correct value of s_{u-2} into the trebling adder during the next cycle. These same sign digits determine the value of d_u and d_{u-1} from which the values of b_u, b_{u-1} can be found using (75).

This mechanization depends on the fact that both possible subtractions will not take place in any cycle. If $d_{u-1} = 1$, it is known that $d_{u-2} = 0$ and the del. $_2$ lines can be adjusted to pass s_{u-3} to the trebling adder.

To obtain three digits in each cycle additional adders must be incorporated to form the correctly signed versions of

$$3s_u - 2\tfrac{1}{2} D, \quad 3s_u - 1\tfrac{1}{2} D, \quad s_u - \tfrac{1}{4} D, \quad \text{and} \quad s_u - 1\tfrac{1}{4} D$$

in addition to the others, so that the possibility of the digital pattern $d_u = 1$, $d_{u-1} = 0$, $d_{u-2} = 1$ can be dealt with.

For parallel machines, the most natural rule is to change the remainder if $|s_u| > \lambda$ independent of D. If λ is chosen as 2^{n-1} this corresponds to shifting the remainder to standard form after each change.

An analysis of the resulting digital pattern is very complex and the author has been unable to solve the problem. It is conjectured that the average number of digits in the resulting representation of a uniformly distributed quotient is half the number of places, but this is based on a dubious hypothesis concerning the distribution of successive remainders.

Conclusions

The application of Boolean algebra to the problems of making fast multipliers and dividers in a binary computing machine results in several practical procedures which have hitherto not been explored.

Acknowledgements

The idea of systematically exploiting an adder subtractor mechanism in multiplication appears first, to the author's knowledge, in M. Lehman's doctorial thesis (3) where an empirical and heuristic analysis is made.

I should like to acknowledge the helpful discussions with M. Lehman on the practical implications of this paper.

REFERENCES

1. A. W. Burks, H. H. Goldstone, and J. von Neumann, *Preliminary Discussion of the Logical Design of an Electronic Computing Instrument*, Part I. Institute of Advanced Studies (Princeton, 1947).
2. R. K. Richards, *Arithmetic Operations in Digital Computers* (Van Nostrand, 1955).
3. M. Lehman, *Parallel Arithmetic Units and their Control*. Ph.D. Thesis, University of London, 1957.

THE QUARTERLY JOURNAL OF MECHANICS AND APPLIED MATHEMATICS

VOLUME XI PART 3 AUGUST 1958

CONTENTS

The Editorial Board gratefully acknowledge the support given by: Blackburn & General Aircraft Limited; Bristol Aeroplane Company; Courtaulds Scientific and Educational Trust Fund; English Electric Company; Hawker Siddeley Group Limited; Imperial Chemical Industries Limited, Metropolitan-Vickers Electrical Company Limited; The Shell Petroleum Co. Limited; Vickers-Armstrongs (Aircraft) Limited.